Università degli Studi di Pavia
Dipartimento di Scienze del Farmaco

IUSS
Scuola Universitaria Superiore Pavia

Counteracting oxidative stress, inflammation and Aβ aggregation with nature-inspired hybrids: relevance for Nrf2 pathway involvement in neurodegeneration and aging

Melania Maria Serafini

Supervisors: Prof. Stefano Govoni

Prof. Cristina Lanni

Prof. Marco Racchi

PhD Director: Prof. Andrea Mattevi

PhD in Biomolecular Sciences and Biotechnologies

XXX cycle, academic years 2014-2017

A Paolo, prezioso compagno di vita e sostegno quotidiano.

*Alla piccola Alice Maria che non vediamo l'ora di conoscere:
grazie per la compagnia che mi hai fatto con i tuoi calcetti
durante questi mesi di stesura della tesi.*

Table of contents

Preface

During my PhD, I carried out the research activity at the Department of Drug Sciences (Pharmacology Section) focusing my attention on the modulation of different pathways involved in the response to oxidative stress, inflammation and amyloid beta peptide (Aβ) aggregation and oligomerization by natural compounds and synthetic molecules inspired by nature.

Oxidative stress and inflammation are common features of different disorders, in particular neurodegenerative diseases, and their homeostasis is impaired during the progression of physiological aging process [1-4]. Moreover, Aβ fibrils formation and accumulation in the brain tissue, is one of the main characteristics of Alzheimer's disease (AD) [5].

As reported in the first chapter of this thesis, thanks to a collaboration with the group of professor Michela Rosini at the Alma Mater Studiorum University of Bologna, we tested a group of newly synthesized molecules inspired by nature for their ability to counteract oxidative stress, Aβ aggregation and oligomerization and to modulate some cellular pathways.

In particular, in Part 1 we studied three compounds (1-3) to investigate the connection between Aβ and oxidative stress, with p53 emerging as a possible mediator of this functional interplay through the zyxin-HIPK2-p53 signaling pathway. The importance of the p53 wild-type conformation and the consequences of the induction of a p53 altered conformation induced by soluble non toxic Aβ, was described in our laboratory in the previous years and has been shown to contribute to the accumulation of cell damage, making cells not able to activate the proper apoptotic program when exposed to *noxae* [6-8]. Here we demonstrate that compound 3 inhibits Aβ fibrilization preventing the formation of cytotoxic stable oligomeric intermediates. Conversely, although to a different extent, all hybrids 1-3 were able

to counteract ROS formation and inhibit Aβ-induced p53 conformational changes, with the stronger antioxidant 2 being significantly more effective.

To go deeper in the characterization of the anti-aggregant ability of 3, in Part 2 I report preliminary data obtained in collaboration with professor Ersilia De Lorenzi at the University of Pavia. We analyzed in capillary electrophoresis the anti-oligomerization properties of compounds 2 and 3, taking 2 as negative control, on the aggregation process of the most amyloidogenic peptide: Aβ42. The analysis was conducted comparing Aβ42 electropherograms with the traces of Aβ42 co-incubated with 2 or 3. Compound 3 confirmed to be a very potent molecule because it inhibited the formation of large oligomers. Moreover also the negative control 2 was able to shift the equilibrium towards non toxic small species, although no activity was detected with thioflavin T-based fluorimetric assay, as shown in Part 1.

Data reported in Part 1 and 2 highlighted the essential role of the catechol moiety in the prevention of Aβ oligomerization and fibrils formation. Starting from the molecule with the most efficacy in counteracting Aβ aggregation, a new library of compounds was synthetized with the attempt to optimize the combination of anti-aggregant and scavenging properties and to dissect the structure-activity relationship (SAR) related to the antioxidant activity.

In aging, oxidant production from several sources is increased, whereas antioxidant enzymes are decreased, and repair systems decline [9]. In the context of AD, oxidative stress is known to trigger the amyloidogenic pathway and to promote Aβ toxicity in a vicious circle [10]. For this reason, in Part 3, we increase the number of molecules analyzed and, supposing the modulation of an intracellular pathway, we focused our attention on the nuclear factor (erythroid-derived 2)-like 2 (Nrf2) transcription factor. Nrf2 is considered the master regulator of the antioxidant cellular response because, once activated, it promotes the transcription of numerous genes acting on different cytoprotective pathways [11].

Starting from 1 as leading compound, that was previously named 3 in part 1 and 2, we confirmed the essential role of the cathecol moiety combined with the thioester function in the prevention of Aβ aggregation and we identified compound 12 as more effective and less toxic than prototype 1. Furthermore, we delineate the general SAR finding that catechol, which become active ortho-quinone on oxidation, should provide neuroprotection in oxidative conditions and α,β-unsaturated carbonyl group, that possesses Michael acceptor functionality, may represent an additional source for Nrf2 activation. Finally, in Part 4, we deepened the mechanism of action of a sub-group of the compounds analyzed in Part 3, on the Nrf2 pathway. Moreover, we investigated the possibility that these molecules exert epigenetic effects by modulating specific microRNAs involved in the antioxidant response. On the basis of our data, we hypotesize that the activation of the Nrf2 pathway is carried out by the interaction of these molecules with the negative regulator Keap1 which binds the transcription factor and recruits a cul-3-ubiquitin ligase. The release of Nrf2 from this complex allows the transctiption factor to migrate from the citoplasm into the nucleus to accomplish its protective functions.

Taking together, data reported in Chapter I lead us to identify and to characterize a group of newly synthetized molecules potentially powerful as pharmacological tools in the modulation of cellular network impaired in neurodegenerative diseases such as the zyxin-HIPK2-p53 signaling pathway and the Nrf2/Aβ axis.

The treatment of AD is still a major challenge: to date, there are not effective disease-modifying treatments available, but only therapeutics that slow down the disease progression and control symptoms in the short-term [12, 13]. There is an enormous global demand for new effective therapies and researchers are investigating different fields. Among others, the integrative approach has gaining relevance as potential strategy. It consists in the use of nutraceuticals

as integrative, complementary and preventive therapy and it emphasizes the importance of diet in fighting not only neurodegenerative disorders, but also the phisiological process of aging.

In the second chapter of this thesis, we focused our attention on two different natural compounds: curcumin and γ-oryzanol which are both commercially available as dietary supplements.

In Part 1, we summarize in a review paper the potential use of curcumin in prevention, treatment and diagnostic of Alzheimer's disease. Curcumin is a natural product extracted from the rhizome of *Curcuma longa*, which has been extensively studied for its numerous properties. In the context of neurodegeneration and AD, curcumin has shown anti-inflammatory, antioxidant and anti-Aβ effects [14]. Although several properties of curcumin have been reported in literature in *in vitro* and *in vivo* studies, clinical trials with curcumin oral administration have failed because of its pharmacokinetic profile [15]. For this reason, we analyzed the literature of the past years to underline the alternative strategies to go beyond these problems.

In Part 2, thanks to a collaboration with the group of professor Daniela Uberti at the University of Brescia, we dissect the mechanism of action of γ-oryzanol demonstrating, for the first time, ist action on the Nrf2 pathway. γ-oryzanol is a ferulate compound very abundant in rice (*Oryza sativa L.*) and it is known for its antioxidant properties [16, 17]. Oxidative stress is not only involved in the pathogenesis of neurodegenerative disorders such as AD, but it is also at the base of some mechanisms involved in aging processes. Thus, counteracting free radical damage through the consumption of dietary antioxidants containing antioxidative phytochemicals, such as γ-oryzanol, become fundamental to maintain body homeostasis, redox balance and to promote a healthy life-style.

Recently, the Nrf2 pathway has been shown to be closely linked to inflammation. Several studies have demonstrated that Nrf2

contributes to the anti-inflammatory process by orchestrating the recruitment of inflammatory cells and regulating gene expression. The Keap1/Nrf2/ARE signaling pathway, not only regulates the antioxidant response, but also the anti-inflammatory gene expression inhibiting the progression of inflammation [18, 19].

Oxidative stress and inflammation, together with autophagy, are keywords of another neurodegenerative disorder: the age-related macular degeneration (AMD) [20-22]. AMD is a severe neurodegenerative disease and a major cause of blindness in the elderly worldwide. AMD phenotype is not homogeneous, the molecular mechanisms of its pathogenesis remain poorly understood and, to date, reliable therapies are completely lacking for the dry form of AMD which is the most common [23, 24]. In the context of a potential therapeutic intervention for AMD, it has been demonstrated that a positive modulation of Nrf2 activity may be protective against oxidative stress and inflammation, thus suggesting the potential use of compounds acting on Nrf2 pathway as therapeutics in some ocular diseases [25, 26]. For this reason, in collaboration with professor Marialaura Amadio of the Department of Drug Sciences at the University of Pavia, we performed some pilot experiments with our Nrf2-activating compounds. These preliminary data are the subject of Chapter III. The collaboration with professor Amadio gave rise to a project funded by the Fondo di Ricerca di Ateneo, Blue Sky Research, in which I am the co-investigator, that will continue at least for the next two years opening future perspective for my work after the end of the PhD.

Finally, during these three years, I was involved in another project whose topic was immunesenescence, defined as the decline in the human immune system that occurs with aging. In this context, I contributed with my skills in cellular biology and biochemistry to the preparation of different published manuscripts that are listed at the end of the thesis.

References

1. Harman D. Aging: a theory based on free radical and radiation chemistry. J Gerontol. 1956 Jul;11(3):298-300.
2. Reuter S, Gupta SC, Chaturvedi MM, Aggarwal BB. Oxidative stress, inflammation, and cancer: how are they linked? Free Radic Biol Med. 2010 Dec 1;49(11):1603-16. doi: 10.1016/j.freeradbiomed.2010.09.006.
3. Olinski R, Siomek A, Rozalski R, Gackowski D, Foksinski M, Guz J, Dziaman T, Szpila A, Tudek B. Oxidative damage to DNA and antioxidant status in aging and age-related diseases. Acta Biochim Pol. 2007;54(1):11-26.
4. Uttara B, Singh AV, Zamboni P, Mahajan RT. Oxidative stress and neurodegenerative diseases: a review of upstream and downstream antioxidant therapeutic options. Curr Neuropharmacol. 2009 Mar;7(1):65-74. doi:10.2174/157015909787602823.
5. Murphy MP, LeVine H 3rd. Alzheimer's disease and the amyloid-beta peptide. J Alzheimers Dis. 2010;19(1):311-23. doi: 10.3233/JAD-2010-1221.
6. Lanni C, Necchi D, Pinto A, Buoso E, Buizza L, Memo M, Uberti D, Govoni S, Racchi M. Zyxin is a novel target for β-amyloid peptide: characterization of its role in Alzheimer's pathogenesis. J Neurochem. 2013 Jun;125(5):790-9. doi:10.1111/jnc.12154.
7. Buizza L, Cenini G, Lanni C, Ferrari-Toninelli G, Prandelli C, Govoni S, Buoso E, Racchi M, Barcikowska M, Styczynska M, Szybinska A, Butterfield DA, Memo M, Uberti D. Conformational altered p53 as an early marker of oxidative stress in Alzheimer's disease. PLoS One. 2012;7(1):e29789. doi:10.1371/journal.pone.0029789.
8. Lanni C, Nardinocchi L, Puca R, Stanga S, Uberti D, Memo M, Govoni S, D'Orazi G, Racchi M. Homeodomain interacting protein kinase 2: a target for Alzheimer's beta

amyloid leading to misfolded p53 and inappropriate cell survival. PLoS One. 2010 Apr 14;5(4):e10171. doi:10.1371/journal.pone.0010171.

9. Zhang H, Davies KJA, Forman HJ. Oxidative stress response and Nrf2 signaling in aging. Free Radic Biol Med. 2015 Nov;88:314-336. doi:10.1016/j.freeradbiomed.2015.05.036.

10. Swomley, A. M., Förster, S., Keeney, J. T., Triplett, J., Zhang, Z., Sultana, R., and Butterfield, D. A. (2014) Abeta, oxidative stress in Alzheimer disease: evidence based on proteomics studies. Biochim. Biophy. Acta 1842, 1248-1257.

11. Itoh K, Chiba T, Takahashi S, Ishii T, Igarashi K, Katoh Y, Oyake T, Hayashi N, Satoh K, Hatayama I, Yamamoto M, Nabeshima Y. An Nrf2/small Maf heterodimer mediates the induction of phase II detoxifying enzyme genes through antioxidant response elements. Biochem Biophys Res Commun. 1997 Jul 18;236(2):313-22.

12. Allgaier M, Allgaier C. An update on drug treatment options of Alzheimer's disease. Front Biosci (Landmark Ed). 2014 Jun 1;19:1345-54.

13. Rafii MS. Update on Alzheimer's disease therapeutics. Rev Recent Clin Trials. 2013 Jun;8(2):110-8.

14. Ammon HP, Wahl MA. Pharmacology of Curcuma longa. Planta Med. 1991 Feb;57(1):1-7.

15. Gupta SC, Patchva S, Aggarwal BB. Therapeutic roles of curcumin: lessons learned from clinical trials. AAPS J. 2013 Jan;15(1):195-218. doi:10.1208/s12248-012-9432-8.

16. Minatel IO, Francisqueti FV, Corrêa CR, Lima GP. Antioxidant Activity of γ-Oryzanol: A Complex Network of Interactions. Int J Mol Sci. 2016 Aug 9;17(8). pii: E1107. doi: 10.3390/ijms17081107.

17. Butsat S, Siriamornpun S. Phenolic acids and antioxidant activities in husk of different Thai rice varieties. Food Sci

Technol Int. 2010 Aug;16(4):329-36. doi:10.1177/1082013210366966.

18. Wardyn JD, Ponsford AH, Sanderson CM. Dissecting molecular cross-talk between Nrf2 and NF-κB response pathways. Biochem Soc Trans. 2015 Aug;43(4):621-6. doi:10.1042/BST20150014.

19. Ahmed SM, Luo L, Namani A, Wang XJ, Tang X. Nrf2 signaling pathway: Pivotal roles in inflammation. Biochim Biophys Acta. 2017 Feb;1863(2):585-597. doi:10.1016/j.bbadis.2016.11.005.

20. Reibaldi M, Longo A, Pulvirenti A, Avitabile T, Russo A, Cillino S, Mariotti C, Casuccio A. Geo-Epidemiology of Age-Related Macular Degeneration: New Clues Into the Pathogenesis. Am J Ophthalmol. 2016 Jan;161:78-93.e1-2. doi:10.1016/j.ajo.2015.09.031.

21. Boya P, Esteban-Martínez L, Serrano-Puebla A, Gómez-Sintes R, Villarejo-Zori B. Autophagy in the eye: Development, degeneration, and aging. Prog Retin Eye Res. 2016 Nov;55:206-245. doi:10.1016/j.preteyeres.2016.08.001.

22. Kaarniranta K, Tokarz P, Koskela A, Paterno J, Blasiak J. Autophagy regulates death of retinal pigment epithelium cells in age-related macular degeneration. Cell Biol Toxicol. 2017 Apr;33(2):113-128. doi: 10.1007/s10565-016-9371-8.

23. Jager RD, Mieler WF, Miller JW. Age-related macular degeneration. N Engl J Med. 2008 Jun 12;358(24):2606-17. doi: 10.1056/NEJMra0801537.

24. Van Lookeren Campagne M, LeCouter J, Yaspan BL, Ye W. Mechanisms of age-related macular degeneration and therapeutic opportunities. J Pathol. 2014 Jan;232(2):151-64. doi: 10.1002/path.4266.

25. Datta S, Cano M, Ebrahimi K, Wang L, Handa JT. The impact of oxidative stress and inflammation on RPE degeneration in

non-neovascular AMD. Prog Retin Eye Res. 2017 Sep;60:201-218. doi: 10.1016/j.preteyeres.2017.03.002.

26. Pujol-Lereis LM, Schäfer N, Kuhn LB, Rohrer B, Pauly D. Interrelation Between Oxidative Stress and Complement Activation in Models of Age-Related Macular Degeneration. Adv Exp Med Biol. 2016;854:87-93. doi:10.1007/978-3-319-17121-0_13.

Chapter I

Part 1.

The following manuscript has been published on ChemMedChem (2016) as:

Nature-inspired multifunctional ligands: focusing on amyloid-based molecular mechanisms of Alzheimer's disease

Elena Simoni,[a] **Melania M. Serafini**,[b,d] Manuela Bartolini,[a] Roberta Caporaso,[a] Antonella Pinto,[b] Daniela Necchi,[b] Jessica Fiori,[a] Vincenza Andrisano,[c] Anna Minarini,[a] Cristina Lanni,*[b] and Michela Rosini*[a]

[a] *Department of Pharmacy and Biotechnology, Alma Mater Studiorum - University of Bologna Via Belmeloro 6, 40126 Bologna, Italy*

[b] *Department of Drug Sciences (Pharmacology Section) University of Pavia, V.le Taramelli 14, 27100 Pavia, Italy*

[c] *Department for Life Quality Studies Alma Mater Studiorum - University of Bologna Corso d'Augusto 237, 47921 Rimini, Italy*

[d] *Scuola Universitaria Superiore IUSS Pavia, P.zza Vittoria 15, 27100 Pavia, Italy*

Nature-Inspired Multifunctional Ligands: Focusing on Amyloid-Based Molecular Mechanisms of Alzheimer's Disease

Elena Simoni,[a] Melania M. Serafini,[b] Manuela Bartolini,[a] Roberta Caporaso,[a] Antonella Pinto,[b] Daniela Necchi,[b] Jessica Fiori,[a] Vincenza Andrisano,[c] Anna Minarini,[a] Cristina Lanni,*[b] and Michela Rosini*[a]

Abstract

The amyloidogenic pathway is a prominent feature of Alzheimer's disease (AD). However, growing evidence suggests that a linear disease model based on amyloid-β peptide (Aβ) alone is not likely to be realistic, thus calling for further investigations on the other actors involved in the play. The pro-oxidant environment induced by Aβ in AD pathology is well established, and a correlation between Aβ, oxidative stress and p53 conformational changes has been suggested. Here, we applied the multifunctional approach to identify allyl thioesters of differently substituted trans-cinnamic acids, whose pharmacological profile was strategically tuned by the hydroxyl substituents on the aromatic moiety. Indeed, only the catechol derivative **3** [S-allyl (*E*)-3-(3,4-dihydroxyphenyl)prop-2-enethioate] inhibited Aβ fibrilization. Conversely, albeit to a different extent, all compounds were able to reduce ROS formation in SH-SY5Y neuroblastoma cells, and to prevent alterations in p53 conformation and activity mediated by soluble sublethal concentrations of Aβ. This may support an involvement of oxidative stress in Aβ function, with p53 emerging as a potential mediator of their functional interplay.

Introduction

Alzheimer's disease (AD) is a progressive neurodegenerative disorder, with a complex interplay of genetic and biochemical factors contributing to the pathological decline. Progression of the disease involves misfolding and aggregation of amyloid-β peptide (Aβ) from soluble non toxic monomers into insoluble fibrils. The most toxic form of Aβ is believed to be soluble oligomers, which are potent mediators of the synaptotoxicity.[1] In AD drug development, programs based on the Aβ cascade hypothesis have dominated research for the past twenty years, and still play a major role in pharmaceutical product pipelines. However, Aβ-centric approaches have not yet resulted in clinically effective drugs. This has raised a degree of skepticism, which has in turn led to review the science underpinning the Aβ model.[2] Besides the consolidated evidence that Aβ might trigger the disease process, intertwined correlations between Aβ and the other main players of the disease have been identified.[3] This has prompted researchers to develop multifunctional anti-amyloid agents[4] that, by acting simultaneously on several AD targets than the amyloidogenic pathway alone, are intended to trigger a synergistic response, with superior efficacy and safety profile.[5] Further, we think that molecules endowed with a multifaceted pharmacology have a great potential in exploring Aβ partnership with other crucial AD features. A deeper comprehension of amyloid-based disease mechanisms might offer the chance for repositioning Aβ in the disease network, being of help in bridging the gap between basic and translational research. In particular, the etiopathogenic loop generated by Aβ and oxidative stress offers a new key for reading Aβ causative role.[6]

Oxidative stress is known to trigger the amyloidogenic pathway and promote Aβ toxicity.[7] On the other hand, several lines of evidence indicate that Aβ exacerbates oxidative stress, with other cellular pathways emerging as determining mediators of this vicious cycle.[8]

In this respect, regulation of p53 conformation and function may represent a crucial feature of this puzzling scenario.

p53 is a tumor suppressor protein primarily involved in cancer biology. However, recent observations have showed that p53 may also play a central role in aging and in neurodegenerative disorders.[9] Conformational changes and functional alterations of p53 have been found in patients with AD.[10] Unfolded p53 is not able to exert its pro-apoptotic activity in AD cells, leading to aberrant cell cycle progression,[11] and to the accumulation of aging-associated abnormalities. p53 is an intrinsically unstable protein, whose conformation and DNA binding domain can be modulated by metal chelators and redox status.[12] In particular, an alteration in oxidative homeostasis, resulting in a subtoxic and chronic ROS exposure, impairs wild-type p53 tertiary structure, inducing a switch toward the not functional unfolded form of p53.[13] The alteration of the physiological functions of p53 can also result from the exposure to soluble non toxic Aβ, and has been shown to be related to the ability of Aβ to interfere with two key proteins, i.e. zyxin and the homeodomain-interacting protein kinase 2 (HIPK2).[14] Zyxin is an adaptor protein identified as a regulator of HIPK2-p53 signaling in response to DNA damage.[15] HIPK2 activity is in turn fundamental in maintaining wild-type p53 function, controlling the destiny of cells when exposed to DNA damaging agents.

In particular, soluble Aβ peptides downregulate zyxin expression, which is fundamental in maintaining HIPK2 stability and in turn p53 activity.[14b] This Aβ-mediated downregulation may be responsible for early pathological changes that precede the amyloidogenic pathway in the neurodegenerative cascade. Therefore, the induction of the unfolded state of p53, by leading to the accumulation of dysfunctional neurons in the CNS, is emerging as a novel amyloid-based mechanism of AD pathogenesis.

As a part of our ongoing work aimed at deepening insight the cross-talk between Aβ functions and oxidative stress in AD, we envisioned

nature as a structural "muse". Natural products offer a great chemical diversity,[16] and have already proven to be a rich source of therapeutics. Polyphenols are widely diffused in nature. They have been shown to modulate several AD pathways, including oxidative injuries and Aβ aggregation.[17] Interestingly, many of them present a hydroxy-cinnamoyl function as a recurring motif. On the other hand, diallyl sulfides are garlic-derived organosulfur compounds carrying allyl mercaptan moieties. They counteract oxidative stress through antioxidant enzyme expression.[18] Herein, we combined these privileged molecular fragments in new chemical entities, affording hybrids **1-3** (Figure 1).

Synthesized compounds were first tested *in vitro* to assess their antiaggregating properties towards Aβ$_{42}$, the most amylodogenic isoform of Aβ. They were then assayed in neuroblastoma cells to explore their ability to counteract oxidative stress and to exert neuroprotective effect against Aβ$_{42}$-induced toxicity.
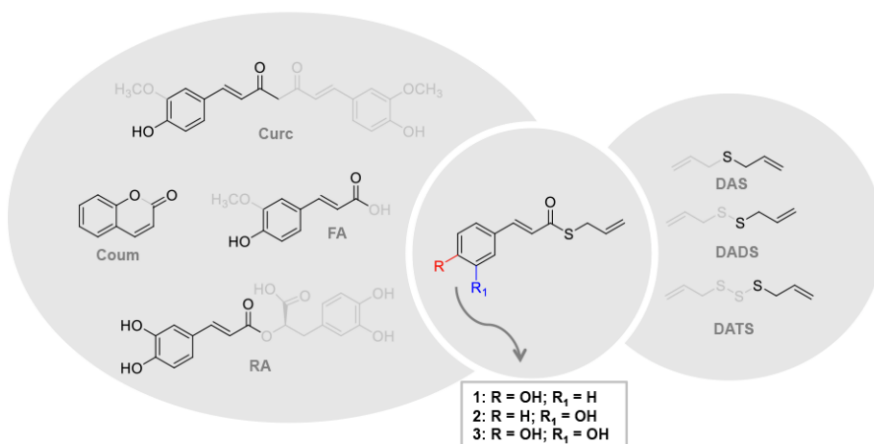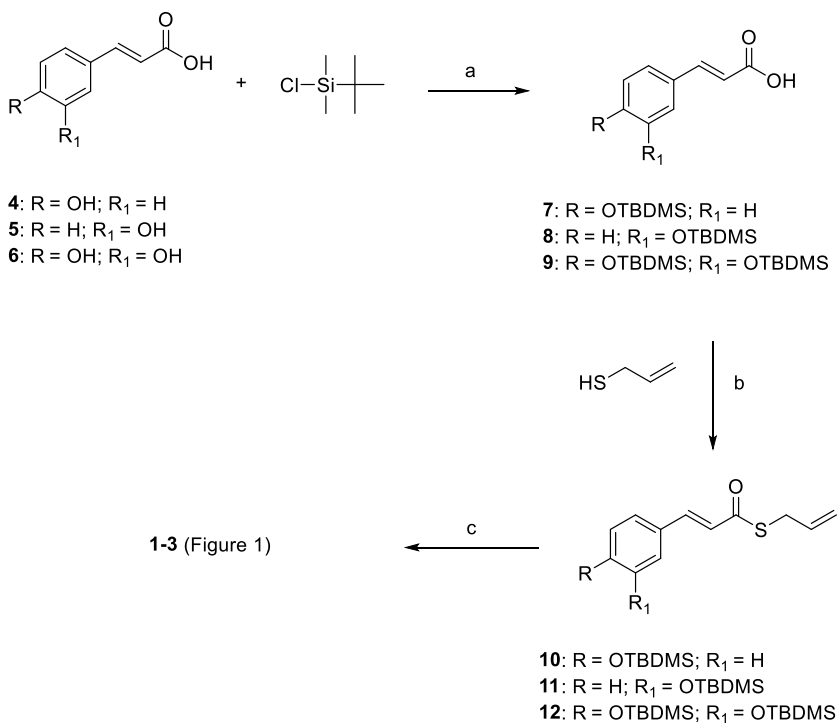

Figure 1. Design strategy for compounds 1-3. Left side: Curc (curcumin), Coum (coumarin), FA (ferulic acid), RA (rosmarinic acid). Right side: DAS (diallyl sulfide), DADS (diallyl disulfide), DATS (diallyl trisulfide).

The efficacy of **1-3** in modulating Aβ-induced conformational state alteration of p53 protein was also investigated. Curcumin was herein the reference compound. Based on its pleiotropic nature, curcumin is a consolidated prototype for AD studies, and it has already provided an outstanding platform for numerous biologically active ligands.[19]

Results and Discussion

Synthetic chemistry. Syntheses of **1**-**3** were carried out in a linear fashion as depicted in Scheme 1. *tert*-Butyldimethylsilyl (TBDMS)-protection of the alcohol followed by coupling reaction with DCC in presence of DMAP gave the intermediates **10-12**. Finally, treatment of **10-12** with tetrabutylammonium fluoride (TBAF) effected desilylation to give the final compounds **1-3**.

4: R = OH; R$_1$ = H
5: R = H; R$_1$ = OH
6: R = OH; R$_1$ = OH

7: R = OTBDMS; R$_1$ = H
8: R = H; R$_1$ = OTBDMS
9: R = OTBDMS; R$_1$ = OTBDMS

1-3 (Figure 1)

10: R = OTBDMS; R$_1$ = H
11: R = H; R$_1$ = OTBDMS
12: R = OTBDMS; R$_1$ = OTBDMS

Scheme 1. **Reaction conditions.** (a) DMF, imidazole, N$_2$, o/n, rt; (b) DCC, DMAP, CH$_2$Cl$_2$, N$_2$, o/n, 0°C-rt; (c) TBAF, THF, N$_2$, 30', room temperature.

Synthesized molecules have been characterized by NMR spectroscopy and ESI mass spectrometry. ^{1}HNMR spectra show that all compounds have an *E* configuration as indicated by the large spin coupling constants (around 16 Hz) of α-H and β-H on double bonds.

Inhibition of Aβ$_{42}$ self-aggregation (ThT-based assay). We have fostered the development of nature-inspired multifunctional ligands as an attractive opportunity to gain insight the cross-talk between oxidative damage and Aβ pathways. Therefore, synthesized compounds were first tested to evaluate their possible anti-aggregating properties by means of a thioflavin T (ThT)-based fluorimetric assay. ThT dye shows a characteristic red shift in the excitation/emission spectrum and an increase in the quantum yield upon binding to fibrillar β-sheet structures.[20] The ThT-based assay is commonly used to monitor Aβ fibrillization and its inhibition.

The evaluation of **1-3** clearly highlights a strong influence of the aryl decoration on the ability to prevent the Aβ$_{42}$ self-assembly process. Interestingly, the catechol moiety (compound **3**) turned out to be essential for activity. **3**, at 1/1 ratio with Aβ$_{42}$ almost completely inhibited Aβ$_{42}$ self-aggregation (% inhibition > 90%), resulting even more effective than curcumin (% inhibition = 73.7%). Noteworthy, in the same experimental conditions, a complete loss of the anti-aggregating efficacy was observed for **1** and **2**, lacking the *m-* or *p-* hydroxyl function, respectively (Figure 2).
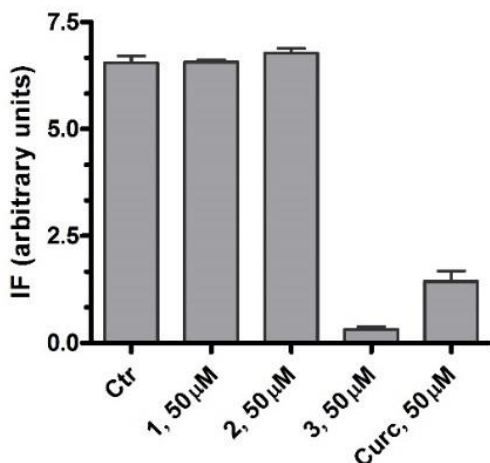
Figure 2. Inhibition Aβ₄₂ aggregation by 1-3 or curcumin (Curc) as determined by a ThT-based assay. ThT-related fluorescence intensity of Aβ₄₂ (50 μM) samples after a 24h-incubation period in the absence (Crtl) or in the presence of the tested compound (50 μM). The values are the mean of two independent measurements each performed in duplicate.

This striking result points to the catechol moiety as a key recognition fragment in amyloid binding. The inhibitory effect exerted by **3** resulted to be concentration-dependent, giving an IC_{50} value of 12.5 ± 0.9 μM. Based on this value, **3** can be considered a good inhibitor of Aβ₄₂ self-aggregation, owning an inhibitory potency similar to the well known multipotent compound bis(7)tacrine (IC_{50} = 8.4 ± 1.4 μM)[21] and derivative D737 (IC_{50} ~ 10 μM),[22] and being only five times less potent than the flavonoid myricetin (2.60 ± 0.33 μM).[23]
To explore the possibility of tuning the anti-aggregating profile of **3**, a detailed structure-activity relationship study is in progress and will be published in due course.

Inhibition of Aβ₄₂ self-aggregation (MS assay). Motivated by the promising results, we sought to gain a deeper understanding of **3**'s mode of action at a molecular level using an orthogonal method, i.e., electrospray ionization-ion trap-mass spectrometry (ESI-IT-MS) in

flow injection mode, which allows to detect and quantitate the monomeric form of Aβ$_{42}$.[23] Amyloid aggregation was monitored by evaluating the Aβ monomer decrease after 24h incubation in the presence and absence of the tested inhibitor, using reserpine as internal standard (IS). In the used experimental conditions, in the absence of any inhibitor, a progressive decrease in the monomer content, expressed as the sum of the native (Aβ$_{42}$ Native) and oxidized form (Aβ$_{42}$ Ox) of Aβ$_{42}$, is observed within 24h, due to inclusion of Aβ monomers into growing stable oligomers.[24] In agreement with this trend, when Aβ$_{42}$ was incubated alone, a dramatic decrease (83%) in monomer content was observed after 24h incubation (Figure 3). Conversely, when treating Aβ$_{42}$ with **3** in a peptide/inhibitor ratio of 1/1, after 24h incubation a high monomer content was detected, meaning that **3** strongly inhibited monomer inclusion into growing amyloid oligomers (Figure 3).
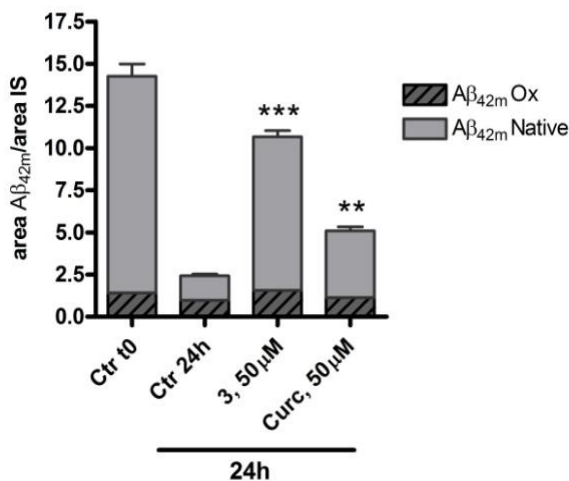

Figure 3. Inhibition of Aβ$_{42}$ aggregation by 3 and curcumin (Curc) as determined by ESI-IT-MS method. The total Aβ$_{42}$ monomer (Aβ$_{42m}$) content in the absence (Ctrl) and in the presence of inhibitor is displayed as the sum of the native (Aβ$_{42}$ Native) and oxidized form (Aβ$_{42}$ Ox) of Aβ$_{42}$. IS stands for internal standard (reserpine). ** $p < 0.01$, *** $p < 0.001$ versus Crtl 24h; Dunnett's Multiple Comparison Test.

Indeed, the residual percentage of $A\beta_{42}$ monomer at 24h was only 17 % in the absence of any inhibitor and 78 %, in the presence of **3**. Curcumin, tested in the same conditions, resulted to be a much weaker inhibitor of the early phase $A\beta_{42}$ aggregation (residual percentage of monomer after 24h incubation = 36 %). These results, other than confirming the antiaggregating activity resulting from the ThT-based assay, also showed that **3** was able to strongly retard the $A\beta$ overall assembly process by acting at monomer level in the early stage of the amyloid aggregation and strongly preventing the formation of stable soluble oligomers. This is of utmost importance because of the cytotoxic effects exerted by soluble aggregation intermediates.[25]

The overall inhibition percentage was $74.5 \pm 6.5\%$, in agreement with data obtained with the ThT fluorometric assay. On the other hand, curcumin showed a % inhibition of $22 \pm 7.6\%$.

Previous studies performed on the natural polyphenol myricetin showed pro-oxidant properties toward $A\beta_{42}$ peptide.[24] These properties can be explained by the well-accepted attitude of polyphenols to act as either antioxidant or pro-oxidant agents.[26] The oxidized form of $A\beta_{42}$ ($A\beta_{42}$ Ox) was shown to be less prone to aggregate than the native one ($A\beta_{42}$ Native), thus accounting for a slower aggregation rate.[27] With these concepts in mind, we sought to verify whether **3**, bearing a catechol moiety, could partially exert its inhibitory activity through an oxidation-based mechanism. Based on the different molecular weight, both the native and oxidized forms of $A\beta_{42}$ can be detected by MS analysis. Worth mentioning, a small percentage of $A\beta_{42}$ Ox is always present in $A\beta_{42}$ commercial samples (around 15%, detectable at t0), and, in agreement with the $A\beta_{42}$ Ox lower inclination to aggregate, the initial content of the oxidized $A\beta$ species just slightly decreases after 24h incubation (Figure 3).[24]

When treating $A\beta_{42}$ samples with **3** in a peptide/inhibitor ratio of 1/1, only a slightly increase of the oxidized species at 24h with respect to the initial content was observed, thus excluding a significant oxidation-mediated mode of inhibition (Figure 3).

Hence, based on these results, a stabilization of the Aβ$_{42}$ monomeric form and inhibition of its inclusion onto the growing oligomers, which greatly retards the overall Aβ assembly process, can be rather postulated.

Protective effect of 3 on Aβ$_{42}$-induced toxicity in SH-SY5Y neuroblastoma cells. To determine whether **3** may exert any neuroprotective effect against Aβ$_{42}$-induced toxicity, a cell viability study in SH-SY5Y human neuroblastoma cells was performed using the MTT assay. Incubation of SH-SY5Y cells with 10 μM Aβ$_{42}$ resulted in a reduction of about 25% of cell viability, which can be ascribed to oligomeric species formation.[28] Non toxic concentrations of **3** and curcumin (5 and 10 μM) were then co-incubated with Aβ$_{42}$. The results depicted in Figure 4 clearly show that **3** is able to exert a dose-dependent protective effect. Indeed, while at 5 μM **3** could not prevent Aβ$_{42}$ cytotoxicity, a strong protective effect was observed when **3** was used at 10 μM. At this concentration, **3** almost completely prevented the Aβ-induced cell death. In the same assay, curcumin was not able to counteract Aβ toxicity even at 10 μM concentration.
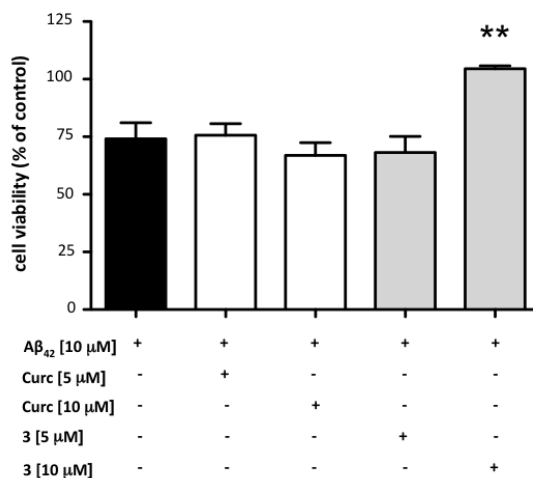
Figure 4. Effect of curcumin (Curc) and compound 3 on Aβ$_{42}$ mediated cytotoxicity in neuroblastoma cells. SH-SY5Y cells were treated for 24 h with curcumin or **3** at 5 μM or 10 μM, and co-incubated with 10 μM Aβ$_{42}$. Cell viability was determined by MTT assay. Data are expressed as % of cell viability versus control. ** $p < 0.01$ versus Aβ$_{42}$; Dunnett's Multiple Comparison Test.

Antioxidant effect on H$_2$O$_2$-induced damage. To determine the potential interest of thioesters **1-3** as antioxidants, we investigated their protective effects against H$_2$O$_2$-induced oxidative damage. ROS scavenging effect was evaluated in neuroblastoma cells by using the fluorescent probe dichlorofluorescin diacetate (DCF-DA) as a specific marker for quantitative intracellular ROS formation. In comparison to untreated neuroblastoma cells (dashed line, Figure 5), the intracellular DCF-fluorescence intensity in H$_2$O$_2$-treated cells significantly increased (grey line, Figure 5). Treatment with curcumin and compounds **1**-**3** significantly suppressed H$_2$O$_2$-induced intracellular ROS production (Figure 5), with **2** being strongly more effective in counteracting ROS formation.
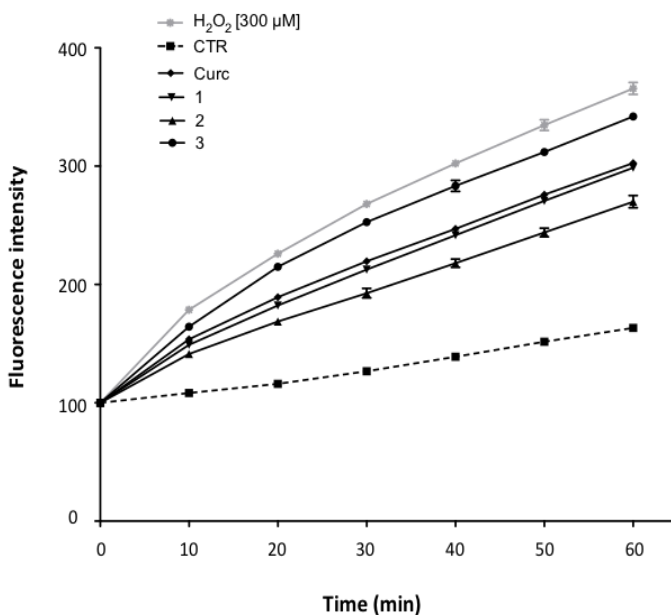
Figure 5. **Compounds 1-3 reverse ROS formation-induced oxidative stress.** Cells were pretreated with curcumin and compounds **1-3** (5 μM) for 24 h and then loaded with 25 μM DCF-DA for 45 min. DCF-DA was removed and cells were then exposed to 300 μM H_2O_2. Intracellular ROS levels were determined based on DCF-fluorescence by fluorescent microplate. Graph shows the intracellular fluorescence intensity of DCF $\pm$ SD in different times treatments. Fluorescence intensity for curcumin and compounds **1-3** at any time is significant with a $p < 0.001$ versus H_2O_2; Dunnett's Multiple Comparison Test.

Effect on zyxin-HIPK2-p53 signaling pathway. The pro-oxidant environment induced by Aβ is well established in AD pathology, and a correlation between Aβ, oxidative stress and p53 conformational changes has already been suggested.[13, 29]

In this context, in our experimental setting we based on data from literature indicating that sublethal concentration of Aβ modulate oxidative stress by inducing high levels of oxidative markers, such as 4-hydroxy-2-nonenal Michael-adducts and 3-nitro-tyrosine, and altered p53 conformation, mainly due to nitration of its tyrosine residues.[30]

However, it is worth to note that Aβ may also act as an antioxidant under specific conditions and this ability seems to be dependent on the peptide concentration.[31]

The mechanisms by which Aβ induces zyxin and HIPK2 deregulation and the consequent p53 conformational change may therefore be related to the capability of the peptide to alter oxidative homeostasis. If this is the case, compounds with antioxidant activity should reduce Aβ-mediated p53 conformational change.

To substantiate this hypothesis, compounds **1-3** were further investigated in a neuroblastoma cell line to verify whether they may affect the alterations in zyxin-HIPK2-p53 pathway mediated by soluble sublethal Aβ concentrations. For these experimental setting, we have diluted Aβ in dimethyl sulfoxide, since evidence from literature indicates that Aβ peptides, when diluted from this solvent, are quite stable and less prone to fibrilization, at near physiologic concentrations.[32]

We first characterized SH-SY5Y neuroblastoma cells in term of HIPK2 and zyxin expression and p53 conformational status. In agreement with our previous data,[14b] a sublethal concentration of Aβ_{42} (10 nM) significantly reduced HIPK2 and zyxin protein levels (Figure 6a).

The conformational status of p53 was analyzed by immunoprecipitation using two conformation-specific antibodies, i.e., PAb1620 and PAb240, which discriminate folded versus unfolded p53 tertiary structure, respectively.[33] As previously verified with other cell lines, also in neuroblastoma cells Aβ_{42} induced the expression of unfolded p53, as recognized by PAb240 antibody (Figure 6b).

On this basis, neuroblastoma cells were then treated with 10 nM Aβ_{42} in the presence or absence of compounds **1-3** at the concentration of 5 μM. When compounds **1-3** were added to the Aβ-pretreated cells, the level of unfolded p53 was significantly lowered as shown by a lower intensity of the PAb240 positive band in comparison with that obtained when cells were treated with Aβ_{42} alone. The ratio between the intensity of the bands immunoreactive to PAb240 and PAb1620, respectively, was comparable to that observed with control cells (Figure 6c), with **2** being significantly more effective.

These data show that pre-treatment of neuroblastoma cells, in particular with compound **2**, for which marked antioxidant properties are not accompanied by any antiaggregating activity, prevented Aβ-induced p53 conformational changes. This finding may support an involvement of the oxidative stress in Aβ function.
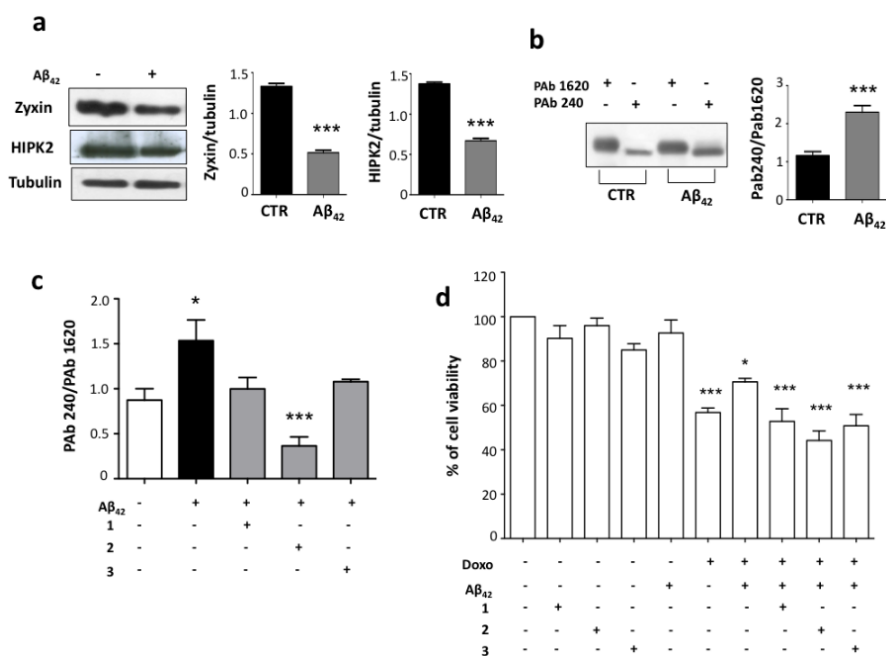
Figure 6. Compounds 1-3 positively modulate the alterations in zyxin-HIPK2-p53 pathway mediated by soluble sublethal Aβ42. (a) Total cell extracts of SH-SY5Y cells, treated with 10 nM Aβ42 for 48 h, were analyzed for zyxin and HIPK2 expression. Anti-tubulin was used as protein loading control. (b) SH-SY5Y cell lysates were immunoprecipitated with PAb240 or PAb1620 antibody. Immunoprecipitates were analyzed by western blot with the CM1 polyclonal anti-p53 antibody. (c) Total cell extracts of SH-SY5Y cells, incubated for 48 h with 10 nM Aβ42 and then treated with 5 μM compounds 1-3 for 24 hours, were analyzed for p53 conformational state. Cell lysates were immunoprecipitated with PAb240 or PAb1620 antibody. Immunoprecipitates were analyzed by western blot with the CM1 polyclonal anti-p53 antibody. After densitometric analysis, data were expressed as integrated density of ratio PAb240/PAb1620 antibodies signal and represent means ± SEM of at least three different experiments. * p < 0.05, *** p < 0.001 vs Aβ treatment; Tukey's Multiple Comparison test. (d) SH-SY5Y cells were incubated with 10 nM Aβ42 for 24 h and then treated for additional 24 h with 5 μM compounds 1-3. Cells were then resuspended in fresh medium and finally exposed to 0.5 μM doxorubicin for 24 h. Cell viability was determined by MTT assay. Data were expressed as % of cell viability versus control. * p < 0.05, *** p < 0.001 versus control; Bonferroni Multiple Comparison test.

Loss of the p53 wild-type conformation and function induced by soluble non toxic Aβ has been shown to contribute to the accumulation of cell damage, making cells not able to activate the proper apoptotic program when exposed to *noxae*.[11a, 14a, 14b] In light of this evidence, we sought to study cell sensitivity to doxorubicin, a genotoxic agent able to induce apoptosis in a p53-dependent manner,[34] following treatment with 10 nM $A\beta_{42}$ in the presence or absence of 5 μM **1-3**. Notably, cells treated with **1-3** and $A\beta_{42}$ showed to be more vulnerable to doxorubicin in comparison with cells treated with $A\beta_{42}$ alone. Doxorubicin induced a reduction of about 30% of cell viability in Aβ-treated cells, while the reduction of cell viability was about 50% in the presence of $A\beta_{42}$ and of each tested compound (Figure 6d). The obtained results indicate that compounds **1-3** may prevent the production of the unfolded isoform of p53 induced by Aβ, making the cells more sensitive and able to respond to an insult.

Conclusions

The amyloidogenic pathway is thought to be crucial to the complex nature of AD. However, Aβ-centric drug programs have had limited success in AD clinical trials, so far. Yet growing evidence suggests that merely hitting Aβ production or aggregation will not be enough to undermine AD architecture, calling for a deeper understanding of Aβ functions. To this aim, we here synthesized nature-inspired compounds **1-3** to investigate the connection between Aβ and oxidative stress, with p53 emerging as a possible mediator of this functional interplay.

Interestingly, the hydroxyl substituents on the aromatic moiety allowed a strategic tuning of compound's pharmacological profile. Notably, out of the three synthesized derivatives, only catechol **3** inhibited Aβ fibrils formation, underling the importance of the catechol moiety. By acting at the early stage of amyloid aggregation, **3** strongly prevented the formation of cytotoxic stable oligomeric intermediates. Conversely, although to a different extent, all hybrids

were able to decrease ROS formation and inhibit Aβ-induced p53 conformational changes, with the stronger antioxidant **2**, which lacks antiaggregating properties, being significantly more effective. These findings suggest the involvement of radical species in the loss of p53 conformation and function induced by subtoxic Aβ. Most importantly, the multifunctional ligand **3**, together with compounds **1** and **2**, in which only the antiaggregating activity was switched off, emerge as promising pharmacologic instruments to deepen insight the molecular mechanisms potentially involved in chronic Aβ injuries.

Experimental Section

Chemistry. *General Chemical methods.* Chemical reagents were purchased from Sigma Aldrich, Fluka and Lancaster (Italy). The course of the reactions was observed by thin layer chromatography (TLC) on 0.20 mm silica gel 60 F254 plates (Merck, Germany), then visualized with an UV lamp. Nuclear magnetic resonance spectra (NMR) were recorded at 400 MHz for ^{1}H and 100 MHz for ^{13}C on Varian VXR 400 spectrometer. Chemical shifts are reported in parts per millions (ppm) relative to tetramethylsilane (TMS), and spin multiplicities are given as s (singlet), br s (broad singlet), d (doublet), t (triplet), q (quartet), or m (multiplet). Direct infusion ESI-MS mass spectra were recorded on a Waters ZQ 4000 apparatus. All final compounds **1−3** are >95% pure by HPLC analyses. The analyses were performed under reversed-phase conditions on a Phenomenex Jupiter C18 (150x4,6 mm I.D.) column, using a binary mixture (A/B) of H$_2$O/acetonitrile (60/40, v/v) as the mobile phase, UV detection at λ = 302 nm and a flow rate of 0.7 mL/min. The liquid chromatograph was by Jasco Corporation (Tokyo, Japan), model PU-1585 UV equipped with a 20 µL loop valve.

General procedure for the intermediates 7-9. To a solution of the appropriate *trans*-cinnamic acid **4-6** (1 equiv) in dry DMF (5 mL) were added TBDMS-Cl (2-3 equiv) and imidazole (5 equiv) under

nitrogen atmosphere. After leaving the reaction at room temperature overnight, the mixture was concentrated to dryness, and the residue purified by column chromatography on silica gel to yield the desired intermediates **7-9.** Compounds **4-6** were even commercially available or synthesized as described in literature for the synthesis of *trans*-cinnamic acid trough Knoevenagel-Doebner reaction.[35]

(*E*)-3-(4-((*tert*-butyldimethylsilyl)oxy)phenyl)acrylic acid (7). Compound **7** was synthesized from **4** (500 mg, 3.04 mmol). Elution with petroleum ether/ethyl acetate (6:4) afforded **7** as a waxy solid: 466 mg (55%); ^{1}H NMR (400 MHz, CDCl$_3$) δ 7.71 (d, *J* = 16.0 Hz, 1H), 7.45 (d, *J* = 8.0 Hz, 2H), 6.85 (d, *J* = 8.0 Hz, 2H), 6.31 (d, *J* = 16.0 Hz, 1H), 0.99 (s, 9H), 0.23 (s, 6H).

(*E*)-3-(3-((*tert*-butyldimethylsilyl)oxy)phenyl)acrylic acid (8). Compound **8** was synthesized from **5** (500 mg, 3.04 mmol). Elution with petroleum ether/ethyl acetate (7:3) afforded **8** as a waxy solid: 370 mg (44%); ^{1}H NMR (400 MHz, CDCl$_3$) δ 7.72 (d, *J* = 16.0 Hz, 1H), 7.24 (t, *J* = 8.0 Hz, 1H), 7.13 (d, *J* = 8.0 Hz, 1H), 7.00 (s, 1H), 6.87 (d, *J* = 8.0 Hz, 1H), 6.40 (d, *J* = 16.0 Hz, 1H), 0.98 (s, 9H), 0.20 (s, 6H).

(*E*)-3-(3,4-bis((*tert*-butyldimethylsilyl)oxy)phenyl)acrylic acid (9). Compound **9** was synthesized from commercially available **6** (500 mg, 2.78 mmol). Elution with petroleum ether/ethyl acetate (8:2) afforded **9** as a waxy solid: 318 mg (28%); ^{1}H NMR (400 MHz, CDCl$_3$) δ 7.64 (d, *J* = 16.0 Hz, 1H), 7.02 (d, *J* = 8.0 Hz, 1H), 7.01 (s, 1H), 6.82 (d, *J* = 8.0 Hz, 1H), 6.22 (d, *J* = 16.0 Hz, 1H), 0.96 (s, 18H), 0.19 (s, 12H).

General procedure for the intermediates 10-12. To an ice-cooled solution of the appropriate acid (**7-9**) (1 equiv) in dry CH$_2$Cl$_2$ (4 mL) was added DCC (1.1 equiv), and DMAP (cat.). The reaction mixture was stirred for 10 min, followed by addition of 2-propene-1-thiol (3 equiv). Stirring was then continued at room temperature overnight,

and the reaction worked up by filtration and evaporation. The crude was purified by chromatography on silica gel.

S-allyl (E)-3-(4-((tert-butyldimethylsilyl)oxy)phenyl)prop-2-enethioate (10). Compound **10** was synthesized from **7** (160 mg, 0.575 mmol). Elution with petroleum ether/ethyl acetate (9.8:0.2) afforded **10** as a waxy solid: 100 mg (52%); ^{1}H NMR (400 MHz, CDCl$_3$) δ 7.57 (d, J = 15.6 Hz, 1H), 7.43 (d, J = 8.0 Hz, 2H), 6.84 (d, J = 8.0 Hz, 2H), 6.59 (d, J = 15.6 Hz, 1H), 5.88-5.83 (m, 1H), 5.28 (d, J = 17.0 Hz, 1H), 5.13 (d, J = 10.0 Hz, 1H), 3.66 (d, J = 6.8, 2H), 0.98 (s, 9H), 0.22 (s, 6H).

S-allyl (E)-3-(3-((tert-butyldimethylsilyl)oxy)phenyl)prop-2-enethioate (11). Compound **11** was synthesized from **8** (370 mg, 1.33 mmol). Elution with petroleum ether/ethyl acetate (9.8:0.2) afforded **11** as a waxy solid: 260 mg (58%); ^{1}H NMR (400 MHz, CDCl$_3$) δ 7.57 (d, J = 15.6 Hz, 1H), 7.15 (t, J = 8 Hz, 1H), 7.13 (s, 1H), 6.88 (d, J = 8.0 Hz, 1H), 6.70 (d, J = 8.0 Hz, 1H), 6.66 (d, J = 16.0 Hz, 1H), 5.88-5.83 (m, 1H), 5.28 (d, J = 16.0 Hz, 1H), 5.13 (d, J = 10.0 Hz 1H), 3.66 (d, J = 6.4 Hz, 2H), 0.97 (s, 9H), 0.20 (s, 6H).

S-allyl (E)-3-(3,4-bis((tert-butyldimethylsilyl)oxy)phenyl)prop-2-enethioate (12). Compound **12** was synthesized from **9** (200 mg, 0.500 mmol). Elution with petroleum ether/ethyl acetate (9.5:0.5) afforded **12** as a waxy solid: 160 mg (70%); ^{1}H NMR (400 MHz, CDCl$_3$) δ 7.49 (d, J = 16 Hz, 1H), 7.00 (d, J = 8.0 Hz, 1H), 6.80 (d, J = 8.0 Hz, 1H), 6.72 (s, 1H), 6.50 (d, J = 16.0 Hz, 1H), 5.76-5.65 (m, 1H), 5.25 (d, J = 16.8 Hz, 1H), 5.09 (d, J = 10.1 Hz, 1H), 3.56 (d, J = 6.8 Hz, 2H), 0.97 (s, 9H), 0.96 (s, 9H), 0.19 (s, 6H), 0.18 (s, 6H).

General procedure for the synthesis of 1-3. To a solution of the appropriate organosilane intermediate **10-12** (1 equiv) in THF (5 mL) was added TBAF (4 equiv) and stirring was continued at room temperature. After 20-30 min, the reaction was quenched by addition of saturated aqueous NH$_4$Cl solution; the aqueous phase was extracted with EtOAc (3 x 10 mL), and the combined organic layers were dried

over Na$_2$SO$_4$. Following evaporation of the solvent, the residue was purified by column chromatography on silica gel.

S-allyl (*E*)-3-(4-hydroxyphenyl)prop-2-enethioate (1). Compound **1** was synthesized from **10** (100 mg, 0.299 mmol). Elution with petroleum ether/ethyl acetate (7:3) afforded **1** as a waxy solid: 30 mg (46%); ^{1}H NMR (400 MHz, CDCl$_3$) δ 7.56 (d, *J* = 16.0 Hz, 1H), 7.42 (d, *J* = 8.0 Hz, 2H), 6.84 (d, *J* = 8.0 Hz, 2H), 6.58 (d, *J* = 16.0 Hz, 1H), 5.88-5.81 (m, 1H), 5.29-5.25 (d, *J* = 17.0 Hz, 1H), 5.13-5.10 (d, *J* = 10.0 Hz, 1H), 3.65 (d, *J* =8.0 Hz, 2H). ^{13}C-NMR (CDCl$_3$, 100 MHz) δ 189.97, 158.23, 140.83, 133.05, 130.44, 126.66, 122.29, 118.02, 116.03, 31.80. MS [ESI$^+$] *m/z* 243 [M+Na]$^+$.

S-allyl (*E*)-3-(3-hydroxyphenyl)prop-2-enethioate (2). Compound **2** was synthesized from **11** (210 mg, 0.63 mmol). Elution with CH$_2$Cl$_2$/MeOH (9.7:0.3) afforded **2** as a waxy solid: 110 mg (79%); ^{1}H NMR (400 MHz, CDCl$_3$) δ 7.54 (d, *J* = 16.0 Hz, 1H), 7.24 (t, *J* = 8.0 Hz, 1H), 7.08 (d, *J* = 8.0 Hz, 1H), 7.02 (s, 1H), 6.90 (d, *J* = 8.0 Hz, 1H), 6.58 (d, *J* = 16.0 Hz, 1H), 6.09 (br s, 1H), 5.88-5.81 (m, 1H), 5.28 (d, *J* = 16.0 Hz, 1H), 5.13 (d, *J* = 10 Hz, 1H), 3.65 (d, *J* = 6.4 Hz, 2H). ^{13}C-NMR (CDCl$_3$, 100 MHz) δ 190.33, 156.20, 140.85, 135.43, 132.75, 130.22, 124.89, 121.12, 118.31, 118.05, 114.91, 31.94. MS [ESI$^-$] *m/z* 219 [M-H]$^-$.

S-allyl (*E*)-3-(3,4-dihydroxyphenyl)prop-2-enethioate (3). Compound **3** was synthesized from **12** (160 mg, 0.344 mmol). Elution with petroleum ether/ethyl acetate (5:5) afforded **3** as a waxy solid: 50 mg (62%); ^{1}H NMR (400 MHz, CD$_3$OD) δ 7.54 (d, *J* = 16.0 Hz, 1H), 7.10 (s, 1H), 7.02 (d, *J* = 8.0 Hz, 1H), 6.84 (d, *J* = 8.0 Hz, 1H), 6.63 (d, *J* = 16.0 Hz, 1H), 5.94-5.87 (m, 1H), 5.31 (d, *J* = 16.8 Hz, 1H), 5.14 (d, *J* = 10.1 Hz, 1H), 3.68 (d, *J* = 6.4 Hz, 2H). ^{13}C-NMR (CD$_3$OD, 100 MHz) δ 189.34, 148.56, 145.47, 141.37, 133.43, 125.91, 122.14, 120.93, 116.56, 115.18, 113.93, 30.94. MS [ESI$^+$] *m/z* 259 [M+Na]$^+$.

Aβ₄₂ self-aggregation: sample preparation. 1,1,1,3,3,3-Hexafluoro-2-propanol (HFIP) pre-treated Aβ₄₂ samples (Bachem AG, Switzerland) were resolubilized with a $CH_3CN/Na_2CO_3/NaOH$ (48.4/48.4/3.2) mixture to have a stable stock solution ([Aβ₄₂] = 500 μM).[36] Tested inhibitors were dissolved in methanol and diluted in the assay buffer. Experiments were performed by incubating the peptide diluted in 10 mM phosphate buffer (pH = 8.0) containing 10 mM NaCl, at 30 °C (Thermomixer Comfort, Eppendorf, Italy) for 24 h (final Aβ concentration = 50 μM) with and without inhibitor.

Inhibition of Aβ₄₂ self-aggregation: ThT assay. Inhibition studies were performed by incubating Aβ₄₂ samples in the assay conditions reported above, with and without tested inhibitors. Inhibitors were first screened at 50 μM in a 1/1 ratio with Aβ₄₂. To quantify amyloid fibril formation, the ThT fluorescence method was used.[20b, 37] After incubation, samples were diluted to a final volume of 2.0 mL with 50 mM glycine-NaOH buffer (pH = 8.5) containing 1.5 μM ThT. A 300-seconds-time scan of fluorescence intensity was carried out (λ_{exc} = 446 nm; λ_{em} = 490 nm), and values at plateau were averaged after subtracting the background fluorescence of 1.5 μM ThT solution. Blanks containing inhibitor and ThT were also prepared and evaluated to account for quenching and fluorescence properties. The fluorescence intensities were compared and the % inhibition was calculated. For compound **3**, the IC_{50} value was also determined. To this aim four increasing concentrations were tested. IC_{50} value was obtained from the % inhibition *vs* log[inhibitor] plot.

Inhibition of Aβ₄₂ self-aggregation by 3: Flow injection-ESI-MS method. Inhibition studies were performed by incubating Aβ₄₂ samples in the assay conditions reported above, with and without the tested inhibitor **3** or curcumin. At t0 and t24h, aliquots with and without inhibitor were analyzed by flow injection-ESI-IT-MS. LC-MS analyses were performed as described in Fiori *et al*.[24]

Briefly, the $A\beta_{42}$ samples were analyzed by 10-µL loop injection after previous addition of reserpine as internal standard. ESI-IT-MS analyses were performed on a Jasco PU-1585 Liquid Chromatograph (Jasco, Tokyo, Japan) interfaced with LCQ Duo Mass Spectrometer (Thermo Finnigan, San Jose, CA, USA) equipped with an electrospray ionization (ESI) source operating with an ion trap analyzer. The mobile phase consisted of 0.1% (v/v) formic acid in acetonitrile/water 30/70. ESI system employed a 4.5 kV spray voltage and a capillary temperature of 200°C. Mass spectra were operated in positive polarity, in the scan range of 200-2000 m/z and at the scan rate of 3 microscans/sec. Single ion monitoring (SIM) chromatograms for the quantitative analysis were reconstructed at the base peaks corresponding to the differently charged amyloid monomer ions (Native, N) and oxidized ions (Ox). The ratio between the total monomer area and the IS area was used for $A\beta_{42}$ monomer determination. The $Area_{total\ monomer}/Area_{IS}$ ratio at t0 is considered as 100% of the monomer content. The results were expressed as means $\pm$ SD of three independent experiments and a p value < 0.05 was considered statistically significant (Dunnett's Multiple Comparison Test).

Reagents for cellular experiments. All culture media, supplements and Foetal Bovine Serum (FBS) were obtained from Euroclone (Life Science Division, Milan, Italy). Electrophoresis reagents were obtained from Bio-Rad (Hercules, CA, USA). All other reagents were of the highest grade available and were purchased from Sigma Chemical Co. (St. Louis, MO, USA) unless otherwise indicated. $A\beta_{42}$ was solubilised in dimethyl sulfoxide (DMSO) at the concentration of 100 µM and frozen in stock aliquots that were diluted at the final concentration of 10 nM prior to use. For each experimental setting, one aliquot of the stock was thawed out and diluted at the final concentration of 10 nM to minimize peptide damage due to repeated freeze and thaw. The $A\beta_{42}$ concentration was chosen following dose

response experiments (data not shown) where maximal modulation of p53 structure and its transcriptional activity[38] was obtained at 10 nM. All the experiments performed with $A\beta_{42}$ were made in 1% of serum. H_2O_2 was diluted to working concentration (1 mM) in phosphate buffer saline (PBS) at the moment of use. Mouse monoclonal anti α-tubulin was purchased from Sigma-Aldrich (St. Louis, MO, USA). Host specific peroxidase conjugated IgG secondary antibodies were obtained from Pierce (Rockford, IL, USA).

Cell cultures. Human neuroblastoma SH-SY5Y cells from European Collection of Cell Cultures (ECACC No. 94030304) were cultured in medium with equal amount of Eagle's minimum essential medium and Nutrient Mixture Ham's F-12, supplemented with 10% foetal bovine serum, glutamine (2mM), penicillin/streptomycin, non-essential aminoacids at 37 °C in 5%CO2/95% air.

Cell viability. The mitochondrial dehydrogenase activity that reduces 3-(4,5-dimethylthiazol-2-yl)-2,5-diphenyl-tetrazolium bromide (MTT, Sigma, St Louis, MO, USA) was used to determine cellular viability, in a quantitative colorimetric assay. At day 0 SH-SY5Y cells were plated at a density of $2x10^4$ viable cells per well in 96-well plates. After treatment, according to the experimental setting, cells were exposed to an MTT solution in PBS (1 mg/mL). Following 4 h incubation with MTT and treatment with SDS for 24 h, cell viability reduction was quantified by using a BIO-RAD microplate reader (Model 550; Hercules, CA, USA).

Measurement of intracellular ROS. DCF-DA (Sigma Aldrich) was used to estimate intracellular ROS. Briefly, cells (2×10^4 cells/well) were pretreated with reference curcumin and compounds **1-3** (5 μM) for 24 h and then loaded with 25 μM DCF-DA at 37°C for 45 min. DCF-DA was removed after centrifuge and cells were resuspended in PBS and then exposed to 300 μM H_2O_2. The results were visualized

using Synergy HT microplate reader (BioTek) with excitation and emission wavelengths of 485 nm and 530 nm, respectively.

Immunodetection of zyxin and HIPK2. Cell monolayers were washed twice with ice cold PBS, lysed on the tissue culture dish by addition of ice-cold lysis buffer (50 mM Tris/HCl pH 7.4, 150mM NaCl, 50 mM EDTA, 0.2 mM 4-(2-aminoethyl) benzenesulfonyl fluoride hydrochloride (AEBSF), 20 µg/ml leupeptin, 25 µg/ml aprotinin, 0,5 µg/ml pepstatin A and 1% Triton X-100) and an aliquot was used for protein analysis with the Pierce Bicinchoninic Acid kit, for protein quantification. Cell lysates were diluted in sample buffer (62.5 mM Tris/HCl pH 6.8, 2% SDS, 10% glycerol, 50 mM dithiothreitol, 0.1% Bromophenol blue) and subjected to Western blot analysis. Proteins were subjected to SDS-PAGE (8%) and then transferred onto PVDF membrane 0,45µm (Immobilion, Millipore Corp, Bedford, MA,USA). The membrane was blocked for 1 h with 5% non-fat dry milk in Tris-buffered saline containing 0.1% Tween 20 (TBST). Membranes were immunoblotted with the rabbit anti human zyxin or HIPK2 polyclonal antibody (at 1:1000 dilution in 5% non fat dry milk, from Cell Signaling Technology, EuroClone, Milan, Italy). The detection was carried out by incubation with horseradish peroxidase conjugated goat anti-rabbit IgG (1:5000 dilution in 5% non fat dry milk, from Pierce, Rockford,IL, USA) for 1 h. The blots were then washed extensively and the proteins of interest were visualized using an enhanced chemiluminescent method (Pierce, Rockford, IL, USA). Tubulin was also performed as a normal control of proteins.

p53 conformational immunoprecipitation. p53 conformational state was analyzed by immunoprecipitation as detailed previously.[10a] Briefly, cells were lysed in immunoprecipitation buffer (10 mM Tris, pH 7.6; 140 mM NaCl; and 0.5% NP40 including protease inhibitors); 100 µg of total cell extracts were used for immunoprecipitation

experiments performed in a volume of 500 µl with 1 µg of the conformation-specific antibodies PAb1620 (wild-type specific) or PAb240 (mutant specific) (Neomarkers, CA, USA). Immunocomplexes were separated by 10% SDS-PAGE and immunoblotting was performed with rabbit anti-p53 antibody (FL393) (Santa Cruz, CA, USA). Immunoreactivity was detected with the ECL-chemiluminescence reaction kit (Amersham, Little Chalfont, UK).

Densitometry and statistics. All the experiments, unless specified, were performed at least three times. Following acquisition of the Western blot image through an AGFA scanner and analysis by means of the Image 1.47 program (Wayne Rasband, NIH, Research Services Branch, NIMH, Bethesda, MD, USA), the relative densities of the bands were analyzed as described previously.[39] The data were analyzed by analysis of variance (ANOVA) followed when significant by an appropriate post hoc comparison test as indicated in figure legend. The reported data are expressed as means $\pm$ SD of at least three independent experiments. A p value < 0.05 was considered statistically significant.

References
1. D. J. Selkoe, Behav Brain Res 2008, 192, 106-113; b) J. Laurén, D. A. Gimbel, H. B. Nygaard, J. W. Gilbert, S. M. Strittmatter, Nature 2009, 457, 1128-1132.

2. E. Karran, M. Mercken, B. De Strooper, Nat Rev Drug Discov 2011, 10, 698-712; b) K. Herrup, Nat Neurosci 2015, 18, 794-799.

3. a) E. Mura, F. Pistoia, M. Sara, S. Sacco, A. Carolei, S. Govoni, Curr Pharm Des 2014, 20, 4121-4139; b) L. M. Ittner, J. Götz, Nat Rev Neurosci 2011, 12, 65-72; c) Z. Esposito, L. Belli, S. Toniolo, G. Sancesario, C. Bianconi, A. Martorana, CNS Neurosci Ther 2013, 19, 549-555.

4. a) E. Viayna, I. Sola, M. Bartolini, A. De Simone, C. Tapia-Rojas, F. G. Serrano, R. Sabaté, J. Juárez-Jiménez, B. Pérez, F. J. Luque, V. Andrisano, M. V. Clos, N. C. Inestrosa, D. Muñoz-Torrero, J Med Chem 2014, 57, 2549-2567; b) E. Nepovimova, E. Uliassi, J. Korabecny, L. E. Peña-Altamira, S. Samez, A. Pesaresi, G. E. Garcia, M. Bartolini, V. Andrisano, C. Bergamini, R. Fato, D. Lamba, M. Roberti, K. Kuca, B. Monti, M. L. Bolognesi, J Med Chem 2014, 57, 8576-8589; c) M. Rosini, E. Simoni, M. Bartolini, E. Soriano, J. Marco-Contelles, V. Andrisano, B. Monti, M. Windisch, B. Hutter-Paier, D. W. McClymont, I. R. Mellor, M. L. Bolognesi, ChemMedChem 2013, 8, 1276-1281; d) M. Rosini, V. Andrisano, M. Bartolini, M. L. Bolognesi, P. Hrelia, A. Minarini, A. Tarozzi, C. Melchiorre, J Med Chem 2005, 48, 360-363; e) M. Rosini, E. Simoni, M. Bartolini, A. Cavalli, L. Ceccarini, N. Pascu, D. W. McClymont, A. Tarozzi, M. L. Bolognesi, A. Minarini, V. Tumiatti, V. Andrisano, I. R. Mellor, C. Melchiorre, J Med Chem 2008, 51, 4381-4384.

5. a) A. Cavalli, M. L. Bolognesi, A. Minarini, M. Rosini, V. Tumiatti, M. Recanatini, C. Melchiorre, J Med Chem 2008, 51, 347-372; b) M. Rosini, Future Med Chem 2014, 6, 485-487; c) A. Anighoro, J. Bajorath, G. Rastelli, J Med Chem 2014, 57, 7874-7887.

6. M. Rosini, E. Simoni, A. Milelli, A. Minarini, C. Melchiorre, J Med Chem 2014, 57, 2821-2831.

7. M. Coma, F. X. Guix, G. Ill-Raga, I. Uribesalgo, F. Alameda, M. A. Valverde, F. J. Muñoz, Neurobiol Aging 2008, 29, 969-980.

8. A. M. Swomley, S. Förster, J. T. Keeney, J. Triplett, Z. Zhang, R. Sultana, D. A. Butterfield, Biochim Biophys Acta 2014, 1842, 1248-1257.

9. a) S. Salvioli, M. Capri, L. Bucci, C. Lanni, M. Racchi, D. Uberti, M. Memo, D. Mari, S. Govoni, C. Franceschi, Cancer Immunol Immunother 2009, 58, 1909-1917; b) W. Chatoo, M. Abdouh, G. Bernier, Antioxid Redox Signal 2011, 15, 1729-1737; c) A. Salminen, K. Kaarniranta, Cell Signal 2011, 23, 747-752.

10. a) D. Uberti, C. Lanni, T. Carsana, S. Francisconi, C. Missale, M. Racchi, S. Govoni, M. Memo, Neurobiol Aging 2006, 27, 1193-1201; b) C. Lanni, M. Racchi, G. Mazzini, A. Ranzenigo, R. Polotti, E. Sinforiani, L. Olivari, M. Barcikowska, M. Styczynska, J. Kuznicki, A. Szybinska, S. Govoni, M. Memo, D. Uberti, Mol Psychiatry 2008, 13, 641-647; c) X. Zhou, J. Jia, Neurosci Lett 2010, 468, 320-325.

11. a) D. Uberti, T. Carsana, E. Bernardi, L. Rodella, P. Grigolato, C. Lanni, M. Racchi, S. Govoni, M. Memo, J Cell Sci 2002, 115, 3131-3138; b) Y. Yang, D. S. Geldmacher, K. Herrup, J Neurosci 2001, 21, 2661-2668.

12. P. Hainaut, J. Milner, Cancer Res 1993, 53, 4469-4473.

13. C. Lanni, M. Racchi, M. Memo, S. Govoni, D. Uberti, Free Radic Biol Med 2012, 52, 1727-1733.

14. a) C. Lanni, L. Nardinocchi, R. Puca, S. Stanga, D. Uberti, M. Memo, S. Govoni, G. D'Orazi, M. Racchi, PLoS One 2010, 5, e10171; b) C. Lanni, D. Necchi, A. Pinto, E. Buoso, L. Buizza, M. Memo, D. Uberti, S. Govoni, M. Racchi, J Neurochem 2013, 125, 790-799; c) E. Mura, S. Zappettini, S. Preda, F.

Biundo, C. Lanni, M. Grilli, A. Cavallero, G. Olivero, A. Salamone, S. Govoni, M. Marchi, PLoS One 2012, 7, e29661.

15. J. Crone, C. Glas, K. Schultheiss, J. Moehlenbrink, E. Krieghoff-Henning, T. G. Hofmann, Cancer Res 2011, 71, 2350-2359.

16. S. Rizzo, H. Waldmann, Chem Rev 2014, 114, 4621-4639.

17. a) C. B. Pocernich, M. L. Lange, R. Sultana, D. A. Butterfield, Current Alzheimer research 2011, 8, 452-469; b) M. Stefani, S. Rigacci, Int J Mol Sci 2013, 14, 12411-12457.

18. S. Kim, H. G. Lee, S. A. Park, J. K. Kundu, Y. S. Keum, Y. N. Cha, H. K. Na, Y. J. Surh, PLoS One 2014, 9, e85984.

19. a) G. Gerenu, K. Liu, J. E. Chojnacki, J. M. Saathoff, P. Martinez-Martin, G. Perry, X. Zhu, H. G. Lee, S. Zhang, ACS Chem Neurosci 2015; b) E. Simoni, C. Bergamini, R. Fato, A. Tarozzi, S. Bains, R. Motterlini, A. Cavalli, M. L. Bolognesi, A. Minarini, P. Hrelia, G. Lenaz, M. Rosini, C. Melchiorre, J Med Chem 2010, 53, 7264-7268.

20. a) M. Groenning, L. Olsen, M. van de Weert, J. M. Flink, S. Frokjaer, F. S. Jørgensen, J Struct Biol 2007, 158, 358-369; b) H. Naiki, K. Higuchi, M. Hosokawa, T. Takeda, Anal Biochem 1989, 177, 244-249.

21. A. Minarini, A. Milelli, V. Tumiatti, M. Rosini, E. Simoni, M. L. Bolognesi, V. Andrisano, M. Bartolini, E. Motori, C. Angeloni, S. Hrelia, Neuropharmacology 2012, 62, 997-1003.

22. A. F. McKoy, J. Chen, T. Schupbach, M. H. Hecht, J Biol Chem 2012, 287, 38992-39000.

23. M. Bartolini, M. Naldi, J. Fiori, F. Valle, F. Biscarini, D. V. Nicolau, V. Andrisano, Anal Biochem 2011, 414, 215-225.

24. J. Fiori, M. Naldi, M. Bartolini, V. Andrisano, Electrophoresis 2012, 33, 3380-3386.

25. a) C. G. Glabe, R. Kayed, Neurology 2006, 66, S74-78; b) M. P. Lambert, A. K. Barlow, B. A. Chromy, C. Edwards, R. Freed, M. Liosatos, T. E. Morgan, I. Rozovsky, B. Trommer,

K. L. Viola, P. Wals, C. Zhang, C. E. Finch, G. A. Krafft, W. L. Klein, Proc Natl Acad Sci U S A 1998, 95, 6448-6453; c) D. M. Walsh, I. Klyubin, J. V. Fadeeva, W. K. Cullen, R. Anwyl, M. S. Wolfe, M. J. Rowan, D. J. Selkoe, Nature 2002, 416, 535-539.

26. S. C. Forester, J. D. Lambert, Mol Nutr Food Res 2011, 55, 844-854.

27. L. Hou, I. Kang, R. E. Marchant, M. G. Zagorski, J Biol Chem 2002, 277, 40173-40176.

28. S. Sabella, M. Quaglia, C. Lanni, M. Racchi, S. Govoni, G. Caccialanza, A. Calligaro, V. Bellotti, E. De Lorenzi, Electrophoresis 2004, 25, 3186-3194.

29. L. R. Borza, Rev Med Chir Soc Med Nat Iasi 2014, 118, 19-27.

30. a) L. Buizza, C. Prandelli, S. A. Bonini, A. Delbarba, G. Cenini, C. Lanni, E. Buoso, M. Racchi, S. Govoni, M. Memo, D. Uberti, Cell Death Dis 2013, 4, e484; b) L. Buizza, G. Cenini, C. Lanni, G. Ferrari-Toninelli, C. Prandelli, S. Govoni, E. Buoso, M. Racchi, M. Barcikowska, M. Styczynska, A. Szybinska, D. A. Butterfield, M. Memo, D. Uberti, PLoS One 2012, 7, e29789; c) G. Cenini, G. Maccarinelli, C. Lanni, S. A. Bonini, G. Ferrari-Toninelli, S. Govoni, M. Racchi, D. A. Butterfield, M. Memo, D. Uberti, Amino Acids 2010, 39, 271-283.

31. D. G. Smith, R. Cappai, K. J. Barnham, Biochim Biophys Acta 2007, 1768, 1976-1990.

32. H. LeVine, Anal Biochem 2004, 335, 81-90.

33. C. Méplan, M. J. Richard, P. Hainaut, Biochem Pharmacol 2000, 59, 25-33.

34. a) K. Hayakawa, M. Hasegawa, M. Kawashima, Y. Nakamura, M. Matsuura, H. Toda, N. Mitsuhashi, H. Niibe, Oncol Rep 2000, 7, 267-270; b) E. Lorenzo, C. Ruiz-Ruiz, A. J. Quesada, G. Hernández, A. Rodríguez, A. López-Rivas, J.

M. Redondo, J Biol Chem 2002, 277, 10883-10892; c) S. Wang, E. A. Konorev, S. Kotamraju, J. Joseph, S. Kalivendi, B. Kalyanaraman, J Biol Chem 2004, 279, 25535-25543.

35. C. N. Xia, H. B. Li, F. Liu, W. X. Hu, Bioorg Med Chem Lett 2008, 18, 6553-6557.

36. M. Bartolini, C. Bertucci, M. L. Bolognesi, A. Cavalli, C. Melchiorre, V. Andrisano, Chembiochem 2007, 8, 2152-2161.

37. H. LeVine, Protein Sci 1993, 2, 404-410.

38. D. Uberti, G. Cenini, L. Olivari, G. Ferrari-Toninelli, E. Porrello, C. Cecchi, A. Pensalfini, A. Pensafini, G. Liguri, S. Govoni, M. Racchi, M. Maurizio, J Neurochem 2007, 103, 322-333.

39. C. Lanni, M. Mazzucchelli, E. Porrello, S. Govoni, M. Racchi, Eur J Biochem 2004, 271, 3068-3075.

Part 2.

The following data were obtained thanks to the collaboration with the Laboratory of Pharmaceutical Analysis and are part of the PhD thesis of Federica Bisceglia, PhD candidate in Chemical and Pharmaceutical Sciences - XXX cycle.

Department of Drug Sciences (Section of Pharmaceutical Chemistry and Technology), University of Pavia, V.le Taramelli 14, 27100 Pavia, Italy.

Supervisor: prof. Ersilia De Lorenzi

Identification of beta-amyloid fibrillogenesis modulators as pharmacological tools in Alzheimer's disease

These preliminary data will be completed in the next months. Then we will work in synergy together to write the manuscript to submit for publication.

Introduction

The aggregation of amyloid beta (Aß) peptides into amyloid fibrils is one of the most important hallmarks of Alzheimer's disease (AD) and amyloid plaques are used as a diagnostic marker. Although the aetiology of AD is still incomplete, compelling evidences indicate that Aß aggregation plays a key role in the onset and progression of the disorder. Therefore, agents able to block or reverse the amyloid process could be an effective approach for treating AD [1]. A variety of anti-amyloid agents have been developed and, according to the amyloid cascade hypothesis, they target the process at different levels. There are different possible therapeutic strategies [2, 3], such as: to stop the production of Aß peptides by inhibiting enzymes involved in the amyloidogenic proteolitic cleavage of the amyloid precursor protein (APP); to enhance the catabolism of Aß peptides *via* an up-regulation of enzymes, such as neprylsin, which degrade Aß and decrease Aß levels in the brain; and to modulate the aggregation of Aß.

In a simplistic view, Aß monomers convert into insoluble fibrils, which constitute amyloid plaques. However, the aggregation of Aß peptides is extremely more complex: monomers interact to form different soluble oligomers involved in many toxic effects; in turn oligomers evolve in bigger aggregates up to insoluble fibrils throughout different and parallel pathways. Indeed, the modulation of the aggregation can focus on the inhibition of the oligomerization process, on the disaggregation of fibrils and of pre-formed aggregates. Another interesting approach is the design of agents which are able to redirect the on-pathway oligomerization that leads to toxic oligomers to the off-pathway process and, thus, to non toxic aggregates [4].

Considering the complexity of the aggregation process and the fact that soluble oligomers and insoluble fibrils represent distinct aggregation pathways, it is evident that a potential inhibitor, to be effective, should block both the oligomerization and the fibrillogenesis.
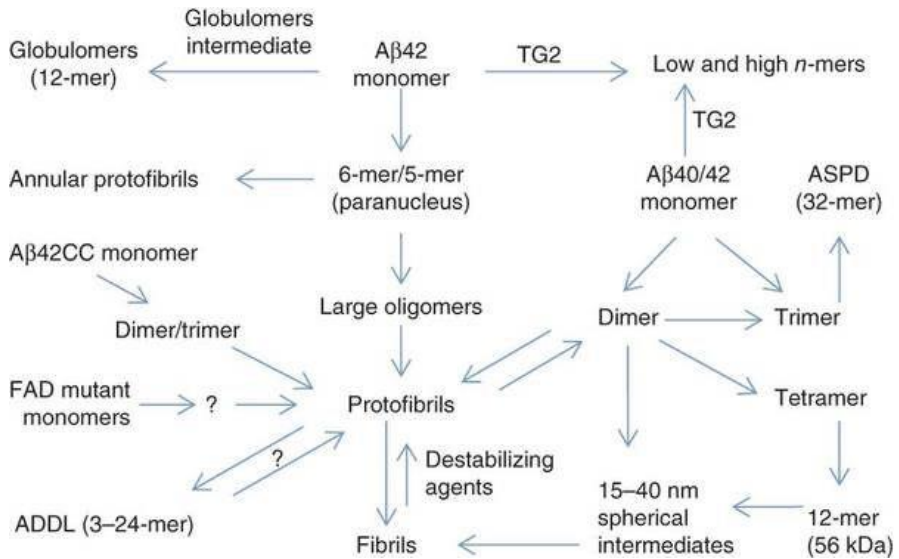
Scheme 1. Overview of Aβ assemblies described in literature [5]

The assays and techniques commonly employed in aggregation studies show limitations in providing simultaneous and comparable information on both fibrils and oligomers [2, 4]. This means that a potential inhibitor of the oligomerization may not be identified by using a specific assay for fibrils, such as thioflavin-T (ThT) fluorescence and, therefore, more than one technique has to be used. Even though the characterization of all Aß assemblies involved in the neurodegeneration is not exhaustive, it is crucial to understand on which particular oligomeric population an inhibitor acts. The transient and non covalent nature of Aß oligomers, the dynamic equilibrium among different populations, which keep on aggregating during the experiments, represent further important issues in the search for modulators of Aß aggregation. For *in vitro* aggregation studies, this results in the set up of reliable and standardized procedures for the preparation of Aß oligomers and for their characterization. This is mandatory for the evaluation of the effects of molecules on the amyloid process [4, 6].

All the disadvantages and limitations of techniques employed for the characterization of Aß aggregates are found also in this context. For example, mass spectrometry (MS) approaches are limited because of the ionization source induced disassembly and the low ionization ability of high molecular weight oligomers; consequently the effect of the inhibitor can be monitored only related to the amount of monomer. Spectroscopic techniques, such as circular dichroism (CD) and ThT fluorescence, provide average information about all species present in the sample [7].

Nevertheless in the context of a multi-methodological approach, the inhibition activity of different small molecules on the amyloidogenic process has been reported. For example, in 2011 Bartolini and co-workers successfully applied matrix-assisted laser desorption/ionization time of flight (MALDI–TOF), electrospray ionization-ion trap (ESI–IT), MS and electrospray ionization quadrupole time of flight MS (ESI–QTOF MS) for measuring the progressive disappearance of Aß42 monomer during inhibition studies with the known Aß inhibitor myricetin [8].

Capillary electrophoresis (CE) can be considered an attractive tool for the identification of entities able to modify the kinetics of formation of Aß oligomers, since it is possible to monitor over time the aggregation of several oligomeric populations. By this separative micro-technique, information about the effect of modulators on the oligomerization can be obtained. Furthermore, CE supported by transmission electron microscopy (TEM), can complete the activity profile of potential modulators [9-12].

CE has been previously used to verify the activity of different agents on the amyloid process. Starting from 2009 De Lorenzi and co-workers have applied an analytical platform based on CE and TEM to identify inhibitors of Aß aggregation. In 2009 two anthraquinone compounds, mitoxantrone and pixantrone, were investigated as Aß oligomerization modulators. Based on the intercalation with topoisomerase II by which they exert their anticancer activity, a

similar mechanism in blocking peptide-peptide interactions was hypothesized. Both were demonstrated to have anti-fibrillogenic activity as well as to reduce or abrogate Aß42 oligomerization in a concentration and time dependent manner [10]. Taverna, Ongeri and co-workers employed CE to determine the effect on oligomer formation exerted by glycosilated compounds [6], by a new class of glycopeptidomimetics [13, 14] and by Aß42 related ß-hairpin peptidomimetics [15]. As assessed by ThT fluorescence and TEM, these compounds prevent the formation of amyloid fibrils and furthermore totally suppress the Aß42-induced toxicity.

The multifactorial nature of AD and the difficulties in obtaining disease-modifying drugs encourage a therapeutic approach based on multitarget-directed ligands (MTDLs). In more recent works by De Lorenzi group [11, 12] CE was used to verify the anti-aggregant activity of multifunctional compounds able to target cholinesterase enzymes (ChEs) and Aß oligomers. By combining a bistacrine scaffold with a hydrophobic peptidomimetic sequence, three compounds have been identified as prototypic of a new class of multifunctional ChEs and Aß42 self-aggregation inhibitors.

A multitude of inhibitors of the Aß fibril formation has been reported in literature. These inhibitors can be classified in three main categories: small molecules, both of natural and synthetic origin, short peptides and antibodies [3].

Among the small molecules, an increasing number of reports have described natural products (NPs) as possible modulators of the amyloid process, such as (-)-epigallocatechin gallate, curcumin, myricetin, rosmarinic acid and many others. NPs represent an important source of novel compounds since by rational design and structural modifications they can be considered as a scaffold for new chemical entities [3].

In this work, we investigate two compounds previously reported in literature for their anti-aggregant activity (as assessed by ThT-based assay and ESI-MS) [16] and/or antioxidant properties. These

molecules have been evaluated as modulators of the amyloid process of Aß42 peptide. In order to assess the effects of these molecules on the aggregation of Aß42, the peptide was co-incubated with the compounds and monitored over time in CE to define the effect of the molecules on specific and characterized oligomeric populations.

Materials and Methods

Reagents. Synthetic Aß42 was purchased from Bachem (Bubendorf, Switzerland) as lyophilized powder and stored at -20°C. 1,1,1,3,3,3-Hexafluoropropan-2-ol (HFIP), dimethylsulfoxide (DMSO), acetonitrile (ACN), sodium carbonate (Na_2CO_3), sodium hydroxide (NaOH) and sodium dodecyl sulphate (SDS) were provided by Merck (Darmstadt, Germany). Ethanol was supplied by Carlo Erba (Cornaredo, Italy). Na_2HPO_4 and NaH_2PO_4 were used for the preparation of the background electrolyte (BGE) in the CE analyses. BGE solutions were prepared daily using Millipore Direct-Q^{TM} deionized water and filtered on 0.45 µm Sartorius membrane filters (Göttingen, Germany). Uncoated fused-silica capillary was from Polymicro Technologies (Phoenix, AZ, USA).

The set of molecules synthesized by Michela Rosini and collaborators at the Alma Mater Studiorum University of Bologna, consists of two compounds (S)-allyl (E)-3-(3-hydroxyphenyl)prop-2-enethioate (**2**) and (S)-allyl (E)-3-(3,4-dihydroxyphenyl)prop-2-enethioate (**3**) already reported in literature [16].
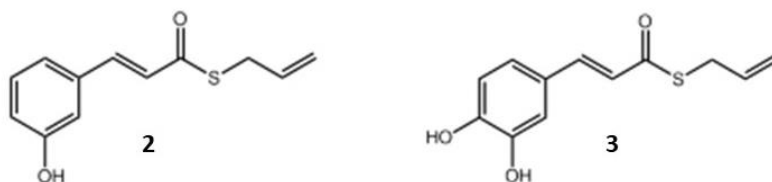

Figure 1. Structure of compounds **2** and **3**.

Sample preparation. Aß42 peptide was solubilized following the procedure of the protocol developed by Bartolini et al. [6]. Briefly, lyophilized Aß42 was dissolved in HFIP. After an appropriate incubation time, the solvent was left to evaporate. Then, the Aß42 aliquots were re-dissolved in a basic mixture (ACN 300 µM, Na_2CO_3 250 mM, NaOH, 48.3:48.3:3.4, v/v/v) to obtain 500 µM Aß42. This solution was finally diluted to the operative concentration (100 µM) with 20 mM phosphate buffer pH=7.4, with or without small molecules. Stock solutions of compounds **2** and **3** (1.53 mM) were prepared in ethanol. When co-incubation studies were carried out, 500 µM Aß42 peptide was dissolved in an appropriately diluted compound solution to keep the peptide concentration at 100 µM and obtain 1:2 peptide/compound ratio. In this way the final percentage of EtOH was lower than 3.26%.

Capillary electrophoresis. CE experiments were performed on an Agilent Technologies 3D CE system with built-in diode-array detector (Waldbronn, Germany). Data were collected and analyzed using a Chemstation A.10.02 software. The uncoated fused-silica capillary (50 µm i.d., 33 cm total length, 24.5 cm effective length) was prepared by flushing 1 M NaOH for 30 minutes, followed by water for 30 minutes and BGE (80 mM Na_2HPO_4/NaH_2PO_4) for 1 hour. The between-run rinsing cycle was carried out by pumping through the capillary 50 mM SDS and water for 1.5 min each, and BGE for 2 min. The injection of the samples was carried out by applying a pressure of 30 mbar for 3 s. The capillaries were thermostated with circulating air at 25°C and separations were carried out at 12 kV (operative current: 75–78 mA) with the anode at the sample injection end. The acquisition wavelength was 200 nm.

Statistical analysis. The data were analyzed by analysis of variance (ANOVA) followed, when significant, by an appropriate post hoc comparison test. The reported data are expressed as mean ± SD or

mean ± SEM of at least three independent experiments. Values of $p < 0.05$ were considered statistically significant.

Results and discussion

The two molecules here analyzed are already reported in literature and have been designed by the group of Michela Rosini and collaborators at the Alma Mater Studiorum University of Bologna in the context of MTDLs to get deeper in understanding the connections between Aß aggregation, oxidative stress and the tumor suppressor p53 [16].

The design strategy of these compounds is based on the combination of chemical functions derived from natural compounds. These chemical groups are related to the modulation of Aß aggregation and to the counteraction of oxidative stress. In particular, the hydroxycinnamoyl function, which is a recurring motif found in many polyphenols, is preserved, since it is related to the ability of polyphenols to modulate several AD pathways such as Aß aggregation and oxidative stress [17, 18], and is combined with the allyl mercaptan moiety of diallyl disulfide, an active principle of garlic endowed with antioxidant activity [19]. Molecules derived from the combination of these two functions are expected to counteract oxidative stress and the aggregation of Aß.

2 and **3** were previously tested for their *in vitro* anti-aggregation activity and for their potential ability to protect neuroblastoma cells from Aß42-induced toxicity and oxidative stress [16]. Results showed that the catechol moiety of **3** was essential for the anti-aggregant activity; indeed **2**, which lacks the *para*-hydroxyl function, did not have effects on the aggregation process, as demonstrated by ThT-based assay. On the other hand, **3** almost completely inhibited the assembly of Aß42 and demonstrated to be more potent than curcumin. Notably, literature reports that the ThT assay is potentially unsuitable as a probe for amyloid fibril formation in the presence of polyphenols like, among many, curcumin and curcumin derivatives, because strong p-p electronic transitions in polyphenols make them

intrinsically fluorescent, thus an interference at the wavelengths of ThT fluorescence is likely to occur [20].

For this reason, to confirm the ThT data, Simoni et al. used ESI-IT MS to finally postulate that **3**, more than curcumin, retards the Aß42 assembly process by stabilization of the monomeric form and inhibition of its inclusion into growing oligomers.

Prompted by the potency of compound **3**, preliminary investigations on its anti-oligomerization activity were carried out by CE, taking compound **2** as negative control.

Our analytical tool has been applied to evaluate the effect of compounds **2** and **3** on the aggregation process of the most amyloidogenic peptide (Aß42).

In order to investigate the potential perturbation of the oligomeric equilibrium induced by compounds, it is necessary to have available a standardized Aß42 aggregation process in the absence of compounds. In our protocol, oligomers are kept in solution for about one month until precipitation into fibrils and small oligomers slowly contribute to the formation of large aggregates. Based on the oligomeric characterization, small oligomers consist of monomers and dimers, whereas the electrophoretic population relative to large aggregates is constituted by assemblies bigger than decamers (peak 3). This oligomeric population builds up over time at the expenses of smaller assemblies (peak 1 and 2) and has demonstrated to be responsible for the toxicity of entire peptide (data not shown).

Since compounds are soluble in pure EtOH, the evaluation of the effect of EtOH at the operative concentrations on the Aß42 aggregation process has also been assessed. To address this issue, the peptide has been solubilized in 3.26% EtOH in phosphate buffer. This is the highest percentage of EtOH that is in contact with the peptide when 100 µM Aß42 samples are coincubated with compounds at the highest concentration tested (50 µM). No differences were detected either in the electrophoretic pattern or in the equilibrium between oligomers. Moreover at this concentration EtOH does not affect the

formation and the morphology of amyloid fibrils as observed by TEM (data not shown).

An important issue in the aggregation studies is the availability of negative controls useful to verify the anti-aggregant properties of small molecules in a more precisely fashion in respect to the mere comparison with the peptide in absence of compounds. Therefore in this study, **2** is considered as the negative control, bearing in mind that abrogation of fibril formation does not necessarily imply anti-oligomeric activity [4, 21].

In Figure 2a), electropherograms acquired at 21 days from the solubilization of Aß42 in the presence or not of 50 µM **3** and 50 µM **2** are reported.

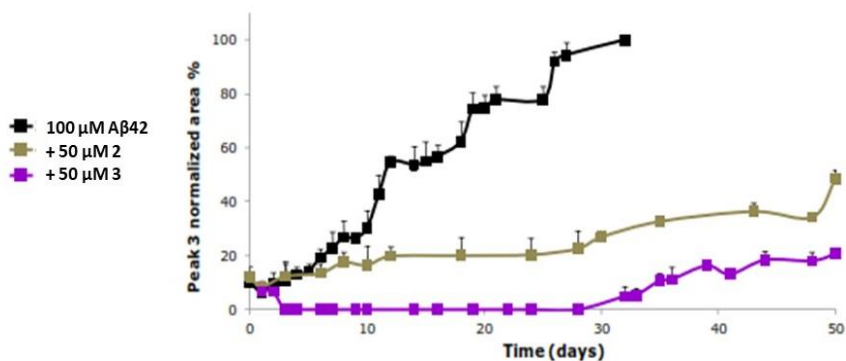a)

Elapsed time from solubilization: 21 days
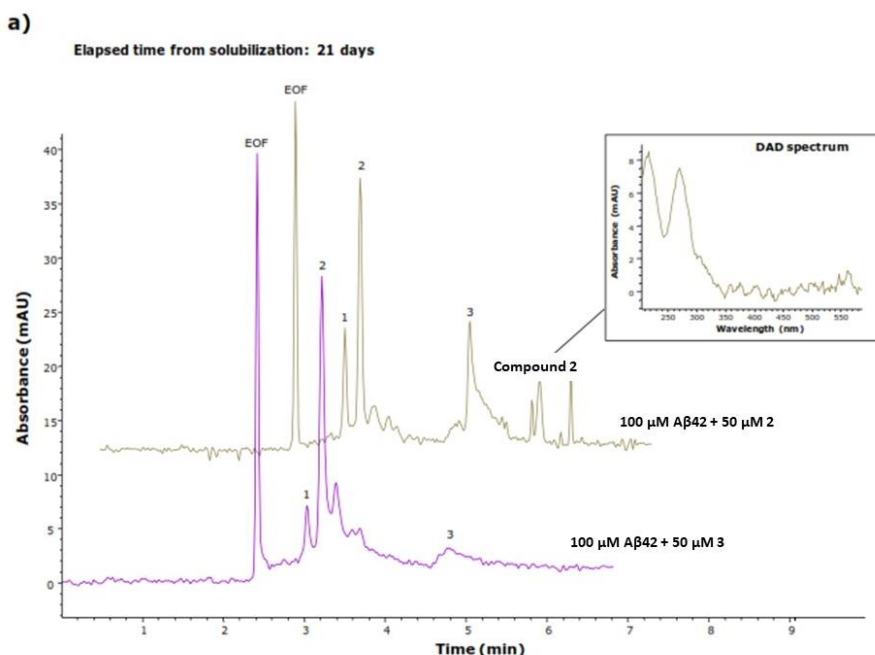
b)
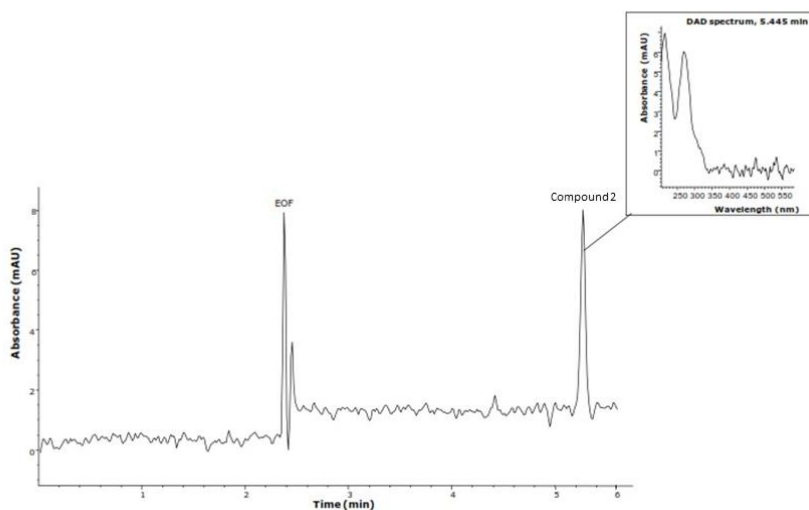
c)

Figure 2. Evaluation of the anti-aggregant activity of compounds 2 and 3. a) Electrophoretic profiles of 100 µM Aß42 alone or in the presence of 50 µM compounds after 21 days from the solubilization. Inset: UV-DAD spectra of peptide Peak 3 and of **2**. **b)** Electropherogram of pure **2** injected in CE and DAD spectrum of 2 peak. **c)** Peak 3 normalized area percentage plot of Aß42 alone and in coincubation with 50 µM **2** or **3**. Data are expressed as mean ± SD, each experimental point is in triplicate.

In the trace relative to the coincubation with **2**, in addition to the electroosmotic flow (EOF) peak and to peaks referred to oligomeric populations (Peaks 1, 2 and 3) another peak is detected over time. It is hypothesized that the species, which migrates slower in respect to Aß42 oligomers, may be the compound **2** itself, as supported by its UV-DAD spectrum in Figure 2a) and 2b). Compound **3** confirms to be very potent, in fact Peak 3 is not detected for long times, as evident from the normalized area plot illustrated in Figure 2c).

Interestingly, from CE analysis, also the negative control **2**, is able to shift the equilibrium towards non toxic small species: although peak 3 is formed over time, its area is significantly smaller than the one of control peptide**.** The fact that the graph in Figure 2c) shows a similar trend for **3** and **2**, although with lower peak 3 area values in presence of **3**, is in strong contrast with the activity found by ThT and ESI-IT MS analyses at the same compound concentration (50 µM).

However, in the work of Simoni et al., data were only produced on overall anti-fibrillogenic activity, as classically assessed by ThT fluorescence, while by ESI-IT MS only the effect on the Aß42 monomer's amount was monitored. Therefore, no information about the activity on soluble oligomers was available.

Conclusions

The peculiar nature of Aß peptides and their high aggregation tendency makes it difficult the assessment of which particular oligomeric population represents the main neurotoxic mediators in AD. This contributes to the lack of effective disease-modifying treatments for the disorder.

Here we shown how a micro-separative technique like CE can play an alternative and unique role in the *in vitro* aggregation studies of Aß oligomers and consequently in the testing of molecules active on the amyloidogenic process. In this way, a very promising molecule, **3**, that was previously identified as anti-aggregant, has confirmed its

properties. In fact, this compound hinders the formation of large toxic oligomers by shifting the equilibrium towards smaller species.

Since oligomers and fibrils can be formed through different pathways, to define an amyloidogenic modulator it is necessary to involve a multi-methodological approach. Following this rationale, here we demonstrated that the CE analysis, combined with ThT and ESI-MS techniques, could be an interesting choice. Type and set up of experiments to be carried out, number of data to be acquired and adequate statistical elaboration are still an issue and this prompts us to investigate further in this direction.

References

1. Chiti F, Dobson CM. Protein Misfolding, Amyloid Formation, and Human Disease: A Summary of Progress Over the Last Decade. Annu Rev Biochem. 2017 Jun 20;86:27-68. doi: 10.1146/annurev-biochem-061516-045115.

2. Walsh DM, Selkoe DJ. A beta oligomers - a decade of discovery. J Neurochem. 2007 Jun;101(5):1172-84. doi:10.1111/j.1471-4159.2006.04426.x.

3. Cheng B, Gong H, Xiao H, Petersen RB, Zheng L, Huang K. Inhibiting toxic aggregation of amyloidogenic proteins: a therapeutic strategy for protein misfolding diseases. Biochim Biophys Acta. 2013 Oct;1830(10):4860-71. doi:10.1016/j.bbagen.2013.06.029.

4. Lee SJ, Nam E, Lee HJ, Savelieff MG, Lim MH. Towards an understanding of amyloid-β oligomers: characterization, toxicity mechanisms, and inhibitors. Chem Soc Rev. 2017 Jan 23;46(2):310-323. doi: 10.1039/c6cs00731g.

5. Benilova I, Karran E, De Strooper B. The toxic Aβ oligomer and Alzheimer's disease: an emperor in need of clothes. Nat Neurosci. 2012 Jan 29;15(3):349-57. doi: 10.1038/nn.3028.

6. Brinet D, Gaie-Levrel F, Delatour V, Kaffy J, Ongeri S, Taverna M. In vitro monitoring of amyloid β-peptide

oligomerization by Electrospray differential mobility analysis: An alternative tool to evaluate Alzheimer's disease drug candidates. Talanta. 2017 Apr 1;165:84-91. doi: 10.1016/j.talanta.2016.12.011.

7. Bartolini M, Bertucci C, Bolognesi ML, Cavalli A, Melchiorre C, Andrisano V. Insight into the kinetic of amyloid beta (1-42) peptide self-aggregation: elucidation of inhibitors' mechanism of action. Chembiochem. 2007 Nov 23;8(17):2152-61. doi:10.1002/cbic.200700427.

8. Bartolini M, Naldi M, Fiori J, Valle F, Biscarini F, Nicolau DV, Andrisano V. Kinetic characterization of amyloid-beta 1-42 aggregation with a multimethodological approach. Anal Biochem. 2011 Jul 15;414(2):215-25. doi:10.1016/j.ab.2011.03.020.

9. Sabella S, Quaglia M, Lanni C, Racchi M, Govoni S, Caccialanza G, Calligaro A, Bellotti V, De Lorenzi E. Capillary electrophoresis studies on the aggregation process of beta-amyloid 1-42 and 1-40 peptides. Electrophoresis. 2004 Oct;25(18-19):3186-94. doi: 10.1002/elps.200406062.

10. Colombo R, Carotti A, Catto M, Racchi M, Lanni C, Verga L, Caccialanza G, De Lorenzi E. CE can identify small molecules that selectively target soluble oligomers of amyloid beta protein and display antifibrillogenic activity. Electrophoresis. 2009 Apr;30(8):1418-29. doi: 10.1002/elps.200800377.

11. Brogi S, Butini S, Maramai S, Colombo R, Verga L, Lanni C, De Lorenzi E, Lamponi S, Andreassi M, Bartolini M, Andrisano V, Novellino E, Campiani G, Brindisi M, Gemma S. Disease-modifying anti-Alzheimer's drugs: inhibitors of human cholinesterases interfering with β-amyloid aggregation. CNS Neurosci Ther. 2014 Jul;20(7):624-32. doi: 10.1111/cns.12290.

12. Butini S, Brindisi M, Brogi S, Maramai S, Guarino E, Panico A, Saxena A, Chauhan V, Colombo R, Verga L, De Lorenzi

E, Bartolini M, Andrisano V, Novellino E, Campiani G, Gemma S. Multifunctional cholinesterase and amyloid Beta fibrillization modulators. Synthesis and biological investigation. ACS Med Chem Lett. 2013 Oct 6;4(12):1178-82. doi: 10.1021/ml4002908.

13. Kaffy J, Brinet D, Soulier JL, Khemtémourian L, Lequin O, Taverna M, Crousse B, Ongeri S. Structure-activity relationships of sugar-based peptidomimetics as modulators of amyloid β-peptide early oligomerization and fibrillization. Eur J Med Chem. 2014 Oct 30;86:752-8. doi: 10.1016/j.ejmech.2014.09.031.

14. Kaffy J, Brinet D, Soulier JL, Correia I, Tonali N, Fera KF, Iacone Y, Hoffmann AR, Khemtémourian L, Crousse B, Taylor M, Allsop D, Taverna M, Lequin O, Ongeri S. Designed Glycopeptidomimetics Disrupt Protein-Protein Interactions Mediating Amyloid β-Peptide Aggregation and Restore Neuroblastoma Cell Viability. J Med Chem. 2016 Mar 10;59(5):2025-40. doi: 10.1021/acs.jmedchem.5b01629.

15. Pellegrino S, Tonali N, Erba E, Kaffy J, Taverna M, Contini A, Taylor M, Allsop D, Gelmi ML, Ongeri S. β-Hairpin mimics containing a piperidine-pyrrolidine scaffold modulate the β-amyloid aggregation process preserving the monomer species. Chem Sci. 2017 Feb 1;8(2):1295-1302. doi:10.1039/c6sc03176e.

16. Simoni E, Serafini MM, Bartolini M, Caporaso R, Pinto A, Necchi D, Fiori J, Andrisano V, Minarini A, Lanni C, Rosini M. Nature-Inspired Multifunctional Ligands: Focusing on Amyloid-Based Molecular Mechanisms of Alzheimer's Disease. ChemMedChem. 2016 Jun 20;11(12):1309-17. doi: 10.1002/cmdc.201500422.

17. Stefani M, Rigacci S. Protein folding and aggregation into amyloid: the interference by natural phenolic compounds. Int

J Mol Sci. 2013 Jun 13;14(6):12411-57. doi: 10.3390/ijms140612411.

18. Pocernich CB, Lange ML, Sultana R, Butterfield DA. Nutritional approaches to modulate oxidative stress in Alzheimer's disease. Curr Alzheimer Res. 2011 Aug;8(5):452-69.

19. Kim S, Lee HG, Park SA, Kundu JK, Keum YS, Cha YN, Na HK, Surh YJ. Keap1 cysteine 288 as a potential target for diallyl trisulfide-induced Nrf2 activation. PLoS One. 2014 Jan 28;9(1):e85984. doi: 10.1371/journal.pone.0085984.

20. Hudson SA, Ecroyd H, Kee TW, Carver JA. The thioflavin T fluorescence assay for amyloid fibril detection can be biased by the presence of exogenous compounds. FEBS J. 2009 Oct;276(20):5960-72. doi:10.1111/j.17424658.2009.07307.x.

21. Necula M, Kayed R, Milton S, Glabe CG. Small molecule inhibitors of aggregation indicate that amyloid beta oligomerization and fibrillization pathways are independent and distinct. J Biol Chem. 2007 Apr 6;282(14):10311-24. doi: 10.1074/jbc.M608207200.

Part 3.

The following manuscript has been published on ACS Chemical Neuroscience (2017) as:

Targeting the Nrf2/amyloid-beta liaison in Alzheimer's disease: a rational approach

Elena Simoni,[1,ϕ] **Melania Maria Serafini**,[2,3,ϕ] Roberta Caporaso,[1] Chiara Marchetti,[1] Marco Racchi,[2] Anna Minarini,[1] Manuela Bartolini,[1] Cristina Lanni,[2] and Michela Rosini[*1]

[1]Department of Pharmacy and Biotechnology, Alma Mater Studiorum - University of Bologna, Via Belmeloro 6, 40126 Bologna, Italy

[2]Department of Drug Sciences (Pharmacology Section), University of Pavia, V.le Taramelli 14, 27100 Pavia, Italy

[3]Scuola Universitaria Superiore IUSS Pavia, P.zza Vittoria 15, 27100 Pavia, Italy

[ϕ] The authors contributed equally to this work

Targeting the Nrf2/Amyloid-Beta Liaison in Alzheimer's Disease: A Rational Approach

Elena Simoni,[†] Melania M. Serafini,[‡,§] Roberta Caporaso,[†] Chiara Marchetti,[†] Marco Racchi,[‡] Anna Minarini,[†] Manuela Bartolini,[†] Cristina Lanni,[‡] and Michela Rosini*,[†]

Abstract

Amyloid is a prominent feature of Alzheimer's disease (AD). Yet, a linear linkage between amyloid-β peptide (Aβ) and the disease onset and progression has recently been questioned. In this context, the crucial partnership between Aβ and Nrf2 pathways is acquiring paramount importance, offering prospects for deciphering the Aβ-centered disease network. Here, we report on a new class of anti-aggregating agents rationally designed to simultaneously activate transcription-based antioxidant responses, whose lead **1** showed interesting properties in a preliminary investigation. Relying on the requirements of Aβ recognition, we identified the catechol derivative **12**. In SH-SY5Y neuroblastoma cells, **12** combined remarkable free radical scavenger properties to the ability to trigger the Nrf2 pathway and induce the Nrf2-dependent defensive gene NQO1 by means of electrophilic activation of the transcriptional response. Moreover, **12** prevented the formation of cytotoxic stable oligomeric intermediates, being significantly more effective, and *per se* less toxic, than prototype **1**. More importantly, as different chemical features were exploited to regulate Nrf2 and Aβ activities, the two pathways could be tuned independently. These findings point to compound **12** and its derivatives as promising tools for investigating the therapeutic potential of the Nrf2/Aβ cellular network, laying foundation for generating new drug leads to confront AD.

Introduction

Alzheimer's disease (AD) is the most common form of neurodegenerative dementia.[1] As for major chronic diseases, its phenotype reflects several pathological processes that interact in a complex network.[2] Despite considerable efforts, the underlying disease mechanisms and their connections are still poorly understood, and it remains unclear whether they participate in neuronal degeneration with causative roles or they merely represent the telltale remains of earlier pathogenic events.

The process of amyloidogenesis is thought to be an important driver of AD. The amyloid-β peptide (Aβ) becomes harmful when Aβ monomers combine in various aggregates to form oligomers and fibrils.[3] Aβ aggregates emerge as manifestations and mediators of a variety of neurobiological events, including inflammatory responses, tau phosphorylation impairment, mitochondrial dysfunction and oxidative damage.[4] Thus, focusing on Aβ alone has probably guided to a simplistic linear disease model, which is now appearing inadequate to represent the complexity of the disease.[5] In this context, the simultaneous observation of multiple components is increasingly being perceived as a more adequate way for addressing Aβ pluralism of causes and effects.[6-9] In this scenario, oxidative stress seems to play an important role, interconnecting diverse AD-related phenomena.[10] Indeed, the pro-oxidant environment induced by Aβ in AD pathology is a consolidated concept.[11] At the same time, oxidative stress is known to trigger the amyloidogenic pathway and promote Aβ toxicity in a vicious circle.[12] This crucial partnership involves the nuclear factor (erythroid-derived 2)-like 2 (Nrf2) transcriptional pathway, an intrinsic mechanism of defense that, under neuropathological conditions, reduces oxidative stress and inflammation by promoting the transcription of cytoprotective genes, including NAD(P)H:quinone reductase (NQO1), heme oxygenase-1 (HO-1), and glutathione S-transferase (GST) to name a few.[13, 14]

The activation of this master regulator occurs by disrupting interaction and binding of Nrf2 to Kelch-like ECH-associated protein 1 (Keap1), a cytosolic Nrf2 repressor that acts as a sensor of oxidative/electrophilic stress.[15] Notwithstanding the extensive oxidative damage characterizing AD, levels of some Nrf2-induced gene products are reduced in AD patients, suggesting disruption of the transcriptional pathway.[16] In addition, recent studies have demonstrated activation of the Keap1-Nrf2 system to be essential for counteracting Aβ-induced toxicity while genetic ablation of Nrf2 worsens amyloid deposition and neuroinflammation in a mouse model of AD.[17]

On these premises, we believe that the identification of pharmacologic tools able to modulate Aβ and/or Nrf2 pathways might contribute to the comprehension of this crucial cross-talk, offering a powerful key for interpreting the mechanistic connection between the process of protein aggregation and tissue degeneration. We have preliminary reported on a set of three molecules as versatile tools for investigating the molecular mechanisms potentially involved in chronic Aβ damage.[18] In particular, we identified the catechol derivative **1**, which joins a remarkable anti-aggregating ability to oxidant properties.

Interestingly, the biological profile of compound **1** was strategically tuned by the hydroxyl substituents on the aromatic moiety, offering a peculiar "on–off" pattern of control of the anti-aggregating efficacy that has contributed to shed light on the interconnection between the overproduction of radical species and Aβ.[18]

On this basis and in the pursuit of more effective molecules, we performed systematic modifications of **1**, by focusing on the aryl substitution pattern, the thioester function, and the aliphatic skeleton (compounds **2-13**, Figure 1).
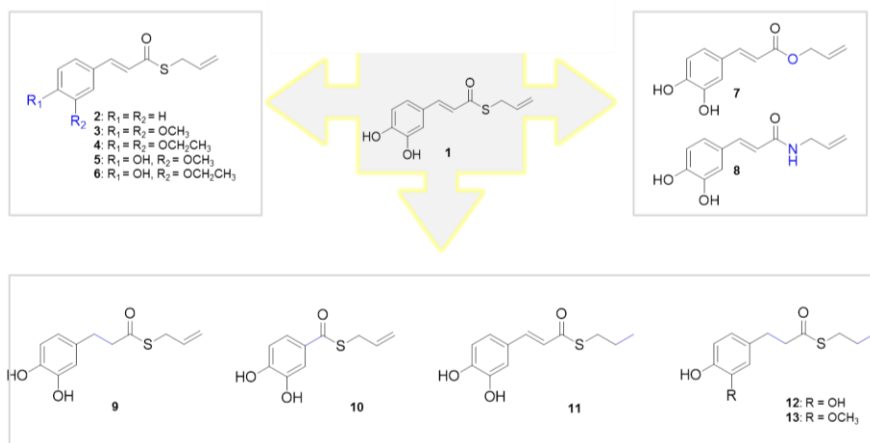
Figure 1. Drug design strategy of compounds **2-13**.

In this paper, we delineate the general structure−activity relationships (SAR) of **2**−**12** by investigating antioxidant and anti-aggregating properties. The efficacy in inhibiting fibrilization of Aβ42, the most amyloidogenic isoform of Aβ, was first studied *in vitro* by a fluorescence-based assay. Compounds were then assayed in human SH-SY5Y neuroblastoma cells to explore their ability to contrast oxidative stress and to exert neuroprotective effect against Aβ42-induced toxicity. To draw connections between the structural requirements involved in inhibition of amyloid aggregation and transcription-based antioxidant responses, selected compounds were studied as Nrf2 inducers in human SH-SY5Y neuroblastoma cells, and the ability of promoting the endogenous up-regulation of the Nrf2-dependent defensive gene NQO1 was also assessed.

Results and Discussion

Syntheses of the thioester derivatives **2**-**4** were accomplished by one pot reaction with minor modifications of literature procedure referred to caffeate esters.[19] As reported in Scheme 1 (method A), this procedure allowed Meldrum's acid mono-thioesterification with allyl sulphide to give the non-isolable intermediate, which was then readily

condensed with the appropriate aldehyde affording cinnamic derivatives **2**-**4** with moderate to good yields.

Unfortunately, this convenient method was not effective to access the phenolic derivatives **5**-**13**. They were therefore synthesized by means of an alternative procedure, which minimized side-reactions and purification efforts (Scheme 1, method B). TBDMS-protected alcohols **14-19** underwent coupling reaction with the appropriate allyl or propyl derivative with DCC in presence of DMAP, to give intermediates **20-28.** Treatment of **20-28** with TBAF effected desilylation to give the final compounds **5**-**13**. ^{1}HNMR spectra show that compounds **2-8** and **11**, featuring a carbon-carbon double bond between the catechol ring and the carbonyl function, have an *E* configuration as indicated by the large spin coupling constants (around 16 Hz) of α-H and β-H on double bonds.
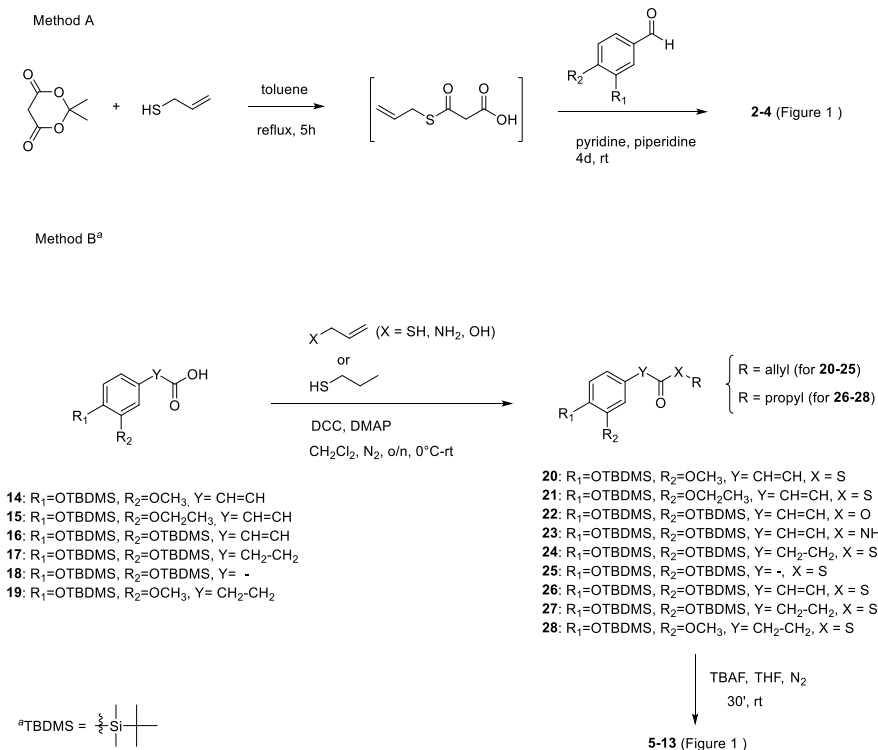
Scheme 1. Syntheses of the thioester derivatives 2-4 (method A) and the phenolic derivatives 5-13 (method B).

Cell toxicity assay. In order to define the range of concentration to be used in cellular experimental settings, the cytotoxicity of compounds **2**-**13** was assessed in SH-SY5Y human neuroblastoma cells, in comparison with **1**. Cells were exposed to the compounds at concentrations ranging from 1 to 12.5 µM for 24 h and cell viability was evaluated by MTT assay. As shown in figure 2, all the compounds were well tolerated (reduction of cell viability of about 10%) at a concentration up to 5 µM, resulting significantly less toxic than prototype **1**, that at this concentration determined a slight decrease (about 20%) of cell viability.
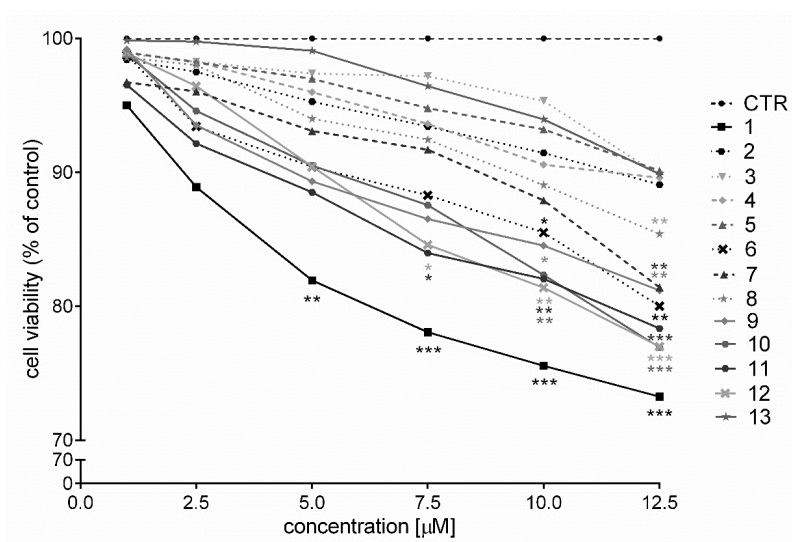
Figure 2. Cellular toxicity of compounds 2-12 on human neuroblastoma SH-SY5Y cells. The cell toxicity profiles of reference compound **1** and the non-(pro)electrophilic derivative **13** are also shown. Cells were treated with 1 µM, 2.5 µM, 5 µM, 7.5 µM, 10 µM and 12.5 µM of each compound for 24 h. Cell viability was assessed by MTT assay. Data are expressed as percentage of cell viability versus CTR; * $p<0.05$, **$p<0.01$, ***$p<0.001$ versus CTR; Dunnett's multiple comparison test.

Inhibition of $A\beta_{42}$ self-aggregation. In our previous study, we identified catechol derivative **1** as a good inhibitor of $A\beta_{42}$ self-aggregation.[18] Its inhibitory effect was studied by a thioflavin T (ThT)-based fluorometric assay, giving an IC_{50} of 12.5 ± 0.9 μM, and confirmed by a mass spectrometry assay,[20] which allowed to detect and quantitate the monomeric form of $A\beta_{42}$. Interestingly, the anti-aggregating profile of **1** seemed to be strictly related to the catechol moiety, as a complete loss of efficacy was observed following single removal of the *m-* or *p*-hydroxyl function.

	Inhibition of $A\beta_{42}$ self-aggregation [a]	
	% inhibition (± SEM) [I] = 50 μM	IC_{50} μM (± SEM)
1	> 90	12.5 ± 0.9
2	< 10	nd
3	< 10	nd
4	< 10	nd
5	< 10	nd
6	< 10	nd
7	68.8 ± 7.9	34.6 ± 6.8
8	36.3 ± 7.6	nd
9	> 90	8.72 ± 0.61
10	49.1 ± 6.3	nd
11	> 90	3.99 ± 0.39
12	> 90	3.80 ± 0.44

[a] Inhibition of $A\beta_{42}$ 50 μM self-aggregation by [I] = 50 μM. The $A\beta_{42}$/inhibitor ratio was equal to 1/1. For compounds showing a % inhibition higher than 50% when screened at 50 μM the IC_{50} value was determined. Values are the mean of two independent experiments each performed in duplicate. nd stands for not determined. SEM = standard error of the mean.

Table 1. Inhibition of $A\beta42$ self-aggregation by compounds 1-12.

Herein, systematic modifications of the aromatic substitution pattern corroborated the importance of the catechol group in inhibiting amyloid aggregation[21] as, in compounds **2**-**6**, the removal or masking into a methoxy- or ethoxy-function of one or both the hydroxyl substituents of **1** resulted in a complete loss of anti-aggregating efficacy (% inhibition at 50 μM <10%, Table 1). Following this observation, catechol-based compounds were studied to assess the role of the thioester function. Replacement of this moiety with an ester or an amide, affording compounds **7** and **8**, respectively, resulted in a gradual decrease in the ability of limiting fibril formation (-CONH-<-COO-<-COS-, Table 1).

Based on these results, we can argue that the catechol motif is essential but not *per se* sufficient to guarantee anti-aggregating efficacy, indicating the thioester moiety as a second requisite of relevance in this respect. Thus, we focused on the chemical link between the above-mentioned key features of **1**. For compound **9**, where saturation of the cinnamoyl double bond avoids conjugation of the catechol moiety and the thioester function, a slight increase in activity is observed with respect to prototype **1** (IC_{50} values equal to 8.72 and 12.5 μM for **9** and **1**, respectively), suggesting that no electronic influence between the two groups is required. Conversely, when the conjugation persists but the distance is shortened, as in **10**, a significant drop in activity is detected (from % inhibition >90 to 49.1 at 50 μM), revealing the importance of the relative position of the catechol group and the thioester side chain in amyloid recognition. Interestingly, the anti-aggregating effect of most active compounds **1** and **9** was further improved by replacing the terminal allyl moiety with an alkyl function, affording **11** (IC_{50} = 3.99 μM) and **12** (IC_{50} = 3.80 μM), respectively. This modification, in addition to potentiating prototype's efficacy, opens perspectives for further functionalization in this position as a promising multitarget drug discovery strategy.[22]

Protective effect of 12 on Aβ₄₂-induced toxicity in SH-SY5Y neuroblastoma cells. Based on the promising data obtained in the in vitro assessment of the anti-aggregating properties of the new derivatives, we studied whether the most active compound **12** could also exert neuroprotective effect against Aβ₄₂-induced toxicity in SH-SY5Y human neuroblastoma cells. Incubation of SH-SY5Y cells with 10 μM Aβ₄₂ resulted in a reduction of about 40% of cell viability (as determined by MTT assay), which can be ascribed to oligomeric species formation.[23]

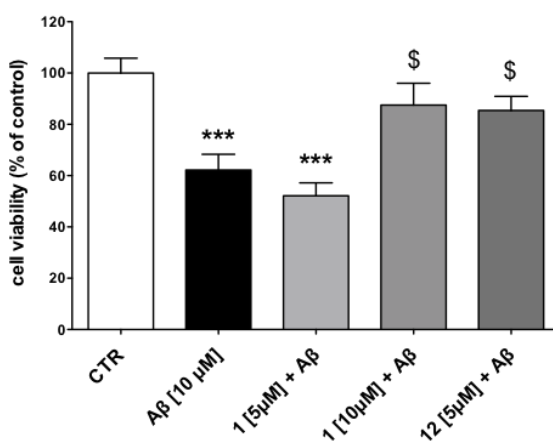**Figure 3. Effect of 1 and 12 on Aβ₄₂-mediated toxicity in neuroblastoma cells.** SH-SY5Y cells were co-incubated for 24 h with 5 μM and 10 μM compound **1** or with 5 μM compound **12** in presence of 10 μM Aβ₄₂. Cell viability was determined by MTT assay. Data are expressed as percentage of cell viability versus CTR; ***$p < 0.001$ versus CTR, $ $p < 0.05$ versus Aβ₄₂; Dunnett's multiple comparison test.

A strong protective effect was observed for compound **12** which, at 5 μM, almost completely prevented the Aβ₄₂-induced cell death, showing to be more effective than **1** that, in the same assay, was not able to counteract Aβ₄₂ toxicity up to 10 μM concentration (Figure 3). These data are in agreement with the inhibitory potency (as IC₅₀ values) determined by ThT-based assay, which showed a 3.3-fold higher anti-aggregating activity for **12** compared to **1** (Table 1).

A good correlation between data obtained by ThT- and cell-based assays was also previously demonstrated by others.[24]

Protective effect towards H_2O_2-induced damage. To determine the potential interest of compounds **2-12** as antioxidants, we evaluated their scavenger ability when co-incubated with 300 µM H_2O_2, using prototype **1** as comparison.
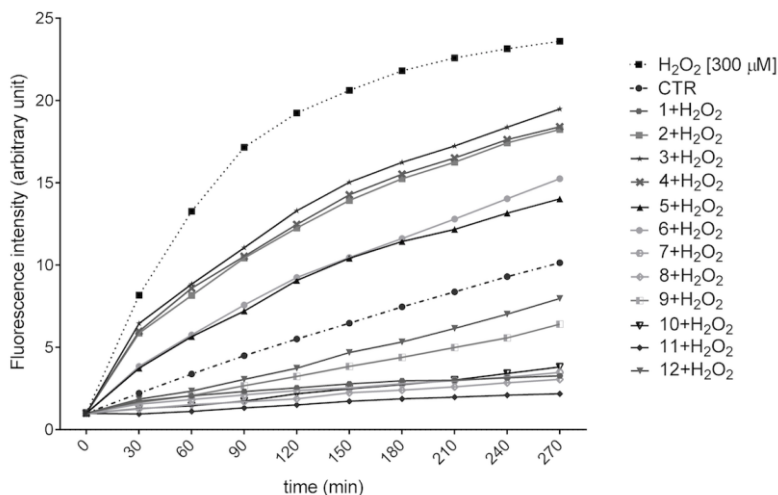

Figure 4. Compounds 1-12 reverse ROS formation induced by H_2O_2-induced oxidative stress in SH-SY5Y neuroblastoma cells. Cells were loaded with 25 mM DCFH-DA for 45 min. DCFH-DA was removed by centrifugation, cells were resuspended in PBS into a black 96-wells plate and exposed to 5 µM concentration of compounds **1-12** and 300 µM H_2O_2. ROS levels were determined from 0 to 270 min using a fluorescence microplate reader. Fluorescence intensity for all compounds is significant at any time from 30 to 270 min with $p < 0.001$ versus H_2O_2. Dunnett's multiple comparison test.

ROS scavenging effects were evaluated in SH-SY5Y cells by using the fluorescent probe dichloro-dihydro-fluorescein diacetate (DCFH-DA) as a specific marker for quantitative intracellular ROS formation. In comparison to untreated cells (dashed line, Figure 4), the intracellular DCFH-fluorescence intensity in H_2O_2-treated cells significantly increased (dotted line, Figure 4).

Treatment with all compounds markedly suppressed H_2O_2-induced intracellular ROS production, albeit to a different extent. In particular, catechol-based derivatives **1** and **7-12** emerged as the most potent antioxidants as, at any time tested, they were able to keep ROS levels below those observed for control (Figure 4). This strong antioxidant activity was particularly evident for compounds where conjugation between the catechol moiety and the carbonyl function (**1**, **7**, **8**, **10** and **11**) occurs, while compounds **9** and **12**, lacking the cinnamoyl double bond, were slightly less effective.

Activation of Nrf2 pathway in neuroblastoma cells. Activation of the Keap1/Nrf2 pathway and the consequent induction of phase 2 antioxidant genes trigger an elaborate network of protective mechanisms against oxidative damage.[25] When exposed to oxidative insults, Keap1 undergoes conformational changes as a result of oxidation at specific cysteine residues. This disrupts Nrf2 binding, promotes Nrf2 translocation into the nucleus and the activation of transcription-mediated protective responses.[26, 27] Interestingly, the Keap1-Nrf2 interaction can also be disrupted by small molecules,[28] most of which have electrophilic properties.[29] Thus, the opportunity for tuning the inducible antioxidant response is offered by Keap1 cysteine residues, which covalently conjugate the electrophilic inducers.[30] Based on these observations, electrophiles and proelectrophiles from synthetic or natural sources have attracted interest from a broad range of researchers in the drug discovery community.[31] In particular, proelectrophile compounds, which include hydroquinone cores of terpenoids and flavonoids, are only converted to their active electrophilic forms in response to pathological oxidation, offering prospects of minimal potential side effects.[32]

Herein, based on the (pro)electrophilic features of compounds **2-12**, we selected a number of catechol-based derivatives to be studied as Nrf2 inducers. First, by acting as the "on" switch for anti-aggregating

activity, the catechol group represented a prerequisite for exploring the amyloid/Nrf2 cellular network. Secondly, catechols, which become active *ortho*-quinones on oxidation, prospect benefits of proelectrophiles, which should provide neuroprotection in oxidative conditions.[33] In addition, catechol-bearing compounds **1** and **7-12** can count on more favorable scavenger abilities (as highlighted by their ability to reverse H_2O_2-induced ROS formation), which can significantly contribute to the overall antioxidant profile of the new molecules.

Thus, catechol derivatives **1** and **7-12** were investigated in SH-SY5Y neuroblastoma cell line to verify whether they may affect the Nrf2 pathway. To note, some of the selected compounds also presented an electrophilic α,β-unsaturated carbonyl group (Michael acceptor functionality), which may represent an additional source for Nrf2 activation. To discriminate the individual contribution of the two (pro)electrophilic features, compound **5**, where the Michael acceptor is not associated to the catechol moiety, and a new compound (**13**) lacking both electrophilic functionalities (purposely synthesized) were tested for comparison. Nrf2 protein levels were evaluated by western immunoblotting in SH-SY5Y cells after treatment for 24 h with compounds **1**, **5** and **7-13** at 5 μM concentration. Interestingly, all compounds with the exception of **13** increased Nrf2 levels when compared to control (Fig. 5a), suggesting that Nrf2 modulation can be driven by both the catechol function and the α,β-unsaturated carbonyl group, while the other structural features seemed to have modest relevance in this respect. In particular, differently from what observed for the anti-aggregating activity, the thioester group is not a key feature for inducing Nrf2 activation, as demonstrated by the strong efficacy elicited by ester derivative **7**.

The lack of efficacy observed for compound **13** suggests that nucleophilic addition of Keap1 cysteine residues to (pro)electrophilic portions of the molecule may represent the initiating event of the transcriptional process. Thus, we focused on the activation of Nrf2

signalling by analyzing its translocation into nucleus and its ability to induce NQO1, a prototypical cytoprotective Nrf2-target gene related to cellular stress response. In particular, we selected compounds **1**, **5**, **7**, **9** and **12**, which increased significantly the protein levels of Nrf2. The selected compounds carry alternatively or simultaneously the two (pro)electrophilic features responsible for Nrf2 induction. Compound **13** was also tested as negative control. All compounds, with the only exception of **13**, induced remarkable Nrf2 nuclear translocation, with catechol derivatives **1**, **7**, **9** and **12** being slightly more effective than **5**, lacking the catechol moiety (Figure 5b).
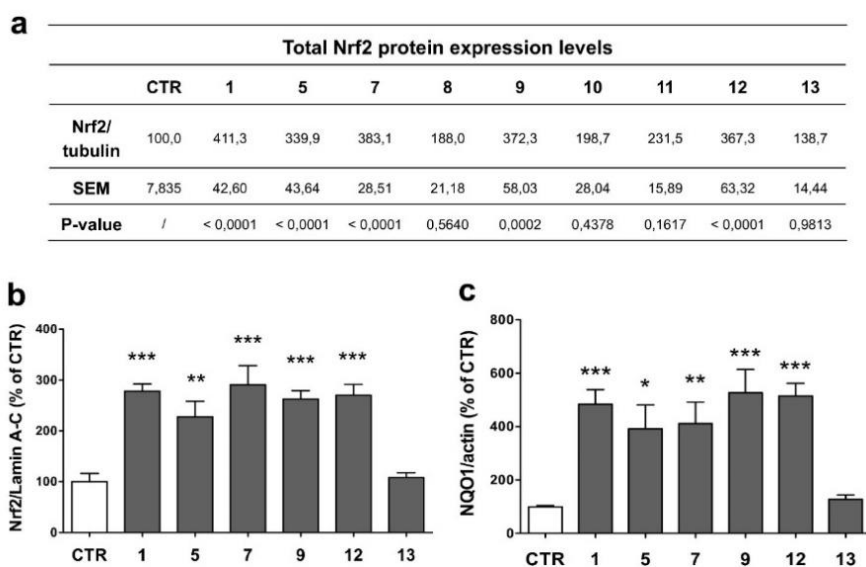
a

		Total Nrf2 protein expression levels								
	CTR	1	5	7	8	9	10	11	12	13
Nrf2/ tubulin	100,0	411,3	339,9	383,1	188,0	372,3	198,7	231,5	367,3	138,7
SEM	7,835	42,60	43,64	28,51	21,18	58,03	28,04	15,89	63,32	14,44
P-value	/	< 0,0001	< 0,0001	< 0,0001	0,5640	0,0002	0,4378	0,1617	< 0,0001	0,9813

Figure 5. Activation of Nrf2-mediated phase II detoxification pathway. a) Total cellular extracts of SH-SY5Y cells treated for 24 h with 5 µM concentration of compounds **1**, **5**, **7-13** were analyzed for Nrf2 expression by western blot. Anti tubulin was used as protein loading control. Results are shown as ratio Nrf2/tubulin (% of CTR) ± SEM. Dunnett's multiple comparison test. **b)** Nuclear cellular extracts of SH-SY5Y cells were treated for 3 h with compounds **1**, **5**, **7**, **9**, **12**, **13** at 5 µM concentration and homogenized to obtain nuclear fraction. Nrf2 expression was determined by western blot. Anti lamin A-C was used as protein loading control. Results are shown as ratio Nrf2/lamin A-C (% of CTR) ± SEM. **p<0.01 and ***p<0.001 versus CTR; Dunnett's multiple comparison test. **c)** Total cellular

extracts of SH-SY5Y cells treated for 24 h with 5 µM concentration of compounds **1**, **5**, **7**, **9**, **12**, **13** were analyzed for NQO1 expression by western blot. Anti-actin was used as protein loading control. Results are shown as ratio NQO1/actin (% of CTR) ± SEM. *$p<0.05$, **$p<0.01$ and ***$p<0.001$ versus CTR; Dunnett's multiple comparison test.

Moreover, when analyzing the induction of NQO1, all the compounds but **13** increased NQO1 levels, with the same trend of activity detected for Nrf2 activation and translocation to the nucleus (Figure 5c). Noteworthy, differently from what recently observed for other multi-electrophile compounds,[34] the combined presence of the two (pro)electrophilic features, as in **1**, did not result in a synergistic efficacy (compare activity of **1** with that of **9** and **12**, which only carry the catechol group). This can be possibly ascribed to the conjugation, occurring in **1**, between the two features, that consequently may not behave as separate entities.

Electrophilic features may account for potential toxicity issues associated with off-target interactions.[34] When studied in SH-SY5Y cells the non-(pro)electrophilic compound **13** was not toxic in the whole range of tested concentrations (cell viability > 90%, Figure 2). Noteworthy, the behavior at 5 µM (concentration of interest for biological activity) of (pro)electrophilic compounds **2-12** was not significantly dissimilar from that of **13**.

Conclusion

Advances in Aβ-centered drug discovery for AD suffer the lack of a molecular mechanistic theory of Aβ causative role. Thus, a deeper comprehension of the intertwined correlation between Aβ and oxidative damage might contribute to the understanding and treatment of the disease. The interest towards this critical partnership is reinforced by the emerging evidence of an aberrant regulation of the Nrf2-mediated antioxidant response in AD, with Aβ contributing to the dysfunctional activation of the transcriptional pathway.

On these bases, in the pursuit of more effective anti-aggregating and antioxidant properties, we herein expanded our previous study on the catechol derivative **1** through systematic modifications of its structure. We also deepened insight the antioxidant profile of the compounds by investigating their ability to trigger the Nrf2 pathway in terms of up-regulation of Nrf2 expression, translocation into the nucleus and induction of the Nrf2-dependent defensive gene NQO1. Interestingly, in SH-SY5Y neuroblastoma cells, all compounds tested exhibited remarkable free radical scavenging properties and protected against oxidative stress by means of electrophilic activation of Nrf2-mediated response. This multimodal behavior was accompanied by a significant reduction of the cytotoxicity with respect to **1**. Relying on the requirements of Aβ recognition, which was driven by the catechol function and the thioester group, we identified compound **12**. It joined the above-mentioned antioxidant effects to a marked ability of preventing the formation of cytotoxic stable oligomeric intermediates, being significantly more effective than prototype **1**. Most importantly, as different chemical features were exploited to regulate Nrf2 and Aβ activities, we could finely and separately tune the two pathways. These findings point to compound **12** and its derivatives as powerful tools for investigating the therapeutic potential of the Nrf2/Aβ cellular network, paving the way for the generation of new drug leads to confront AD.

Experimental Section
Chemistry. *General Chemical methods.* Chemical reagents were purchased from Sigma Aldrich, Fluka and Lancaster (Italy). The course of the reactions was observed by TLC on 0.20 mm silica gel 60 F254 plates (Merck, Germany), then visualized with an UV lamp. Nuclear magnetic resonance spectra (NMR) were recorded at 400 MHz for ^{1}H and 100 MHz for ^{13}C on Varian VXR 400 spectrometer. Chemical shifts are reported in parts per millions (ppm) relative to tetramethylsilane (TMS), and spin multiplicities are given as s

(singlet), br s (broad singlet), d (doublet), t (triplet), q (quartet), or m (multiplet). Direct infusion ESI-MS mass spectra were recorded on a Waters ZQ 4000 apparatus. Final compounds **1−13** were >95% pure as determined by HPLC analyses. The analyses were performed under reversed-phase conditions on a Phenomenex Jupiter C18 (150x4.6 mm I.D.) column, using a binary mixture of H_2O/acetonitrile (60/40, v/v for **2**, **5**, **6**; 30/70, v/v for **3,4**; 65/35, v/v for **7**, **10**, **11**; 70/30, v/v for **8**; 50/50, v/v for **9**, **12**, **13**) as the mobile phase, UV detection at λ = 302 nm (for **2**-**8**, **10**) or 254 nm (for **9**, **12**, **13**) and a flow rate of 0.7 mL/min. Analyses were performed on a liquid chromatograph model PU-1585 UV equipped with a 20 µL loop valve (Jasco Europe, Italy).

General procedure for the target compounds 2-4. To a solution of Meldrum's acid (1 equiv, 114.13 mg, 4.05 mmol) in toluene (8 mL) was slowly added 2-propene-1-thiol (1 equiv, 300 mg, 4.05 mmol). The mixture was refluxed for 7 h. After the formation of the intermediate, the reaction was cooled to room temperature followed by sequential addition of the appropriate aldehyde (0.4 equiv), pyridine (400 µL) and piperidine (40 µL). The stirring continued at room temperature 4 days. Following evaporation of the solvent, the residue was purified by column chromatography on silica gel to yield the desired cinnamic derivatives **2**-**4**.

***S*-allyl(*E*)-3-phenylprop-2-enethioate (2).** **2** was synthesized from benzaldehyde (170 mg, 1.6 mmol). Elution with petroleum ether/ethyl acetate (9.7:0.3) afforded **2** as a waxy solid: 108 mg (33%). ^{1}H NMR (400 MHz, CDCl$_3$) δ 7.58 (d, *J*=15.6 Hz, 1H), 7.47-7.44 (m, 2H), 7.32-7.29 (m, 3H), 6.67 (d, *J*=15.6 Hz, 1H), 5.89-5.79 (m, 1H), 5.26 (dd, [1]*J*=16.8 Hz, [2]*J*=1.2 Hz, 1H), 5.10 (d, *J*=10 Hz, 1H), 3.64 (d, *J*=6.8 Hz, 2H). ^{13}C NMR (100 MHz, CDCl$_3$) δ 190.04, 140.63, 134.06, 133.19, 130.58, 128.94 (2 C), 128.43 (2 C), 124.75, 117.99, 31.80. MS [ESI[+]] *m/z* 227 [M+Na][+].

***S*-allyl(*E*)-3-(3,4-dimethoxyphenyl)prop-2-enethioate (3).** **3** was synthesized from 3,4-dimethoxybenzaldehyde (266 mg, 1.6 mmol).

Elution with petroleum ether/ethyl acetate (7:3) afforded **3** as a white solid: 220 mg (52%), m.p.= 123 °C. ^{1}H NMR (400 MHz, CDCl$_3$) δ 7.57 (d, J=16 Hz, 1H), 7.13 (dd, [1]J=8 Hz, [2]J=2 Hz, 1H), 7.05 (d, J=2Hz, 1H), 6.86 (d, J=8 Hz, 1H), 6.59 (d, J=16 Hz, 1H), 5.91-5.84 (m, 1H), 5.29 (d, J=19.6, 1H), 5.13 (d, J=11.6, 1H), 3.92 (s, 6H), 3.67 (d, J=8 Hz, 2H). ^{13}C-NMR (100 MHz, CDCl$_3$) δ 188.88, 151.44, 149.25, 140.77, 133.21, 126.95, 123.26, 122.58, 117.86, 111.04, 109.74, 55.98 (2 C), 31.71. MS [ESI[+]] m/z 265 [M+1][+].

S-allyl(*E*)-3-(3,4-diethoxyphenyl)prop-2-enethioate (4). 4 was synthesized from 3,4-diethoxybenzaldehyde (310 mg, 1.6 mmol). Cristallization from ethanol gave **4** as a white solid: 220 mg (47%), m.p. =145 °C; ^{1}H NMR (400 MHz, CDCl$_3$) δ 7.53 (d, J=15.6 Hz, 1H), 7.09-7.05 (m, 2H), 6.83 (d, J=8 Hz, 1H), 6.57 (d, J=15.6 Hz, 1H), 5.89-5.83 (m, 1H), 5.27 (d, J=17.2 Hz, 1H), 5.11 (d, J=10.4 Hz, 1H), 4.13-4.08 (m, 4H), 3.66 (d, J=6.8 Hz, 2H), 1.47-1.44 (m, 6H). ^{13}C-NMR (100 MHz, CDCl$_3$) δ 188.76, 151.28, 148.79, 140.90, 133.27, 126.75, 123.21, 122.36, 117.78, 112.63, 112.0, 64.58 (2 C), 31.67, 14.74 (2 C). MS [ESI[+]] m/z 315 [M+Na][+].

General procedure for the intermediates 14-19. To a solution of the appropriate commercially available acid (1 equiv) in dry DMF (5 mL) were added TBDMS-Cl (2-3 equiv) and imidazole (5 equiv) under nitrogen atmosphere. After leaving the reaction to room temperature overnight, the mixture was concentrated to dryness, and the residue purified by column chromatography on silica gel to yield the desired intermediates **14-19**. Experimental data of known compounds **14** and **16-19** were in agreement with the literature.

(*E*)-3-(4-((*tert*-butyldimethylsilyl)oxy)-3-ethoxyphenyl) acrylic acid (15). 15 was synthesized from (*E*)-3-(3-ethoxy-4-hydroxyphenyl)acrylic acid (500 mg, 2.40 mmol). Elution with petroleum ether/ethyl acetate/methanol (5:4.5:0.5) afforded **15** as a waxy solid: 325 mg (42%); ^{1}H NMR (400 MHz, CDCl$_3$) δ 7.70 (d, J=15.6 Hz, 1H), 7.03 (s, 1H), 7.02 (d, J=4.0 Hz, 1H), 6.84 (d, J=4.0

Hz, 1H), 6.30 (d, *J*=15.6 Hz, 1H), 4.04 (q, *J*=7.2 Hz, 2H), 1.45 (t, *J*=6.8 Hz, 3H), 0.99 (s, 9H), 0.17 (s, 6H). ^{13}C NMR (100 MHz, CDCl$_3$) 171.57, 152.21, 148.89, 147.65, 126.62, 122.91, 121.31, 114.01, 111.09, 64.93, 31.76, 25.61 (3 C), 14.73, -4.61 (2 C).

General procedure for the intermediates 20-28. To an ice-cooled solution of the appropriate protected acid (**14-19**) (1 equiv) in dry CH$_2$Cl$_2$ (4 mL) was added DCC (1.1 equiv), and DMAP (cat.). The reaction mixture was stirred for 10 min, followed by addition of the appropriate nucleophile (3 equiv). Stirring was then continued at room temperature overnight, and the reaction worked up by filtration and evaporation. The crude was purified by chromatography on silica gel.

S-**allyl(*E*)-3-(4-((*tert*-butyldimethylsilyl)oxy)-3-methoxy phenyl)prop-2-enethioate (20). 20** was synthesized from **14**[35] (410 mg, 1.33 mmol) and 2-propene-1-thiol. Elution with petroleum ether/ethyl acetate (9.4:0.6) afforded **20** as a waxy solid: 330 mg (68%); ^{1}H NMR (400 MHz, CDCl$_3$) δ 7.48 (d, *J*=15.6 Hz, 1H), 6.98-6.95 (m, 2H), 6.76 (d, *J*=8 Hz, 1H), 6.50 (d, *J*=15.6 Hz, 1H), 5.80-5.76 (m, 1H), 5.21 (d, *J*=18 Hz, 1H), 5.05 (d, *J*=10 Hz, 1H), 3.76 (s, 3H), 3.59 (d, *J*=6.80 Hz, 2H), 0.91 (s, 9H), 0.09 (s, 6H). ^{13}C NMR (100 MHz, CDCl$_3$) 174.87, 151.23, 147.94, 140.97, 133.25, 127.84, 122.81, 122.66, 121.14, 117.84, 111.00, 55.44, 31.70, 25.63 (3 C), 18.46, -4.61 (2 C).

S-**allyl(*E*)-3-(4-((*tert*-butyldimethylsilyl)oxy)-3-ethoxy phenyl)prop-2-enethioate (21). 21** was synthesized from **15** (200 mg, 0.62 mmol) and 2-propene-1-thiol. Elution with petroleum ether/ethyl acetate (9.5:0.5) afforded **21** as a waxy solid: 130 mg (55%); ^{1}H NMR (400 MHz, CDCl$_3$) δ 7.50 (d, *J*=16 Hz, 1H), 7.00-6.89 (m, 2H), 6.79 (d, *J*=8 Hz, 1H), 6.52 (d, *J*=16 Hz, 1H), 5.86-5.77 (m, 1H), 5.22 (d, *J*=17.2 Hz, 1H), 5.10 (d, *J*=10 Hz, 1H), 4.01 (q, *J*=6.4 Hz, 2H), 3.62 (d, *J*=6.8 Hz, 2H), 1.41 (t, *J*=6.4 Hz, 3H), 0.96 (s, 9H), 0.03 (s, 6H). ^{13}C NMR (100 MHz, CDCl$_3$) δ 189.04, 146.34,

145.99, 140.85, 132.27, 125.39, 124.69, 122.15, 117.64, 114.96, 111.02, 64.93, 31.90, 24.93 (3 C), 18.66, 14.35, -4.31 (2 C).

Allyl(*E*)-3-(3,4-bis((*tert*-butyldimethylsilyl)oxy)phenyl) acrylate (22). 22 was synthesized from **16**[35] (190 mg, 0.465 mmol) and allyl alcohol. Elution with petroleum ether/ethyl acetate (9.5:0.5) afforded **22** as a waxy solid: 120 mg (57%); ^{1}H NMR (400 MHz, CDCl$_3$) δ 7.57 (d, *J*=16 Hz, 1H), 6.99 (s, 1H), 6.98 (d, *J*=8 Hz, 1H) 6.80 (d, *J*=8 Hz, 1H) 6.23 (d, *J*=16 Hz, 1H), 6.00-5.98 (m, 1H), 5.34 (d, *J*=16 Hz, 1H), 5.24 (d, *J*=11 Hz, 1H), 4.67 (d, *J*=6 Hz, 2H), 0.97 (s, 9H), 0.96 (s, 9H), 0.19 (s, 6H), 0.18 (s, 6H). ^{13}C NMR (100 MHz, CDCl$_3$) δ 169.8, 146.93, 146.04, 143.71, 133.03, 126.06, 122.03, 118.64, 115.29, 114.85, 114.00, 30.07, 26.63 (6 C), 18.56 (2 C), -4.21 (4 C).

(*E*)-*N*-allyl-3-(3,4-bis((*tert*-butyldimethylsilyl)oxy)phenyl) acrylamide (23). 23 was synthesized from **16**[35] (400 mg, 0.978 mmol) and allylamine. Elution with petroleum ether/ethyl acetate (8:2) afforded **23** as a waxy solid: 100 mg (23%); ^{1}H NMR (400 MHz, CDCl$_3$) δ 7.49 (d, *J*=15.6 Hz, 1H), 6.98 (s, 1H), 6.96 (d, *J*=8 Hz, 1H), 6.77 (d, *J*=8 Hz, 1H), 6.21 (d, *J*=15.6 Hz, 1H), 5.91-5.80 (m, 1H), 5.81 (br s, 1H), 5.21 (d, *J*=17.2 Hz, 1H), 5.13 (d, *J*=11.6 Hz, 1H), 3.99 (d, *J*=5.6 Hz, 2H), 0.97 (s, 9H), 0.96 (s, 9H), 0.19 (s, 6H), 0.18 (s, 6H). ^{13}C NMR (100 MHz, CDCl$_3$) δ 166.95, 147.31, 145.20, 141.17, 133.93, 127.02, 121.55, 117.63, 115.34, 114.80, 113.52, 41.20, 25.63 (6 C), 18.76 (2 C), -4.11 (4 C).

***S*-allyl 3-(3,4-bis((*tert*-butyldimethylsilyl)oxy)phenyl) propanethioate (24). 24** was synthesized from **17**[36] (300 mg, 0.73 mmol) and 2-propene-1-thiol. Elution with petroleum ether/ethyl acetate (9.7:0.3) afforded **24** as a waxy solid: 200 mg (59%); ^{1}H NMR (400 MHz, CDCl$_3$) δ 6.71(d, *J*=8 Hz, 1H), 6.62-6.57 (m, 2H), 5.78-5.73 (m, 1H), 5.20 (dd, [1]*J*=16.8 Hz, [2]*J*=1.2 Hz, 1H), 5.07 (d, *J*=8 Hz, 1H), 3.51 (d, *J*=8 Hz, 2H), 2.84-2.77 (m, 4H), 0.97 (s, 18H), 0.17 (s, 12H). ^{13}C-NMR (100 MHz, CDCl$_3$) δ 198.09, 146.78 (2 C), 145.42, 133.22, 121.34, 121.24, 121.10, 117.99, 45.79, 31.09, 30.86, 26.09 (6 C), 18.57 (2 C), -3.96 (4 C).

S-allyl 3,4-bis((*tert*-butyldimethylsilyl)oxy)benzothioate (25). 25 was synthesized from **18**[37] (330 mg, 0.862 mmol) and 2-propene-1-thiol. Elution with petroleum ether/ethyl acetate (8:2) afforded **25** as a waxy solid: 130 mg (34%); ^{1}H NMR (400 MHz, CDCl$_3$) δ 7.51-7.47 (m, 2H), 6.84 (d, J=8 Hz, 1H), 5.88 (m, 1H), 5.30 (d, J=17.2 Hz, 1H), 5.13 (d, J=10 Hz, 1H), 3.69 (d, J=6.8 Hz, 2H), 0.99 (s, 18H), 0.22 (s, 12H). ^{13}C NMR (100 MHz, CDCl$_3$) δ 190.30, 151.34, 146.49, 134.01, 130.94, 120.42, 117.82, 115.96, 114.76, 32.28, 25.72 (6 C), 18.57 (2 C), -4.06 (4 C).

S-propyl(*E*)-3-(3,4-bis((*tert*-butyldimethylsilyl)oxy) phenyl)prop-2-enethioate (26). 26 was synthesized from **16**[35] (480 mg, 1.174 mmol) and 1-propanethiol. Elution with petroleum ether/ethyl acetate (9.8:0.2) afforded **26** as a waxy solid: 430 mg (78%); ^{1}H NMR (400 MHz, CDCl$_3$) δ 7.49 (d, J=16 Hz, 1H), 7.05-7.01 (m, 2H), 6.82 (d, J=8.4 Hz, 1H), 6.52 (d, J=16 Hz, 1H), 2.99 (t, J=7.2 Hz, 2H), 1.70-1.64 (m, 2H), 1.03-0.97 (m, 18H + 3H), 0.21 (s, 12H). ^{13}C NMR (100 MHz, CDCl$_3$) δ 190.70, 145.84, 144.52, 141.95, 126.95, 122.98, 121.65, 115.54, 114.83, 32.14, 24.08, 25.52 (6 C), 18.53 (2 C), 13.32, -4.16 (4 C).

S-propyl 3-(3,4-bis((*tert*-butyldimethylsilyl)oxy)phenyl) propanethioate (27). 27 was synthesized from **17**[36] (300 mg, 0.73 mmol) and 1-propanethiol. Elution with petroleum ether/ethyl acetate (9.7:0.3) afforded **27** as a waxy solid: 342 mg (44%); ^{1}H NMR (400 MHz, CDCl$_3$) δ 6.72 (d, J= 8 Hz, 1H), 6.64 (s, 1H), 6.61 (d, J=8 Hz, 1H), 2.86-2.79 (m, 6H), 1.60-1.55 (m, 2H), 0.99-0.93 (m, 18H+3H), 0.18 (s, 12H). ^{13}C NMR (100 MHz, CDCl$_3$) δ 198.86, 146.74, 145.35, 133.35, 121.33, 121.25, 121.06, 45.91, 30.94, 30.87, 26.07 (6 C), 23.07, 18.54 (2 C), 13.45, -3.98 (4 C).

S-propyl 3-(4-((*tert*-butyldimethylsilyl)oxy)-3-methoxy phenyl)propanethioate (28). 28 was synthesized from **19**[38] (110 mg, 0.35mmol) and 1-propanethiol. Elution with petroleum ether/ethyl acetate (9.5:0.5) afforded **28** as a pale oil: 70 mg (54%); ^{1}H NMR (400MHz, CDCl$_3$) δ 6.75 (d, J=8 Hz, 1H), 6.67 (d, J=2 Hz, 1H), 6.63

(dd, ^1J=8 Hz, ^2J=2 Hz, 1H), 3.78 (s, 3H), 2.91-2.86 (m, 2H), 2.85-2.82 (m, 4H), 1.62-1.56 (m, 2H), 0.99 (s, 9H), 0.97-0.94 (m, 3H), 0.14 (s, 6H). ^{13}C NMR (100MHz, CDCl$_3$) δ 198.96, 150.90, 143.55, 143.55, 133.69, 120.90, 112.54, 55.57, 45.95, 31.38, 30.88, 25.83 (3 C), 23.06, 18.53, 13.39, -4.56 (2 C).

General procedure for the synthesis of 5-13. To a solution of the appropriate organosilane intermediate **20-28** (1 equiv) in THF (5 mL) was added TBAF (4 equiv) and stirring was continued at room temperature. After 20-30 min, the reaction was quenched by addition of saturated aqueous NH$_4$Cl solution; the aqueous phase was extracted with EtOAc (3 x 10 mL), and the combined organic layer was dried over Na$_2$SO$_4$. Following evaporation of the solvent, the residue was purified by column chromatography on silica gel.

***S*-allyl(*E*)-3-(4-hydroxy-3-methoxyphenyl)prop-2-enethioate (5).** **5** was synthesized from **20** (330 mg, 0.91mmol). Elution with petroleum ether/ethyl acetate (8.5:1.5) afforded **5** as a waxy solid: 140 mg (62%); ^{1}H NMR (400 MHz, CDCl$_3$) δ 7.54 (d, *J*=15.6 Hz, 1H), 7.08 (d, *J*=8 Hz, 1H), 7.01 (s, 1H), 6.90 (d, *J*=8 Hz, 1H), 6.56 (d, *J*=15.6 Hz, 1H), 5.90 (br s, 1H), 5.87-5.80 (m, 1H), 5.27 (d, *J*=16.8 Hz, 1H), 5.11 (d, *J*=10 Hz, 1H), 3.92 (s, 3H), 3.65 (d, *J*=7.6 Hz, 2H). ^{13}C NMR (100 MHz, CDCl$_3$) δ 188.91, 148.31, 146.79, 140.95, 133.23, 126.57, 123.66, 122.35, 117.86, 114.81, 109.49, 55.98, 31.71. MS [ESI$^-$] m/z 249 [M-1]$^-$.

***S*-allyl(*E*)-3-(3-ethoxy-4-hydroxyphenyl)prop-2-enethioate (6). 6** was synthesized from **21** (120 mg, 0.317 mmol). Elution with petroleum ether/ethyl acetate (8.5:1.5) afforded **6** as a waxy solid: 50 mg (60%); ^{1}H NMR (400 MHz, CDCl$_3$) δ 7.52 (d, *J*=15.6 Hz, 1H), 7.06 (d, *J*=8 Hz, 1H), 6.99 (s, 1H), 6.90 (d, *J*=8 Hz, 1H), 6.54 (d, *J*=15.6 Hz, 1H), 5.90 (br s, 1H), 5.89-5.84 (m, 1H), 5.26 (d, *J*=16.8 Hz, 1H), 5.10 (d, *J*=9.6 Hz, 1H), 4.13 (q, *J*=7.2 Hz, 2H), 3.64 (d, *J*=7.2 Hz, 2H), 1.45 (t, *J*=7.2 Hz, 3H). ^{13}C NMR (100 MHz, CDCl$_3$) δ 188.94, 148.44, 146.09, 141.05, 133.25, 126.49, 123.49, 122.25,

117.84, 114.76, 110.42, 64.63, 31.70, 14.75. MS [ESI$^+$] *m/z* 265 [M+1]$^+$; [ESI$^-$] *m/z* 263 [M-1]$^-$.

Allyl (*E*)-3-(3,4-dihydroxyphenyl)acrylate (7).[19] **7** was synthesized from **22** (120 mg, 0.267 mmol). Elution with petroleum ether/ethyl acetate (5:5) afforded **7** as a waxy solid: 43 mg (73%); ^{1}H NMR (400 MHz, CDCl$_3$) δ 7.59 (d, *J*=16 Hz, 1H), 7.09 (s, 1H), 6.98 (d, *J*=8 Hz, 1H), 6.86 (d, *J*=8 Hz, 1H), 6.26 (d, *J*=16 Hz, 1H), 5.97-5.93 (m, 1H), 5.35(d, *J*=17.2 Hz, 1H), 5.26(d, *J*=10.4 Hz, 1H), 4.70 (d, *J*=5.6 Hz, 2H). ^{13}C NMR (100 MHz, CDCl$_3$) δ 167.8, 146.63, 145.65, 143.91, 132.03, 127.26, 122.53, 118.44, 115.49, 114.97, 114.40, 29.67. MS [ESI$^+$] *m/z* 221 [M+1]$^+$; [ESI$^-$] *m/z* 219 [M-1]$^-$.

(*E*)-*N*-allyl-3-(3,4-dihydroxyphenyl)acrylamide (8).[39] **8** was synthesized from **23** (100 mg, 0.224 mmol). Elution with CHCl$_3$/MeOH (9.7:0.3) afforded **8** as a waxy solid: 40 mg (81%); ^{1}H NMR (400 MHz, CD$_3$OD) δ 7.39 (d, *J*=15.6 Hz, 1H), 6.99 (s, 1H), 6.89 (d, *J*=8 Hz, 1H), 6.74 (d, *J*=8 Hz, 1H), 6.37 (d, *J*=15.6 Hz, 1H), 5.91-5.82 (m, 1H), 5.18(d, *J*=17.2 Hz, 1H), 5.11 (d, *J*=13.2 Hz, 1H), 3.89 (d, *J*=7.2 Hz, 2H). ^{13}C NMR (100 MHz, CD$_3$OD) δ 167.75, 147.41, 145.30, 141.14, 134.03, 126.82, 120.75, 116.63, 115.04, 114.90, 113.68, 41.50. MS [ESI$^+$] *m/z* 220 [M+1]$^+$; [ESI$^-$] *m/z* 218 [M-1]$^-$.

S-allyl 3-(3,4-dihydroxyphenyl)propanethioate (9). 9 was synthesized from **24** (130 mg, 0.28 mmol). Elution with petroleum ether/ethyl acetate (5.5:4.5) afforded **9** as a waxy oil: 45 mg (67%); ^{1}H NMR (400 MHz, CDCl$_3$) δ 6.77 (d, *J*=8 Hz, 1H), 6.69 (s, 1H), 6.61 (d, *J*=8 Hz, 1H), 5.84-5.73 (m, 1H), 5.22 (d, *J*=17.2 Hz, 1H), 5.10 (d, *J*=10.8 Hz, 1H), 3.53 (d, *J*=7.2 Hz, 2H), 2.89-2.80 (m, 4H). ^{13}C NMR (100 MHz, CDCl$_3$) δ 199.25, 143.71, 142.18, 132.95 (2 C), 120.77, 118.18, 115.56, 115.50, 45.68, 31.96, 30.91. MS [ESI$^+$] *m/z* 261 [M+Na]$^+$.

S-allyl 3,4-dihydroxybenzothioate (10). 10 was synthesized from **25** (130 mg, 0.296 mmol). Elution with dichloromethane/methanol (9.8:0.2) afforded **10** as a dark oil: 15 mg (20%); ^{1}H NMR (400 MHz,

CD$_3$OD) δ 7.41-7.38 (m, 2H), 6.81 (d, J=8.4 Hz, 1H), 5.91-5.82 (m, 1H), 5.27 (d, J=16.8 Hz, 1H), 5.09 (d, J=9.6 Hz, 1H), 3.66 (d, J=6.8 Hz, 2H). ^{13}C NMR (100 MHz, CD$_3$OD) δ 191.30, 152.35, 146.49, 135.01, 130.24, 121.53, 117.92, 115.92, 114.96, 32.38. MS [ESI$^+$] m/z 209 [M+1]$^+$.

S-propyl (*E*)-3-(3,4-dihydroxyphenyl)prop-2-enethioate (11). 11 was synthesized from **26** (430 mg, 0.921 mmol). Elution with dichloromethane/methanol (9.6:0.4) afforded **11** as a pale oil: 63 mg (30%); ^{1}H NMR (400 MHz, CDCl$_3$) δ 7.50 (d, J=15.6 Hz, 1H), 7.10 (s, 1H), 7.02 (d, J=8 Hz, 1H), 6.88 (d, J=8 Hz, 1H), 6.56 (d, J=15.6 Hz, 1H), 2.98 (t, J=7.2 Hz, 2H), 1.69-1.64 (m, 2H), 1.00 (t, J=7.2 Hz, 3H). ^{13}C NMR (100 MHz, CDCl$_3$) δ 191.80, 146.88, 144.02, 140.92, 127.25, 122.98 (2 C), 115.74, 114.93, 31.13, 23.08, 13.52. MS [ESI$^-$] m/z 237 [M-1]$^-$.

S-propyl 3-(3,4-dihydroxyphenyl)propanethioate (12). 12 was synthesized from **27** (119 mg, 0.25 mmol). Elution with petroleum ether/ethyl acetate (5.5:4.5) afforded **12** as a waxy oil: 41 mg (66%); ^{1}H NMR (400 MHz, CDCl$_3$) δ 6.76 (d, J=8.4 Hz, 1H), 6.68 (d, J=2 Hz 1H),6.59 (dd, ^1J=8.4, ^2J=2 Hz 1H), 2.86-2.81 (m, 6H), 1.58-1.57 (m, 2H), 0.94 (t, J=7.2 Hz, 3H). ^{13}C NMR (100 MHz, CDCl$_3$) δ 200.23, 143.60, 142.07, 132.89, 120.61, 115.44, 115.39, 45.71, 30.92, 30.88, 22.82, 13.27. MS [ESI$^+$] m/z 263 [M+Na]$^+$.

S-propyl 3-(4-hydroxy-3-methoxyphenyl)propanethioate (13). 13 was synthesized from **28** (70 mg, 0.189 mmol). Elution with petroleum ether/ethyl acetate (5.5:4.5) afforded **13** as a pale oil: 45 mg (94%); ^{1}H NMR (400 MHz, CDCl$_3$) δ 6.83-6.81 (m, 1H), 6.68 (s, 1H), 6.66 (d, J=2 Hz, 1 H), 3.86 (s, 3H), 2.92-2.80 (m, 6H), 1.61-1.56 (m, 2 H), 0.95 (t, J=8 Hz, 3H). ^{13}C NMR (100 MHz, CDCl$_3$) δ 199.14, 146.62, 144.23, 132.25, 121.10, 114.56, 111.14, 56.07, 46.15, 31,47, 30.10, 23.16, 13.51. MS [ESI$^+$] (m/z) 277 [M+Na]$^+$.

Sample preparation for Aβ₄₂ self-aggregation.

1,1,1,3,3,3-Hexafluoro-2-propanol (HFIP)-pretreated $A\beta_{42}$ samples (Bachem AG, Switzerland) were resolubilized with a CH_3CN/0.3 mM Na_2CO_3/250 mM NaOH (48.4:48.4:3.2) mixture to have a stable stock solution ($[A\beta_{42}]$=500 μM).[20, 40] Tested inhibitors were dissolved in MeOH and diluted in the assay buffer. Experiments were performed by incubating the peptide diluted in 10 mM phosphate buffer (pH 8.0) containing 10 mM NaCl at 30°C (Thermomixer Comfort, Eppendorf, Italy) for 24 h (final Aβ concentration=50 μM) with and without inhibitor.

Inhibition of Aβ₄₂ self-aggregation: ThT assay. Inhibition studies were performed by incubating $A\beta_{42}$ samples in the assay conditions reported above, with and without tested inhibitors. Inhibitors were first screened at 50 μM in a 1:1 ratio with $A\beta_{42}$. To quantify amyloid fibril formation, the ThT fluorescence method was used.[41] After incubation, samples were diluted to a final volume of 2.0 mL with 50 mM glycine-NaOH buffer (pH = 8.5) containing 1.5 μM ThT. A 300-seconds-time scan of fluorescence intensity was carried out (λ_{exc} = 446 nm; λ_{em} = 490 nm), and values at plateau were averaged after subtracting the background fluorescence of 1.5 μM ThT solution. Blanks containing inhibitor and ThT were also prepared and evaluated to account for quenching and fluorescence properties. The fluorescence intensities were compared and the % inhibition was calculated. For compounds **7**, **9**, **11** and **12**, the IC_{50} value was also determined. To this aim four increasing concentrations were tested. IC_{50} value was obtained from the % inhibition *vs* log[inhibitor] plot.

Reagents for cellular experiments. All culture media, supplements and Foetal Bovine Serum (FBS) were obtained from Euroclone (Life Science Division, Milan, Italy). Electrophoresis reagents were obtained from Bio-Rad (Hercules, CA, USA). All other reagents were of the highest grade available and were purchased from Merck KGaA

(Darmstadt, Germany) unless otherwise indicated. $A\beta_{42}$ was solubilized in dimethyl sulfoxide (DMSO) at the concentration of 100 µM and frozen in stock aliquots. All the experiments performed with $A\beta$ were made in 1% of serum. H_2O_2 was diluted to working concentration (300 µM) in phosphate buffer saline (PBS) at the moment of use.

Cell cultures. Human neuroblastoma SH-SY5Y cell line from European Collection of Cell Cultures (ECACC No. 94030304) were cultured in medium with equal amount of Eagle's minimum essential medium and Nutrient Mixture Ham's F-12, supplemented with 10% foetal bovine serum, glutamine (2mM), penicillin/streptomycin, non-essential aminoacids at 37 °C in 5% CO_2/95% air.

Cell viability. The mitochondrial dehydrogenase activity that reduces 3-(4,5-dimethylthiazol-2-yl)-2,5-diphenyl-tetrazolium bromide (MTT, Sigma, St Louis, MO, USA) was used to determine cellular viability, in a quantitative colorimetric assay. At day 0 SH-SY5Y cells were plated at a density of 2.5×10^4 viable cells per well in 96-well plates. After treatment, according to the experimental setting, cells were exposed to an MTT solution in PBS (1 mg/mL). Following 4 h incubation with MTT and treatment with SDS for 24 h, cell viability reduction was quantified by using a Synergy HT multi-detection microplate reader (Bio-Tek).

Measurement of intracellular ROS. DCFH-DA (Merck KGaA, Darmstadt, Germany) was used to estimate intracellular ROS. Two different experimental settings were performed. First, cells were loaded with 25 µM DCFH-DA for 45 min. After centrifugation DCFH-DA was removed and cells were exposed to 5 µM of compounds **1-13** and 300 µM H_2O_2. Alternatively, cells (2×10^4 cells/well) were pretreated to compounds **1-13** (5 µM) for 24 h and then loaded with 25 µM DCFH-DA at 37°C for 45 min. DCFH-DA

was removed after centrifuge and cells were resuspended in PBS and then exposed to 300 μM H_2O_2. The results were visualized using Synergy HT multi-detection microplate reader (BioTek) with excitation and emission wavelengths of 485 nm and 530 nm, respectively.

Immunodetection of Nrf2 and NQO-1. Cell monolayers were washed twice with ice cold PBS, lysed on the tissue culture dish by addition of ice-cold lysis buffer (50 mM Tris/HCl pH 7.4, 150 mM NaCl, 50 mM EDTA, 0.2 mM 4-(2-aminoethyl) benzenesulfonyl fluoride hydrochloride (AEBSF), 20 µg/mL leupeptin, 25 µg/mL aprotinin, 0,5 µg/mL pepstatin A and 1% Triton X-100) and an aliquot was used for protein analysis with the Bradford assay, for protein quantification. Cell lysates were diluited in sample buffer (62.5 mM Tris/HCl pH 6.8, 2% SDS, 10% glycerol, 50 mM dithiothreitol, 0.1% Bromophenol blue) and subjected to Western blot analysis. Proteins were subjected to SDS-PAGE (10%) and then transferred onto PVDF membrane 0,45 µm (Merck KGaA Darmstadt, Germany). The membrane was blocked for 1 h with 5% BSA in Tris-buffered saline containing 0.1% Tween 20 (TBST). Membranes were immunoblotted with the rabbit anti human Nrf2 polyclonal antibody (at 1:2000 in 5% BSA) and the mouse anti-NQO-1 monoclonal antibody (1:1000 in 5% BSA) (Novus, Bio-techne Minneapolis, USA). The detection was carried out by incubation with horseradish peroxidase conjugated goat anti-rabbit IgG for Nrf-2 or rabbit anti-mouse for NQO-1 (1:5000 dilution in 5% BSA, from Merck KGaA Darmstadt, Germany) for 1 h. The blots were then washed extensively and the proteins of interest were visualized using an enhanced chemiluminescent method (Pierce, Rockford, IL, USA). Tubulin was also performed as a normal control of proteins (Merck KGaA Darmstadt, Germany).

Subcellular fractionation for Nrf2 nuclear translocation. 5×10^6 SH-SY5Y cells were seeded in 100mm^2 dishes and treated for 3 h with 5

μM compounds **1**, **5**, **7**, **9**, **11**, **13**; afterwards the medium was removed, and cells were washed twice with ice-cold PBS. Cells were subsequently homogenized 15 times using a glass-glass dounce homogenizer in 0.32 M sucrose buffered with 20 mM Tris-HCl (pH 7.4) containing 2 mM EDTA, 0,5 mM EGTA, 50 mM β-mercaptoethanol, and 20μg/mL leupeptin, apotrinin and pepstatin. The homogenate was centrifuged at 300×g for 5 min to obtain the nuclear fraction. An aliquot of the nuclear fraction was used for protein assay by the Bradford method, whereas the remaining was boiled for 5 min after dilution with sample buffer and subjected to polyacrylamide gel electrophoresis and immunoblotting as described.

Densitometry and statistics. All the experiments, unless specified, were performed at least three times. Following acquisition of the Western blot image through an AGFA scanner and analysis by means of the Image 1.47 program (Wayne Rasband, NIH, Research Services Branch, NIMH, Bethesda, MD, USA), the relative densities of the bands were expressed as arbitrary units and normalized to data obtained from control sample run under the same conditions. Data were analyzed by analysis of variance (ANOVA) followed when significant by an appropriate post hoc comparison test as indicated in figure legend. The reported data are expressed as means ± SEM of at least three independent experiments. A p value < 0.05 was considered statistically significant.

Author Contributions

M.R., C.L., E.S. participated in research design; M.R., C.L., M.B. and E.S. analysed results and wrote the manuscript with input from all coauthors; M.R., C.L., M.B., A.M., M.R., E.S. conceived the methodology, designed experiments and analysed data. E.S., R.C. and C.M. afforded synthesis and characterization of compounds; M.B. ran experiments on amyloid aggregation; M.M.S. performed cellular experiments.

Abbreviations

AD, Alzheimer's disease; Aβ, amyloid-β peptide; ANOVA, analysis of variance; DCFH-DA, dichlorodihydrofluorescein diacetate; DCC, *N*,*N*'-dicyclohexylcarbodiimide; DMAP, 4-dimethylaminopyridine; DMF, *N*,*N*-dimethylformamide; DMSO, dimethyl sulfoxide; ESI-MS, electrospray ionisation mass spectrometry; FBS, Foetal Bovine Serum, GST, glutathione S-transferase; HPLC, high performance liquid chromatography; HO-1, heme oxygenase-1; Keap 1, Kelch-like ECH-associated protein 1; MTT, 3-(4,5-dimethylthiazol-2-yl)-2,5-diphenyl-tetrazolium bromide; NMR, nuclear magnetic resonance; NQO1, NAD(P)H:quinone reductase; Nrf2, nuclear factor (erythroid-derived 2)-like 2; PBS, phosphate buffer saline; ppm, parts per millions; SAR, structure-activity relationships; TBDMS, *tert*-butyldimethylsilyl; TBAF, tetrabutylammonium fluoride; TBDMS-Cl, *tert*-butyldimethylsilyl chloride; TBST, Tris-buffered saline containing 0.1% Tween 20; THF, tetrahydrofuran; TLC, thin layer chromatography; TMS, tetramethylsilane; ThT, thioflavin T; UV, ultraviolet.

References

1. Winblad, B., Amouyel, P., Andrieu, S., Ballard, C., Brayne, C., Brodaty, H., Cedazo-Minguez, A., Dubois, B., Edvardsson, D., Feldman, H., Fratiglioni, L., Frisoni, G. B., Gauthier, S., Georges, J., Graff, C., Iqbal, K., Jessen, F., Johansson, G., Jönsson, L., Kivipelto, M., Knapp, M., Mangialasche, F., Melis, R., Nordberg, A., Rikkert, M. O., Qiu, C., Sakmar, T. P., Scheltens, P., Schneider, L. S., Sperling, R., Tjernberg, L. O., Waldemar, G., Wimo, A., and Zetterberg, H. (2016) Defeating Alzheimer's disease and other dementias: a priority for European science and society. Lancet Neurol. 15, 455-532.

2. Iqbal, K., and Grundke-Iqbal, I. (2010) Alzheimer's disease, a multifactorial disorder seeking multitherapies. Alzheimers Dement. 6, 420-424.

3. Reiman, E. M. (2016) Alzheimer's disease: Attack on amyloid-β protein. Nature 537, 36-37.

4. Kuruva, C. S., and Reddy, P. H. (2017) Amyloid beta modulators and neuroprotection in Alzheimer's disease: a critical appraisal. Drug Discov. Today 22, 223-233.

5. Herrup, K. (2015) The case for rejecting the amyloid cascade hypothesis. Nat. Neurosci. 18, 794-799.

6. Rosini, M., Simoni, E., Bartolini, M., Soriano, E., Marco-Contelles, J., Andrisano, V., Monti, B., Windisch, M., Hutter-Paier, B., McClymont, D. W., Mellor, I. R., and Bolognesi, M. L. (2013) The bivalent ligand approach as a tool for improving the in vitro anti-Alzheimer multitarget profile of dimebon. ChemMedChem 8, 1276-1281.

7. Viayna, E., Sola, I., Bartolini, M., De Simone, A., Tapia-Rojas, C., Serrano, F. G., Sabaté, R., Juárez-Jiménez, J., Pérez, B., Luque, F. J., Andrisano, V., Clos, M. V., Inestrosa, N. C., and Muñoz-Torrero, D. (2014) Synthesis and multitarget biological profiling of a novel family of rhein derivatives as disease-modifying anti-Alzheimer agents. J. Med. Chem. 57, 2549-2567.

8. Prati, F., De Simone, A., Bisignano, P., Armirotti, A., Summa, M., Pizzirani, D., Scarpelli, R., Perez, D. I., Andrisano, V., Perez-Castillo, A., Monti, B., Massenzio, F., Polito, L., Racchi, M., Favia, A. D., Bottegoni, G., Martinez, A., Bolognesi, M. L., and Cavalli, A. (2015) Multitarget drug discovery for Alzheimer's disease: triazinones as BACE-1 and GSK-3β inhibitors. Angew. Chem. Int. Ed. Engl. 54, 1578-1582.

9. Minarini, A., Milelli, A., Tumiatti, V., Rosini, M., Simoni, E., Bolognesi, M. L., Andrisano, V., Bartolini, M., Motori, E.,

Angeloni, C., and Hrelia, S. (2012) Cystamine-tacrine dimer: a new multi-target-directed ligand as potential therapeutic agent for Alzheimer's disease treatment. Neuropharmacology 62, 997-1003.

10. Rosini, M., Simoni, E., Milelli, A., Minarini, A., and Melchiorre, C. (2014) Oxidative stress in Alzheimer's disease: are we connecting the dots? J. Med. Chem. 57, 2821-2831.

11. Butterfield, D. A., Swomley, A. M., and Sultana, R. (2013) Amyloid β-peptide (1-42)-induced oxidative stress in Alzheimer disease: importance in disease pathogenesis and progression. Antioxid. Redox. Signal. 19, 823-835.

12. Swomley, A. M., Förster, S., Keeney, J. T., Triplett, J., Zhang, Z., Sultana, R., and Butterfield, D. A. (2014) Abeta, oxidative stress in Alzheimer disease: evidence based on proteomics studies. Biochim. Biophy. Acta 1842, 1248-1257.

13. Wilson, A. J., Kerns, J. K., Callahan, J. F., and Moody, C. J. (2013) Keap calm, and carry on covalently. J. Med. Chem. 56, 7463-7476.

14. Itoh, K., Chiba, T., Takahashi, S., Ishii, T., Igarashi, K., Katoh, Y., Oyake, T., Hayashi, N., Satoh, K., Hatayama, I., Yamamoto, M., and Nabeshima, Y. (1997) An Nrf2/small Maf heterodimer mediates the induction of phase II detoxifying enzyme genes through antioxidant response elements. Biochem. Biophys. Res. Commun. 236, 313-322.

15. Lu, M. C., Ji, J. A., Jiang, Z. Y., and You, Q. D. (2016) The Keap1-Nrf2-ARE Pathway As a Potential Preventive and Therapeutic Target: An Update. Med. Res. Rev. 36, 924-963.

16. Ramsey, C. P., Glass, C. A., Montgomery, M. B., Lindl, K. A., Ritson, G. P., Chia, L. A., Hamilton, R. L., Chu, C. T., and Jordan-Sciutto, K. L. (2007) Expression of Nrf2 in neurodegenerative diseases. J. Neuropathol. Exp. Neurol. 66, 75-85.

17. Joshi, G., Gan, K. A., Johnson, D. A., and Johnson, J. A. (2015) Increased Alzheimer's disease-like pathology in the APP/ PS1ΔE9 mouse model lacking Nrf2 through modulation of autophagy. Neurobiol. Aging 36, 664-679.

18. Simoni, E., Serafini, M. M., Bartolini, M., Caporaso, R., Pinto, A., Necchi, D., Fiori, J., Andrisano, V., Minarini, A., Lanni, C., and Rosini, M. (2016) Nature-Inspired Multifunctional Ligands: Focusing on Amyloid-Based Molecular Mechanisms of Alzheimer's Disease. ChemMedChem 11, 1309-1317.

19. Xia, C. N., Li, H. B., Liu, F., and Hu, W. X. (2008) Synthesis of trans-caffeate analogues and their bioactivities against HIV-1 integrase and cancer cell lines. Bioorg. Med. Chem. Lett. 18, 6553-6557.

20. Bartolini, M., Naldi, M., Fiori, J., Valle, F., Biscarini, F., Nicolau, D. V., and Andrisano, V. (2011) Kinetic characterization of amyloid-beta 1-42 aggregation with a multimethodological approach. Anal. Biochem. 414, 215-225.

21. Simoni, E., Caporaso, R., Bergamini, C., Fiori, J., Fato, R., Miszta, P., Filipek, S., Caraci, F., Giuffrida, M. L., Andrisano, V., Minarini, A., Bartolini, M., and Rosini, M. (2016) Polyamine Conjugation as a Promising Strategy To Target Amyloid Aggregation in the Framework of Alzheimer's Disease. ACS Med. Chem. Lett. 7, 1145-1150.

22. Rosini, M., Simoni, E., Caporaso, R., and Minarini, A. (2016) Multitarget strategies in Alzheimer's disease: benefits and challenges on the road to therapeutics. Future Med. Chem. 8, 697-711.

23. Sabella, S., Quaglia, M., Lanni, C., Racchi, M., Govoni, S., Caccialanza, G., Calligaro, A., Bellotti, V., and De Lorenzi, E. (2004) Capillary electrophoresis studies on the aggregation process of beta-amyloid 1-42 and 1-40 peptides. Electrophoresis 25, 3186-3194.

24. Pouplana, S., Espargaro, A., Galdeano, C., Viayna, E., Sola, I., Ventura, S., Muñoz-Torrero, D., and Sabate, R. (2014) Thioflavin-S staining of bacterial inclusion bodies for the fast, simple, and inexpensive screening of amyloid aggregation inhibitors. Curr. Med. Chem. 21, 1152-1159.

25. Baird, L., and Dinkova-Kostova, A. T. (2011) The cytoprotective role of the Keap1-Nrf2 pathway. Arch. Toxicol. 85, 241-272.

26. Suzuki, T., and Yamamoto, M. (2015) Molecular basis of the Keap1-Nrf2 system. Free Radic Biol Med 88, 93-100.

27. Abed, D. A., Goldstein, M., Albanyan, H., Jin, H., and Hu, L. (2015) Discovery of direct inhibitors of Keap1-Nrf2 protein-protein interaction as potential therapeutic and preventive agents. Acta Pharm. Sin. B 5, 285-299.

28. Jiang, Z. Y., Lu, M. C., and You, Q. D. (2016) Discovery and Development of Kelch-like ECH-Associated Protein 1. Nuclear Factor Erythroid 2-Related Factor 2 (KEAP1:NRF2) Protein-Protein Interaction Inhibitors: Achievements, Challenges, and Future Directions. J. Med. Chem. 59, 10837-10858.

29. Magesh, S., Chen, Y., and Hu, L. (2012) Small molecule modulators of Keap1-Nrf2-ARE pathway as potential preventive and therapeutic agents. Med. Res. Rev. 32, 687-726.

30. Kobayashi, M., and Yamamoto, M. (2006) Nrf2-Keap1 regulation of cellular defense mechanisms against electrophiles and reactive oxygen species. Adv. Enzyme Regul. 46, 113-140.

31. Satoh, T., Stalder, R., McKercher, S. R., Williamson, R. E., Roth, G. P., and Lipton, S. A. (2015) Nrf2 and HSF-1 Pathway Activation via Hydroquinone-Based Proelectrophilic Small Molecules is Regulated by Electrochemical Oxidation Potential. ASN Neuro. 7.

32. Satoh, T., McKercher, S. R., and Lipton, S. A. (2014) Reprint of: Nrf2/ARE-mediated antioxidant actions of pro-electrophilic drugs. Free Radic. Biol. Med. 66, 45-57.

33. Lipton, S. A., Rezaie, T., Nutter, A., Lopez, K. M., Parker, J., Kosaka, K., Satoh, T., McKercher, S. R., Masliah, E., and Nakanishi, N. (2016) Therapeutic advantage of pro-electrophilic drugs to activate the Nrf2/ARE pathway in Alzheimer's disease models. Cell Death Dis. 7, e2499.

34. Deny, L. J., Traboulsi, H., Cantin, A. M., Marsault, É., Richter, M. V., and Bélanger, G. (2016) Bis-Michael Acceptors as Novel Probes to Study the Keap1/Nrf2/ARE Pathway. J. Med. Chem. 59, 9431-9442.

35. Rattanangkool, E., Kittikhunnatham, P., Damsud, T., Wacharasindhu, S., and Phuwapraisirisan, P. (2013) Quercitylcinnamates, a new series of antidiabetic bioconjugates possessing α-glucosidase inhibition and antioxidant. Eur. J. Med. Chem. 66, 296-304.

36. Allegretta, G., Weidel, E., Empting, M., and Hartmann, R. W. (2015) Catechol-based substrates of chalcone synthase as a scaffold for novel inhibitors of PqsD. Eur. J. Med. Chem. 90, 351-359.

37. Cervellati, R., Galletti, P., Greco, E., Cocuzza, C. E., Musumeci, R., Bardini, L., Paolucci, F., Pori, M., Soldati, R., and Giacomini, D. (2013) Monocyclic β-lactams as antibacterial agents: facing antioxidant activity of N-methylthio-azetidinones. Eur. J. Med. Chem. 60, 340-349.

38. Toneto Novaes, L. F., Martins Avila, C., Pelizzaro-Rocha, K. J., Vendramini-Costa, D. B., Pereira Dias, M., Barbosa Trivella, D. B., Ernesto de Carvalho, J., Ferreira-Halder, C. V., and Pilli, R. A. (2015) (-)-Tarchonanthuslactone: Design of New Analogues, Evaluation of their Antiproliferative Activity on Cancer Cell Lines, and Preliminary Mechanistic Studies. ChemMedChem 10, 1687-1699.

39. Rajan, P., Vedernikova, I., Cos, P., Berghe, D. V., Augustyns, K., and Haemers, A. (2001) Synthesis and evaluation of caffeic acid amides as antioxidants. Bioorg. Med. Chem. Lett. 11, 215-217.

40. Bartolini, M., Bertucci, C., Bolognesi, M. L., Cavalli, A., Melchiorre, C., and Andrisano, V. (2007) Insight into the kinetic of amyloid beta (1-42) peptide self-aggregation: elucidation of inhibitors' mechanism of action. ChemBioChem 8, 2152-2161.

41. Naiki, H., Higuchi, K., Hosokawa, M., and Takeda, T. (1989) Fluorometric determination of amyloid fibrils in vitro using the fluorescent dye, thioflavin T1. Anal. Biochem. 177, 244-249.

Part 4.

The following manuscript is in preparation for the submission to Free Radical Biology and Medicine as:

Modulation of the oxidative stress response through the activation of the Nrf2 pathway by nature-inspired hybrids

Melania Maria Serafini,[1,2] Michele Catanzaro,[1] Elena Simoni,[3] Marco Dacrema,[1] Marco Racchi,[1] Michela Rosini,[3] Maria Daglia,[1] and Cristina Lanni[*1]

[1]*Department of Drug Sciences (Pharmacology Section), University of Pavia, V.le Taramelli 14, 27100 Pavia, Italy*

[2]*Scuola Universitaria Superiore IUSS Pavia, P.zza Vittoria 15, 27100 Pavia, Italy*

[3]*Department of Pharmacy and Biotechnology, Alma Mater Studiorum - University of Bologna, Via Belmeloro 6, 40126 Bologna, Italy*

Introduction

Every single cell in the human organism is continuously producing reactive oxygen and nitrogen species (ROS/RNS) as a physiological consequence of cellular energy metabolism reactions occurring in mitochondria. Furthermore, free radicals can be induced by exposure to different exogenous or endogenous insults. At low concentrations ROS/RNS play an important role in many physiological processes, but high levels of these free radicals can react with macromolecules such as proteins, lipids and nucleic acids, inducing modifications that can negatively affect cell function and lead to cell death. For this reason, organisms possesses antioxidant systems which act on ROS/RNS levels, bringing them under control by counteracting any increases. Oxidative stress is thus defined as the imbalance between oxidants and antioxidants, leading to the loss of redox signalling, the disruption of redox control, and possibly to molecular damage [1]. Oxidative stress is at the basis of many diseases, not often as a triggering cause, but more frequently as a mechanism that sustains other pathological processes promoting the progression of disease [2-4]. The identification of new molecules acting as modulators of this chain is therefore an open field of research, due to their potential application in a range of different disorders. In recent years increasing importance has been given to molecules with antioxidant properties. Nature has been found to be a rich source of compounds capable of modulating several protective pathways, and thus counteracting oxidative injuries.

The nuclear factor erythroid 2-related factor 2 (Nrf2) pathway is the main intrinsic mechanism of defense against oxidative stress in the cell [5]. The activation of this master regulator occurs in a redox-sensitive manner and induces the translocation of the Nrf2 transcription factor itself into the nucleus, where it binds to antioxidant response elements (ARE), also named electrophile-responsive element (EpRE), a cis-acting enhancer sequence located in the promoter region of genes encoding antioxidant and phase II

detoxifying enzymes such as NAD(P)H: quinone reductase-1 (NQO1), heme oxygenase-1 (HO-1) and glutathione S-transferase (GST).

In our previous papers, we identified newly-synthetized compounds inspired by nature. The main structure of these hybrids consists of diallyl sulfide (DAS), a garlic-derived organosulfur compound, and a phenolic ring which is a common feature of such molecules as curcumin, rosmarinic acid and coumarin, well known for their antioxidant properties [6-8]. Our previous data demonstrated the ability of these nature-inspired hybrids to act as scavenger agents in the presence of oxidant stressors [9, 10]. In particular, we identified a catechol derivative (compound 1) with remarkable anti-aggregating ability and antioxidant properties [9, 10]. Further to this molecule, other nature-inspired molecules have been designed by varying the length and/or the nature of the tether between the (pro-) electrophilic functions of compound 1.

The aim of this paper has been to use analysis of intracellular defensive pathways to better investigate the antioxidant activity and potency of structure-based selected natural hybrids, in comparison to that of two reference molecules: curcumin (CUR) and dimethyl fumarate (DMF).

CUR has been extensively studied in different pathological contexts and, while to date there are no confirmed applications in humans due to the failure of clinical trials, its antioxidant properties are well-known and confirmed by a plethora of publications [11-14].

DMF has been recently approved by the Food and Drug Administration (FDA) for the treatment of multiple sclerosis (MS) and its anti-inflammatory and antioxidant properties are reported in literature [reviewed in 15].

Based on our previous results, we have deepened our studies on the mechanism of action of selected nature-inspired hybrids on the Nrf2 cellular pathway, investigating their ability to modulate the expression of the Nrf2 transcription factor and its negative regulator

Keap1. In addition, we have further investigated the ability of our compounds to exert epigenetic effects, modulating specific miRNAs. MicroRNAs are small non-coding RNA molecules of about 22 nucleotides which play a role in RNA-silencing and post-transcriptional regulation of gene expression. In recent years, growing evidence has supported the ability of different natural products, such as polyphenols in general and curcumin in particular, to interact with selected miRNAs, thus targeting multiple genes and showing pleiotropic activity [16-20]. In line with these premises, the investigation of miRNA modulation could potentially be important in providing novel insights for a better understanding of the antioxidant activities of natural products and nature-inspired hybrids.

Material and Methods

Reagents. Nature-inspired hybrids, CUR and DMF were solubilized in DMSO (Merck KGaA, Darmstadt Germany) at stock concentrations and frozen ($-20°C$) in aliquots that were diluted immediately prior to use. For each experimental setting, one stock aliquot was thawed out and diluted to minimize compound damage due to repeated freeze and thaw cycles. The final concentration of DMSO in culture medium was <0.1%. Cell culture media and all supplements were from Merck (Merck KGaA, Darmstadt Germany). Rabbit polyclonal anti-human Nrf2 (NBP1-32822), mouse monoclonal anti-human NQO1 (NB200-209), and rabbit polyclonal anti-human HO-1 (NBP1-31341) antibodies were purchased from Novus (Biotechne, Minneapolis USA). Mouse monoclonal anti-human Keap1 antibody (MAB3024) was purchased from R&D Systems (Biotechne, Minneapolis USA). Mouse monoclonal anti-β-actin (612656) and mouse anti-lamin A/C (612162) antibodies were purchased from BD Biosciences (Franklin Lakes, NJ, USA). Finally, mouse anti-α-tubulin (sc-5286) and mouse anti GSS (sc-166882) antibodies were purchased from Santa Cruz Biotechnology (Dallas, Texas USA).

Cell cultures. All culture media, supplements and Foetal Bovine Serum (FBS) were purchased from Sigma Aldrich (Merck KGaA, Darmstadt Germany). Human neuroblastoma SH-SY5Y cells from the European Collection of Cell Cultures (ECACC No. 94030304) were cultured in a medium with equal amounts of Eagle's minimum essential medium and Nutrient Mixture Ham's F-12, supplemented with 10% heat-inactivated FBS, 2 mM glutamine, 0.1 mg/mL streptomycin, 100 IU·mL penicillin and non-essential aminoacids at 37 °C in 5% CO_2 and 95% air atmosphere.

Subcellular fractionation for the immunodetection of nuclear Nrf2. The expression of Nrf2 in nuclear cell lysates was assessed using Western blot analysis. Cell monolayers were washed twice with ice-cold PBS, harvested and subsequently homogenized 15 times using a glass-glass dounce homogenizer in ice-cold fractionation buffer (20 mM Tris/HCl pH 7.4, 2 mM EDTA, 0.5 mM EGTA, 0.32 M sucrose, 50 mM β-mercaptoethanol). The homogenate was centrifuged at 300×g for 5 min to obtain the nuclear fraction. An aliquot of the nuclear extract was used for protein quantification, whereas the remainder was prepared for western blot by mixing the nuclear cell lysate with 2X sample buffer (125 mM Tris-HCl pH 6.8, 4% SDS, 20% glycerol, 6% β-mercaptoethanol, 0.1% bromophenol blue) and then denaturing at 95°C for 5 min. Equivalent amounts of nuclear extracted proteins were loaded into a SDS-PAGE gel, electrophoresed under reducing conditions, transferred to a PVDF membrane (Merck KGaA, Darmstadt Germany) and then blocked for 1 h with 5% w/v BSA in Tris-buffered saline containing 0.1% Tween 20 (TBS-T). Membranes were immunoblotted with rabbit anti-human Nrf2 (1:2000) diluted in 5% w/v BSA in TBS-T. Detection was carried out by incubation with horseradish peroxidase conjugated goat anti-rabbit IgG (1:5000 dilution in 5% w/v BSA in TBS-T) for 1 h at room temperature. Membranes were then washed three times with TBS-T and proteins of interest were visualized using an enhanced

chemiluminescent reagent (Pierce, Rockford, IL, USA). Lamin A/C was performed as a control for gel loading.

Immunodetection of Nrf2, Keap1, NQO1, HO-1 and GSS. The expression of Nrf2, Keap1, NQO1, HO-1 and GSS in whole cell lysates was assessed by Western blot analysis. After treatment, cell monolayers were washed twice with ice-cold PBS, lysed on the culture dish by the addition of ice-cold homogenization buffer (50 mM Tris-HCl pH 7.5, 150 mM NaCl, 5 mM EDTA, 0.5% Triton X-100 and protease inhibitor mix) and an aliquot was used for protein quantification. Western blotting samples and SDS-PAGE gel electrophoresis were carried out as previously described. The proteins were visualized using primary antibodies for Nrf2 (1:2000) Keap1 (1:1000), NQO1 (1:2000), HO-1 (1:2000) or GSS (1:1000) and secondary horseradish peroxidase conjugated antibody (1:5000) diluted in 5% w/v BSA in TBS-T. Signal development was carried out using an enhanced chemiluminescent method (Pierce, Rockford, IL, USA). β-Actin or α-tubulin were performed as a control for gel loading.

Real-time PCR (RT-PCR). For RNA extraction, 2×10^6 cells were used. Total RNA was extracted using RNeasy Plus Mini Kit (Qiagen, Valencia, CA, USA) following the manufacturer's instructions. QuantiTect reversion transcription kit and QuantiTect Sybr Green PCR kit (Qiagen, Valencia, CA, USA) were used for cDNA synthesis and gene expression analysis, following the manufacturer's specifications. Nrf2, Keap1, NQO1, HO-1, GSS and GAPDH primers were provided by Qiagen. GAPDH was used as an endogenous reference. After the extraction procedure, the quantification of RNA was performed using a spectrophotometric method with FLUOstar® Omega (BMG LABTECH, Ortenberg, Germania), using the LVIS plate and following instructions from the instrument's operating manual: 2 µl of extracted RNA were spotted on the microdrop wells,

the absorbance was then read at 260 nm and 280 nm. The concentration of RNA was assessed using the 260 nm absorbance value, and the purity of the samples by calculating the 260/280 absorbance ratio. After quantification a RTII Retrotrascription Kit (Qiagen) was used to promote the retrotrascription of exclusively mature miRNA, with the following protocol: x µl of template RNA, where x is the number of µl according to the starting concentration of RNA as suggested for the procedure, were added to 2 µl of 5X HiSpec buffer, 2 µl of 10X mi Script Nucleic mix and 2 µl of miScript Reverse Transcriptase. Finally, RNAse-free water was added to reach a final volume of 20 µl. During the preparation of the mixture the samples were stored in ice, and then incubated in the SimpliAmp Thermal Cycler (ThermoFisher Scientific, Waltham, Massachusetts, USA) at 37 C° for 60 minutes and then at 95 C° for 5 minutes, to inactivate the transcriptase mixture. The cDNA of each sample was diluited with RNase-free water prior to start the Real Time PCR Procedure. To verify the expression of the miRNA targets a miScript® miRNA PCR Array (Qiagen) was used and, following the manufacturer's instructions, we performed the Real time PCR using StepOnePlus RT-PCR (Applied Biosystem, Foster City, California, USA). The primers were purchased from Qiagen, and in particular, specific forward primers were contained the in miScript® miRNA PCR Array, unlike the reverse primers, which were contained in the in miScript SYBR® Green PCR Array. The mixture used for the amplification of cDNA was suitable for the 96 well plates, in detail, 1375 µl of 2X Quantitect SYBR Green PCR Master Mix were added to 275 µl 10X miScript Universal Primer and 1000 µl of RNase free water. A volume of 24 µl of the previous mixture was added to each well. At the end 1 µl of cDNA sample was added to reach a final volume of 25 µl. For each plate the amplification conditions were set as shown: 95 °C for 15 minutes, 94 °C for 15 seconds, 55 °C for 30 seconds and, finally, 70 °C for 30 seconds. The last three steps were repeated for 45 cycles.

SNORD61 and RNU6-6P were used as endogenous controls to normalize the data obtained.

Densitometry and statistics. All experiments, unless specified, were performed at least three times with representative results being shown. Data are expressed as mean ± SEM. The acquisition of the Western blotting images was done through a scanner and the relative densities of the bands were analyzed with ImageJ software. Statistical analyses were performed using InStat software version 6.0 (GraphPad Software, La Jolla, CA, USA). Statistical differences were determined by analysis of variance (ANOVA) followed, when significant, by an appropriate post hoc test as indicated in figure legends. In order to investigate whether the treatments have influenced miRNA expression, we used Linear Mixed Models, including treatments as fixed terms and plates as random effects. In all miRNA figures shown, the points indicate the mean value, while the bars represent the standard error of the mean. In all reported statistical analyses, effects were designated as significant if p-value < 0.05. Statistical analyses were performed using R software version 3.4.1 [21].

Results

Modulation of Nrf2 and its negative regulator Keap1. In order to understand the molecular mechanisms at the basis of the antioxidant activity of newly-synthetized compounds inspired by nature, we decided to investigate the role of Nrf2 pathway as this plays a key role in orchestrating cellular antioxidant defenses and in maintaining redox homeostasis.

To analyze the activation of the Nrf2-mediated detoxification pathway we performed RT-PCR and western immunoblotting on SH-SY5Y human neuroblastoma cells exposed to 1, 5, 7, 9, 12, 13 and CUR at a concentration of 5μM or 20 μM DMF for 24 h.

These concentrations were chosen based on literature data [10, 22] and on cell viability assays on our cellular model (data not shown).
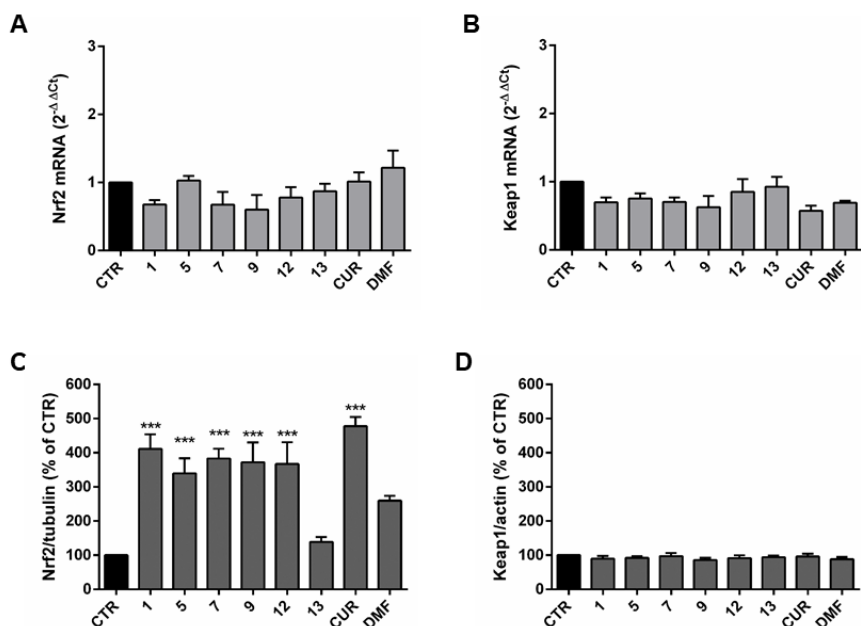

Figure 1. Activation of Nrf2-mediated phase II detoxification pathway. RNA from total cellular extracts of SH-SY5Y cells treated for 24 h with 5 μM of compounds were analyzed for Nrf2 **(A)** and Keap1 **(B)** mRNA expression by RT-PCR. GAPDH was used as housekeeping gene. Results are shown as average ± SEM; no statistically significant data with Dunnett's multiple comparison test. Cellular extracts of SH-SY5Y cells treated for 24 h with compounds at 5 μM were analyzed for Nrf2 **(C)** and Keap1 **(D)** protein levels by Western blot. Anti-tubulin was used as protein loading control. Results are shown as ratio (% of CTR) ± SEM; *$p < 0.05$, **$p < 0.01$ and ***$p < 0.001$ versus CTR; Dunnett's multiple comparison test.

All compounds tested did not affect the mRNA expression of Nrf2 (Figure 1A) and Keap1 (Figure 1B) or the protein levels of Keap1 (Figure 1D). However, a strong increase in Nrf2 protein expression (Figure 1C) is induced by CUR and all hybrid compounds with the exception of 13. DMF treatment, though it did not produce statistically significant results in our experimental setting, showed a trend of increase with a mean value that is more than double that of the control (mean: 259.93 % of CTR). Altogether, these results show that all tested compounds, with the exception of 13, can modulate Nrf2 protein levels, but do not act at the transcriptional level.

In basal conditions, the Nrf2 transcription factor is found in the cytoplasm bound to the Keap1 protein. Keap1 recruits the Cul3 ubiquitin-E3 ligase which adds ubiquitin molecules to the Nrf2 protein, and the ubiquitinated Nrf2 is directed towards the proteasome to be degraded [23, 24].

Our data demonstrates that there is no change in the transcription levels of Nrf2 and Keap1 and in the protein levels of Keap1, and the increase in Nrf2 protein levels in the whole cell is therefore not due to a decreased transcription or translation of the negative regulator Keap1. On the basis of these results, we hypothesized that the compounds might interact with Keap1 molecules preventing their binding to Nrf2, and thus the recruitment of the Cul3 ubiquitin-E3 ligase and the ubiquitination process. Free Nrf2 in the cytoplasm could then escape proteasome targeting and migrate into the nucleus to carry out its activities as a transcription factor.

Nuclear translocation of the Nrf2 transcription factor. We further examined the potency of these compounds in terms of inducing the nuclear localization of Nrf2 in neuroblastoma cells, this property being necessary to assess the complete activation of the Nrf2 pathway, in comparison with CUR and DMF. Simultaneously, in order to determine the specific moieties responsible for the activation of the transcription factor, a structure–activity relationship (SAR) was

conducted on these compounds. Data from literature suggested that the nucleophilic (catechol) moiety and/or the electrophilic (Michael acceptor) moiety are important for Nrf2 induction [25, 26] and the six hybrids investigated differ from each other by the presence or absence of these two functional groups (Scheme 1). In fact, 1 and 7 have a double bond in the lateral chain which might act as a Michael acceptor and posses the catecholic group, 9 and 12 are without the double bond, 5 is without the catechol group and 13 is lacking both nucleophilic and electrophilic moieties. Moreover, we investigated the action of CUR and DMF as positive controls.
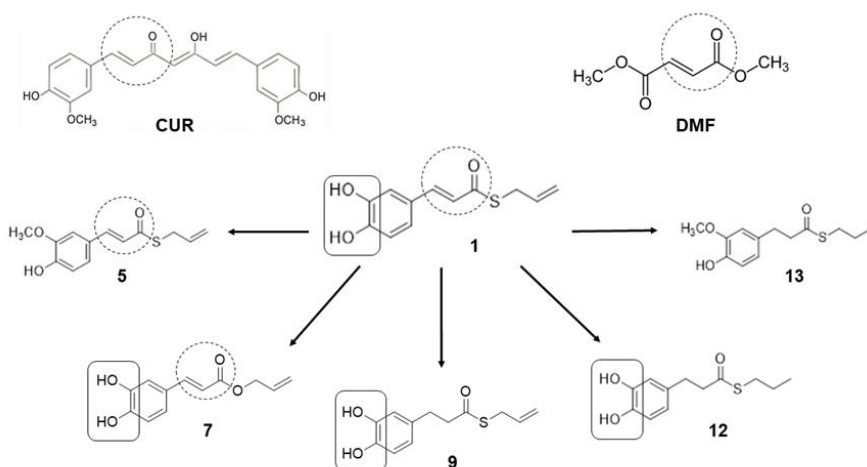
Scheme 1. Chemical structure of nature-inspired new hybrids. Dashed line circle boxes represent Michael acceptor electrophilic functions. Full line squared box represent catechol nucleophilic functions.

SH-SY5Y cells were treated with different concentrations of compounds: 5 µM, 500 nM and 50 nM of 1, 5, 7, 9, 12, 13 and CUR or 20 µM, 2 µM and 200 nM of DMF. The concentrations of DMF were chosen based on literature data [27-29] and preliminary experiments on our cell model (data not shown). As shown in figure 2, all tested compounds, with the exception of 13, induced nuclear translocation of Nrf2 at their highest concentration.

Moreover, 1 and 12 also significantly induced Nrf2 nuclear localization at the lower 500 nM concentration, thus revealing themselves to be more potent than the reference compounds curcumin and DMF. None of the molecules were found to act on the Nrf2 pathway at the lowest concentrations investigated.
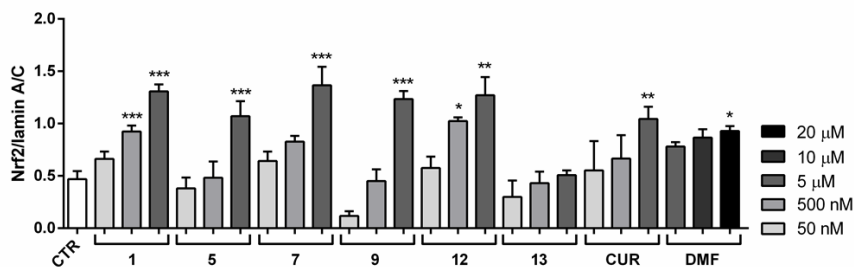

Figure 2. Nrf2 nuclear translocation. Nuclear cellular extracts of SH-SY5Y cells were treated for 3 h at 5 µM, 500 nM and 50 nM. Nrf2 expression in the nucleus was determined by Western blot. Anti-lamin A/C was used as protein loading control. Results are shown as ratio Nrf2/lamin A/C ± SEM; *$p < 0.05$, **$p < 0.01$ and ***$p < 0.001$ versus CTR; Dunnett's multiple comparison test.

Activation of the Nrf2 target genes. To complete the analysis of the activation of the Nrf2 pathway, the expression of two Nrf2 target genes has been further evaluated. Once in the nucleus, Nrf2 binds to the ARE sequences in the promoter region of its target genes inducing phase II cytoprotective genes related to the cellular stress response, such as NAD(P)H quinone oxidoreductase-1 (NQO1) and heme oxygenase-1 (HO-1). mRNA and protein levels of these two genes were evaluated by RT-PCR and western immunoblotting in SH-SY5Y neuroblastoma cells treated with 5 µM 1, 5, 7, 9, 12, 13 and CUR, or 20 µM DMF for 24 h. As shown in figure 3, all compounds, with the exception of 13 and CUR, induced an increase in NQO1 mRNA levels (Figure 3A) followed by the increase in NQO1 protein (Figure 3C).

In a similar way, the mRNA (Figure 3B) and protein (Figure 3D) levels of HO-1 are positively modulated by all hybrids except for 13 and CUR. The increase in the transcription and translation of two Nrf2 target genes demonstrated the complete activation of the Nrf2 pathway.
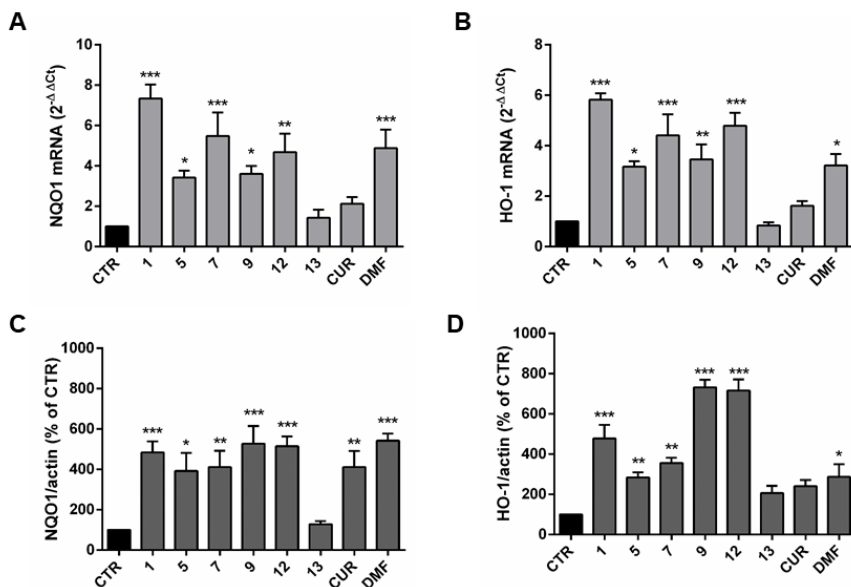

Figure 3. Nrf2 target activation. RNA from total cellular extracts of SH-SY5Y cells treated for 24 h with 5 μM of compounds were analyzed for NQO1 **(A)** and HO-1 **(B)** mRNA expression by RT-PCR. GAPDH was used as housekeeping gene. Results are shown as average ± SEM; *$p < 0.05$, **$p < 0.01$ and ***$p < 0.001$ versus CTR; Dunnett's multiple comparison test. Cellular extracts of SH-SY5Y cells treated for 24 h with compounds at 5 μM were analyzed for NQO1 **(C)** and HO-1 **(D)** protein levels by Western blot. Anti-actin was used as protein loading control. Results are shown as ratio (% of CTR) ± SEM; *$p < 0.05$, **$p < 0.01$ and ***$p < 0.001$ versus CTR; Dunnett's multiple comparison test.

To better understand the discrepancy between the obtained data and the loss of efficacy of CUR on target gene activation in comparison with the nature-inspired hybrid compounds, we further evaluated

whether the duration of the treatment used for the investigation of the mRNA and protein levels of Nrf2 target genes was consistent. We thus performed a time course with compound 1, as an example of the most potent hybrid compound, and CUR. SH-SY5Y cells were treated with 5 μM 1 or CUR for 3, 6, 9 and 16 h. NQO1 (Figure 4A and 4B) and HO-1 (Figure 4C and 4D) mRNA are differently regulated in time with NQO1 slowly increasing and HO-1 being boosted for 3 h and then decreasing with time.
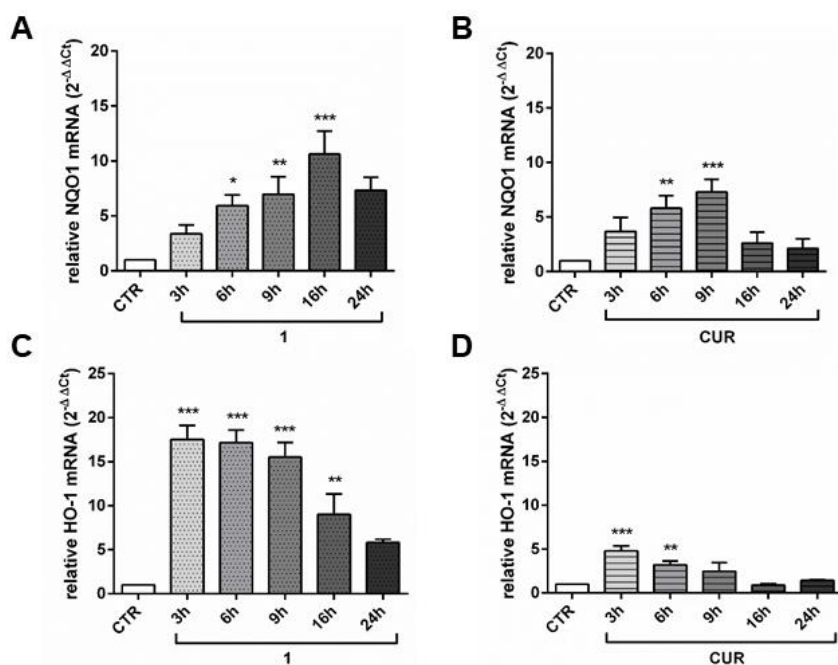

Figure 4. Time course of NQO1 and HO-1 mRNA modulation. RNA from total cellular extracts of SH-SY5Y cells treated for 3, 6, 9 and 16 h with 5 μM of compounds 1 and CUR were analyzed for NQO1 (**A, B**) or HO-1 (**C, D**) relative mRNA expression by RT-PCR. GAPDH was used as housekeeping gene. Results are shown as average ± SEM; *$p < 0.05$, **$p < 0.01$ and ***$p < 0.001$ versus CTR; Dunnett's multiple comparison test.

Treatment with compound 1 induced a significant increase in relative NQO1 mRNA levels from 6 h to 16 h, whereas CUR treatment induced an increase at 6 h which reached a peak at 9 h and then lost statistical significance by 16 h. On the contrary, the treatment with compound 1 induced a strong increase in HO-1 mRNA levels, already statistically significant at 3 h, then decreasing with time. The effect of curcumin is similar to that of hybrid 1, though the increase in the HO-1 mRNA levels is smaller. Taken together, these results could explain the previous data on NQO1 and HO-1 mRNA levels at 24 h.

Modulation of hsa-miR-125b-5p. To evaluate the mechanism through which structure-based selected natural hybrids exert their antioxidant activity, in comparison to CUR, we determined the expression levels of hsa-miR-125b-5p in SH-SY5Y cell cultures treated with 1, 5, 7, 9, 12, 13 compounds and CUR at different concentrations (5 µM, 500 nM and 50 nM).
Literature data indicate that hsa-miR-125b-5p is involved in the oxidative stress response, showing mRNA targets coding for glutathione sythetase (GSS). Total RNA was extracted from treated and control cells, as according to the Material and Methods section, and RT-PCR assays were performed.
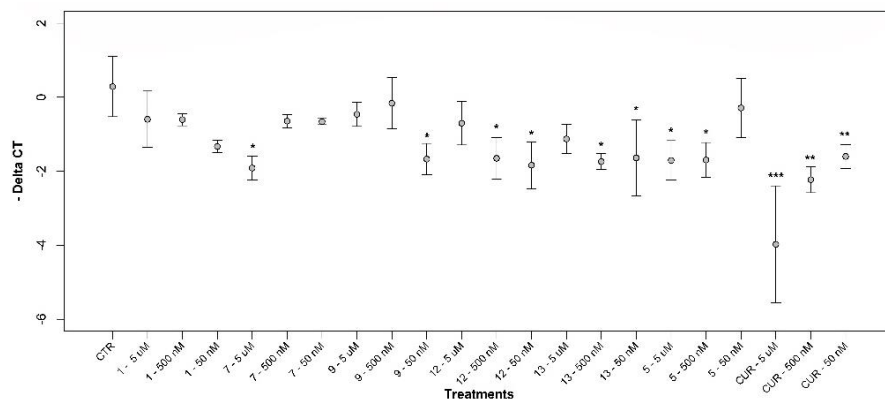
Figure 5. hsa-miR-125b-5p modulation. Expression levels (-Delta CT) of hsa-miR-125b-5p in human neuroblastoma SH-SY5Y cells treated with compounds and CUR at different concentrations (50 nM, 500 nM and 5 μM); *p < 0.05, **p < 0.01 and ***p < 0.001 versus CTR.

As far as hsa-miR-125b-5p is concerned, the results obtained following statistical analysis suggest that the expression levels of this miRNA are downregulated after treatment with CUR at all concentrations (Figure 5). In addition, statistically significant differences were registered for the following treatments: 5 (5 μM and 500 nM), 7 (5 μM), 9 (50 nM), 12 (500 nM and 50 nM), 13 (500 nM and 50 nM). The decrease of hsa-miR-125b-5p after the treatments with 1, 5, 7, 9, 12, 13 compounds and CUR at different concentrations, confirms that they have the capacity to modulate miRNAs involved in protection against oxidative stress.
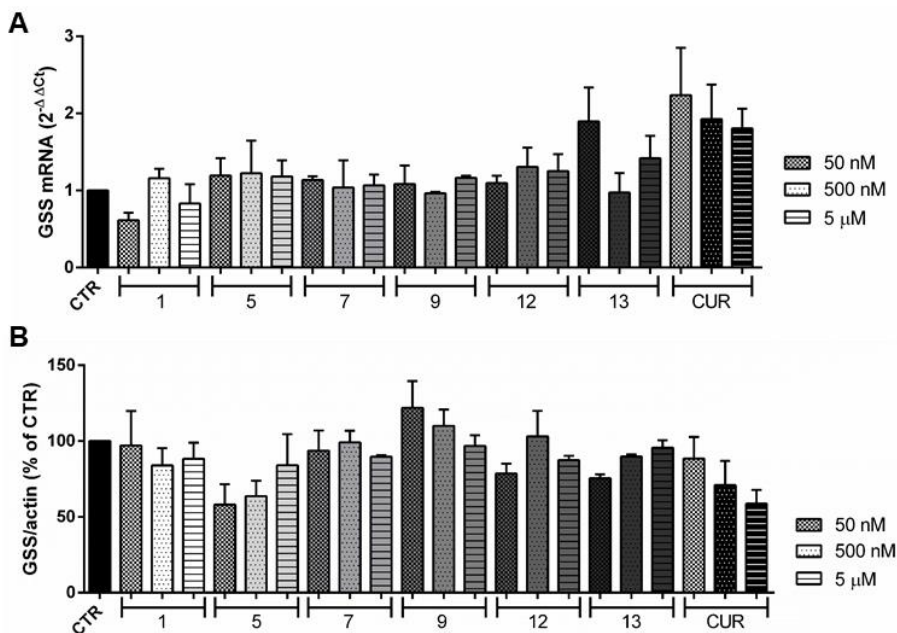
Figure 6. GSS mRNA and protein expression. (A) RNA from total cellular extracts of SH-SY5Y cells treated for 24 h with 5 μM, 500 nM or 50 nM of compounds were analyzed for GSS mRNA expression by RT-PCR. GAPDH was used as housekeeping gene. Results are shown as average ± SEM. **(B)** Cellular extracts of SH-SY5Y cells treated for 24 h with 5 μM, 500 nM or 50 nM compounds were analyzed for GSS protein levels by Western blot. Anti-actin was used as protein loading control. Results are shown as ratio (% of CTR) ± SEM.

Nevertheless, the tested compounds did not increased the expression levels of mRNA coding for GSS (Figure 6 A) and did not modify the expression levels of the protein itself (Figure 6 B), suggesting that the process of GSS synthesis is regulated by other molecular mechanisms and the modulation of this mRNA is not strictly under the control of miR-125-5p, which could act with other miRNAs, giving rise to synergistic and/or antagonistic effects.

References

1. Sies H, Jones D. Oxidative Stress, 2nd edition in Fink G. (Ed.), Encyclopedia of Stress, 3, Elsevier, Amsterdam (2007) 45-48.
2. Reuter S, Gupta SC, Chaturvedi MM, Aggarwal BB. Oxidative stress, inflammation, and cancer: how are they linked? Free Radic Biol Med. 2010 Dec 1;49(11):1603-16. doi: 10.1016/j.freeradbiomed.2010.09.006.
3. Dias V, Junn E, Mouradian MM. The role of oxidative stress in Parkinson's disease. J Parkinsons Dis. 2013;3(4):461-91. doi: 10.3233/JPD-130230.
4. Cheignon C, Tomas M, Bonnefont-Rousselot D, Faller P, Hureau C, Collin F. Oxidative stress and the amyloid beta peptide in Alzheimer's disease. Redox Biol. 2017 Oct 18;14:450-464. doi: 10.1016/j.redox.2017.10.014.
5. Baird L, Dinkova-Kostova AT. The cytoprotective role of the Keap1-Nrf2 pathway. Arch Toxicol. 2011 Apr;85(4):241-72. doi: 10.1007/s00204-011-0674-5.

6. Ho CY, Cheng YT, Chau CF, Yen GC. Effect of diallyl sulfide on in vitro and in vivo Nrf2-mediated pulmonic antioxidant enzyme expression via activation ERK/p38 signaling pathway. J Agric Food Chem. 2012 Jan 11;60(1):100-7. doi:10.1021/jf203800d.

7. Nabavi SF, Tenore GC, Daglia M, Tundis R, Loizzo MR, Nabavi SM. The cellular protective effects of rosmarinic acid: from bench to bedside. Curr Neurovasc Res.2015;12(1):98-105.

8. Witaicenis A, Seito LN, da Silveira Chagas A, de Almeida LD Jr, Luchini AC, Rodrigues-Orsi P, Cestari SH, Di Stasi LC. Antioxidant and intestinal anti-inflammatory effects of plant-derived coumarin derivatives. Phytomedicine. 2014 Feb 15;21(3):240-6. doi: 10.1016/j.phymed.2013.09.001.

9. Simoni E, Serafini MM, Caporaso R, Marchetti C, Racchi M, Minarini A, Bartolini M, Lanni C, Rosini M. Targeting the Nrf2/Amyloid-Beta Liaison in Alzheimer's Disease: A Rational Approach. ACS Chem Neurosci. 2017 Jul 19;8(7):1618-1627. doi: 10.1021/acschemneuro.7b00100.

10. Simoni E, Serafini MM, Bartolini M, Caporaso R, Pinto A, Necchi D, Fiori J, Andrisano V, Minarini A, Lanni C, Rosini M. Nature-Inspired Multifunctional Ligands: Focusing on Amyloid-Based Molecular Mechanisms of Alzheimer's Disease. ChemMedChem. 2016 Jun 20;11(12):1309-17. doi: 10.1002/cmdc.201500422.

11. Darvesh AS, Carroll RT, Bishayee A, Novotny NA, Geldenhuys WJ, Van der Schyf CJ. Curcumin and neurodegenerative diseases: a perspective. Expert Opin Investig Drugs. 2012 Aug;21(8):1123-40. doi: 10.1517/13543784.2012.693479.

12. Vera-Ramirez L, Pérez-Lopez P, Varela-Lopez A, Ramirez-Tortosa M, Battino M, Quiles JL. Curcumin and liver disease.

Biofactors. 2013 Jan-Feb;39(1):88-100. doi: 10.1002/biof.1057.

13. Shen LR, Parnell LD, Ordovas JM, Lai CQ. Curcumin and aging. Biofactors. 2013 Jan-Feb;39(1):133-40. doi: 10.1002/biof.1086.

14. Nabavi SF, Thiagarajan R, Rastrelli L, Daglia M, Sobarzo-Sánchez E, Alinezhad H, Nabavi SM. Curcumin: a natural product for diabetes and its complications. Curr Top Med Chem. 2015;15(23):2445-55.

15. Suneetha A, Raja Rajeswari K. Role of dimethyl fumarate in oxidative stress of multiple sclerosis: A review. J Chromatogr B Analyt Technol Biomed Life Sci. 2016 Apr 15;1019:15-20. doi: 10.1016/j.jchromb.2016.02.010.

16. Howell JC, Chun E, Farrell AN, Hur EY, Caroti CM, Iuvone PM, Haque R. Global microRNA expression profiling: curcumin (diferuloylmethane) alters oxidative stress-responsive microRNAs in human ARPE-19 cells. Mol Vis. 2013;19:544-60.

17. Curti V, Capelli E, Boschi F, Nabavi SF, Bongiorno AI, Habtemariam S, Nabavi SM, Daglia M. Modulation of human miR-17-3p expression by methyl 3-O-methyl gallate as explanation of its *in vivo* protective activities. Mol Nutr Food Res. 2014 Sep;58(9):1776-84. doi: 10.1002/mnfr.201400007.

18. Liang Z, Xi Y. MicroRNAs mediate therapeutic and preventive effects of natural agents in breast cancer. Chin J Nat Med. 2016 Dec;14(12):881-887. doi:10.1016/S1875-5364(17)30012-2.

19. Pandima Devi K, Rajavel T, Daglia M, Nabavi SF, Bishayee A, Nabavi SM. Targeting miRNAs by polyphenols: Novel therapeutic strategy for cancer. Semin Cancer Biol. 2017 Feb 7. doi:10.1016/j.semcancer.2017.02.001.

20. Curti V, Di Lorenzo A, Rossi D, Martino E, Capelli E, Collina S, Daglia M. Enantioselective modulatory effects of

naringenin enantiomers on the expression levels of miR-17-3p involved in endogenous antioxidant defenses. Nutrients. 2017 Feb 28;9(3). pii: E215. doi: 10.3390/nu9030215.

21. R core Team (2017). R: A language and environment for statistical computing. R foundation for statistical computing. Vienna, Austria. URL https://www.R-poject.org/.

22. Brennan MS, Matos MF, Li B, Hronowski X, Gao B, Juhasz P, Rhodes KJ, Scannevin RH. Dimethyl fumarate and monoethyl fumarate exhibit differential effects on KEAP1, NRF2 activation, and glutathione depletion in vitro. PLoS One. 2015 Mar20;10(3):e0120254. doi: 10.1371/journal.pone.0120254.

23. Itoh K, Wakabayashi N, Katoh Y, Ishii T, Igarashi K, Engel JD, Yamamoto M. Keap1 represses nuclear activation of antioxidant responsive elements by Nrf2 through binding to the amino-terminal Neh2 domain. Genes Dev. 1999 Jan 1;13(1):76-86. doi:10.1101/gad.13.1.76

24. Kobayashi A, Kang MI, Okawa H, Ohtsuji M, Zenke Y, Chiba T, Igarashi K, Yamamoto M. Oxidative stress sensor Keap1 functions as an adaptor for Cul3-based E3 ligase to regulate proteasomal degradation of Nrf2. Mol Cell Biol. 2004 Aug;24(16):7130-9. doi: 10.1128/MCB.24.16.7130-7139.2004.

25. Tanigawa S, Fujii M, Hou DX. Action of Nrf2 and Keap1 in ARE-mediated NQO1 expression by quercetin. Free Radical Biol Med 2007; 42:1690-703.

26. Sirota R, Gibson D, Kohen R. The role of the catecholic and the electrophilic moieties of caffeic acid in Nrf2/Keap1 pathway activation in ovarian carcinoma cell lines. Redox Biol 2015; 4:48-59.

27. Scannevin RH, Chollate S, Jung MY, Shackett M, Patel H, Bista P, Zeng W, Ryan S, Yamamoto M, Lukashev M, Rhodes KJ. Fumarates promote cytoprotection of central nervous

system cells against oxidative stress via the nuclear factor(erythroid-derived 2)-like 2 pathway. J Pharmacol Exp Ther. 2012 Apr;341(1):274-84. doi: 10.1124/jpet.111.190132.

28. Jing X, Shi H, Zhang C, Ren M, Han M, Wei X, Zhang X, Lou H. Dimethyl fumarate attenuates 6-OHDA-induced neurotoxicity in SH-SY5Y cells and in animal model of Parkinson's disease by enhancing Nrf2 activity. Neuroscience. 2015 Feb 12;286:131-40. doi: 10.1016/j.neuroscience.2014.11.047.

29. Campolo M, Casili G, Lanza M, Filippone A, Paterniti I, Cuzzocrea S, Esposito E. Multiple mechanisms of dimethyl fumarate in amyloid β-induced neurotoxicity in human neuronal cells. J Cell Mol Med. 2017 Oct 9. doi: 10.1111/jcmm.13358.

Chapter II

Part 1.

The following review has been published on Pharmacological Research (2017) as:

Curcumin in Alzheimer's disease: can we think to new strategies and perspectives for this molecule?

Melania Maria Serafini,[a,b] Michele Catanzaro,[b] Michela Rosini,[c] Marco Racchi,[b] and Cristina Lanni[*,b]

[a] Scuola Universitaria Superiore IUSS Pavia, P.zza Vittoria 15, 27100 Pavia, Italy

[b] Department of Drug Sciences (Pharmacology Section), University of Pavia, V.le Taramelli 14, 27100 Pavia, Italy

[c] Department of Pharmacy and Biotechnology, Alma Mater Studiorum - University of Bologna, Via Belmeloro 6, 40126 Bologna, Italy

Review

Curcumin in Alzheimer's disease: Can we think to new strategies and perspectives for this molecule?

Melania Maria Serafini [a,b], Michele Catanzaro [b], Michela Rosini [c], Marco Racchi [b], Cristina Lanni [b,*]

Abstract

Population aging is an irreversible global trend with economic and socio-political consequences. One of the most invalidating outcomes of aging in the elderly is cognitive decline, leading to dementia and often related to neurodegenerative disorders. Among these latter, Alzheimer's disease (AD) is the major cause of dementia, affecting more than 30 million of individuals worldwide. To date, the treatment of AD remains a challenge because of an incomplete understanding of the events that lead to the selective neurodegeneration typical of Alzheimer's brains. There is an enormous global demand for new effective therapies and researchers are investigating new fields. One promising strategy is the use of nutraceuticals as integrative, complementary and preventive therapy. Curcumin is one example of natural product with anti-AD properties, with promising potential for prevention, treatment and diagnostic. The limitations in the use of curcumin as therapeutic are represented by its pharmacokinetics profile and the low bioavailability after oral administration. However, curcumin has been the focus of intense research for new drug development. Here we analyzed some new approaches that have been applied in the attempt to improve its use, particularly new formulations, changes in the way of administration, nanotechnology-based delivery systems and the hybridization strategy.

Keywords

Curcumin, Alzheimer's disease, alternative formulations, curcuminoids, hybrids

Introduction

One of the most important demographic trends facing the world is the aging of the population. As the life expectancy has increased, the high prevalence of chronic disabilities represents one of the major causes of upward burden on the economy of Health Services, requiring a long-term clinical management of the affected subjects. Moreover, the morbidity often observed in aged people increases the healthcare costs since requires multiple intervention approaches. Among different comorbidities, cognitive decline leading to dementia remains the most invalidating one, because of the lack of efficacious treatments and its hard impact on both healthcare workers and families.

The major cause of dementia among the elderly is Alzheimer's disease (AD) and current estimations predict that the number of people with dementia will increase and triple by 2050 [1]. For this reason, AD is a growing socio-economic problem worldwide and many researchers are focusing their efforts to come up with a cure. AD is a neurodegenerative disease clinically characterized by progressive loss of memory and cognitive functions. The main microscopic pathological features of AD include accumulation of intracellular fibrillary tangles (NFT) and extracellular senile plaques of β-amyloid peptide (Aβ), chronic neuro-inflammation, synaptic and neuronal loss. From the macroscopic point of view, brain atrophy is consistent with a brain volume and weight decrease [2]. The treatment of AD remains a major challenge because of an incomplete understanding of the events that lead to the selective neurodegeneration typical of Alzheimer's brains. To date, there are not yet effective disease-modifying treatments available, but only therapeutics that slow down the disease progression and control

symptoms in the short-term [3-4]. The failure of approved drugs to revert the disease is due to the lack of an early diagnosis for AD: synaptic loss, neuronal loss and brain shrinkage are already significant by the time of symptoms onset and AD diagnosis. There is an enormous global demand for new effective therapies and researchers are investigating different fields. One promising strategy is the cell-based therapy that aims at repopulation and regeneration of neuronal networks in AD brain. Some first clinical trials (NCT01297218 and NCT01696591) concluded that the neuroprotective effect of mesenchymal stem cells intracranial injections (MSCs), frequently reported in AD animal models, was not evident [5], but other trials are ongoing or recruiting patients. Another strategy deeply investigated in the last few years is the immunotherapy targeting Aβ peptide and/or tau protein, the two pathognomonic signs of the disease. Both, Aβ-directed immunization and tau immunotherapy have shown promising results in AD transgenic mouse models [6], but the translation to safe and efficient therapy for humans is still a challenge [7]. In this review we will focus our attention on another approach based on an integrative, complementary and preventive therapy for neurodegenerative disorders with alternative therapeutics, such as nutraceuticals.

Natural products have already proven to be a rich source of therapeutics and, by offering a great chemical diversity, they can be of inspiration to create new bioactive compounds. Curcumin is one example of natural product with several properties useful in different clinical fields [8-10], whose antioxidant, Aβ-binding and anti-inflammatory properties make it a potential therapeutic for AD prevention, treatment and diagnostic.

Curcumin and its potential in Alzheimer's disease

Curcumin is a natural product found in turmeric (*Curcuma longa*), a spice herb member of the ginger family (*Zingiberaceae*). Its chemical name is 1,7-bis[4-hydroxy-3-methoxyphenyl]-1,6-heptadiene-3,5-

dione, also named diferuloylmethane, and it constitutes the 2-5% of the turmeric root. Dried turmeric root was a traditional remedy of Chinese medicine and Ayurvedic indian medicine since ancient times; it was used in the treatment of different pathologies such as skin diseases, wounds, rheumatisms, asthma, allergies, sinusitis, hepatic disorders, intestinal worms, generic inflammation and oxidative stress conditions [11]. Commercially available curcumin is a combination of three molecules, together called curcuminoids. Curcumin is the most representative (60-70%), followed by demethoxycurcumin (DMC, 20-27%) and bisdemethoxycurcumin (BDMC, 10-15%). Curcuminoids differ in potency and efficacy, with no clear supremacy of curcumin over the other two compounds or the whole mixture, thus suggesting that DMC and BDMC significantly contributed to the curcuminoid mixture effectiveness, that is not only due to curcumin. This concept is well reviewed by Ahmed and Gilani [12] in the context of Alzheimer's disease. The authors listed numerous papers that have demonstrated the neuroprotective potential of curcuminoids *in vitro* and *in vivo*, suggesting that curcuminoids act through multiple mechanisms as a mixture, but the contribution of the single components is distinct for activity and potency. For example, curcumin is more effective in inhibiting acetilcholinesterase activity [13], in protecting PC12 cells and HUVEC cells against Aβ [14-15], whereas DMC and BDMC have a stronger antioxidant activity measured with the DPPH (1,1-diphenyl-2-picrylhydrazyl) assay [15] and an higher IC_{50} in the inhibition of Aβ 1-42 fibrillogenesis [16]. Concerning the potential effects of curcumin, in particular in AD, it can prevent AD development thanks to its anti-inflammatory [17-21] and antioxidant properties [22-24]. *In vitro* studies have shown that curcumin can bind Aβ, thus influencing the peptide aggregation and inhibiting fibrils formation and elongation [25]. Moreover, curcumin can enhance Aβ cellular uptake [26] avoiding plaques deposition and preventing cellular insults induced by the peptide [16] and it can also downregulate Aβ production through BACE1 (beta-site APP-

cleaving enzyme) expression [27]. *In vivo*, curcumin is able to rescue the distorted neuritic morphology near Aβ plaques [28], to decrease Aβ serum level as well as Aβ burden in the brain, especially in the neocortex and in the hippocampus, and to attenuate inflammation and microglia activation in AD mouse models [29]. Furthermore, curcumin can modulate tau protein processing and phosphorylation avoiding NFTs formation [recently reviewed by 30-31] (Fig. 1).
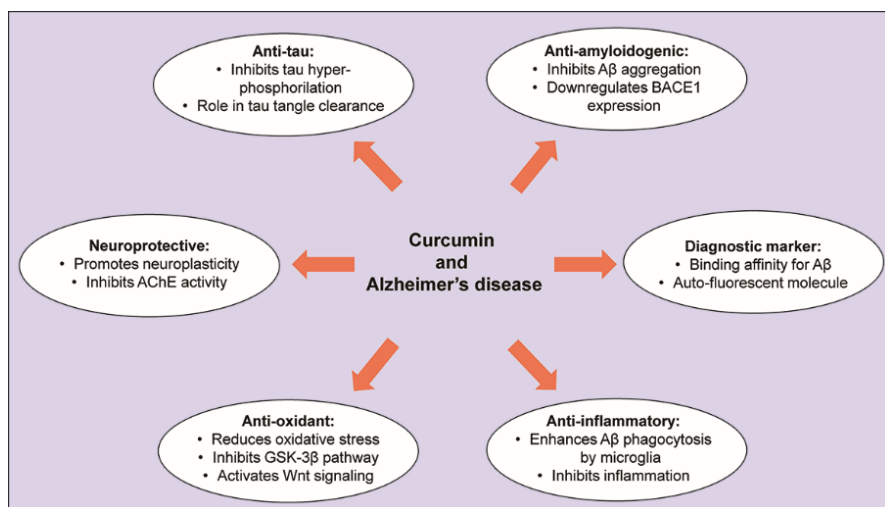

Figure 1: Curcumin activities in Alzheimer's disease. Mechanisms of action of curcumin related to Alzheimer's disease pathological features. Figures have been done following the guidelines reported in [102].

Interestingly, curcumin has been shown to have a potential in the diagnostic field. Thanks to its fluorescent properties and Aβ-binding ability, curcumin has been also suggested as a detection agent for the early diagnosis of plaques deposition in the brain [32].

These findings were very promising; however, despite curcumin has a very safe nutraceutical profile with low side-effects and it has been reported to be well tolerated at doses up to 8 grams per day in humans, the attempts to use curcumin in a therapeutic field were discouraging because the translation of these studies in clinical trials was not very

successful [33]. Moreover, doubts about curcumin potential therapeutic use have recently raised because its classification as a PAINS (pan-assay interference compounds) candidate. PAINS are compounds that show activity in multiple assay, not through a specific interaction with the target, but by interfering with the assay readout. Curcumin has numerous PAINS-type characteristics such as redox activity, metal chelation properties, auto-fluorescence and covalent protein labeling [34]. For this reason, results obtained with methods that can involve PAINS-like behaviors, need to be verified with other techniques to be confirmed. The classification of curcumin as a PAINS candidate is a very recent issue, and published data regarding the bioactivity of curcumin have to be read with a critical view. The limitations in the use of curcumin as therapeutic are represented by its pharmacokinetics profile. Curcumin is nearly insoluble in water, has a short half-life and a low bioavailability [35]. After oral administration it is rapidly metabolized by conjugation, sulfation and glucuronidation in the intestinal wall and in the liver and then excreted in feces. Moreover, it is chemically instable at neutral physiological pH and photodegradable, making its handling complicated and restricting its applications.

In addition to curcumin limitations, also the patient recruitment for clinical trial is challenging. AD is a multiple-stages pathology with different pathological markers, clinical features, and a final diagnosis only *post-mortem*. The patient recruitment is often based on the score in MMSE (Mini-Mental State Examination) that correlates with the severity of dementia, allowing the classification in no cognitive impairment, mild cognitive impairment and severe cognitive impairment. This classification correlates only partially with the pathological hallmarks observed in the brain, thus indicating that the sample of the patient are heterogeneous and not homogeneous as expected. To overcome these pharmaceutical issues related to curcumin pharmacokinetics and to improve therapeutic efficacy, new strategies have been applied and have been deepened in this review:

new formulations, a change in the way of administration, alternative drug delivery taking advantage from the development of nanotechnology-based delivery systems, such as nanoparticles, liposomes and hydrogels and, finally, the hybridization approach.

Alternative formulations for curcumin

Considering the not significant results of the numerous clinical trials on humans [33-34], the oral administration of curcumin is not recommended. For this reasons alternative formulations have been tested *in vitro* and *in vivo*, with the final goal of optimizing curcumin absorption and efficacy.

The first approach for an alternative formulation was based on the combination of curcumin with other natural products as co-adjuvants. Piperine (1-piperoylpiperidine), an alkaloid extracted from black pepper fruits (*Piper nigrum*) and present also in long pepper (Piper longum) and other piper species (*Piperaceae*), was known for its ability to enhance the bioavailability of numerous drugs and phytochemicals thanks to its inhibition of uridine 5'-diphospho-glucuronosyltransferase (UDP-glucuronosyltransferase) [36]. In the context of AD, it was demonstrated, *in vivo,* that piperine significantly improved spatial memory because of its cytoprotective effect and the inhibition of AChE in hippocampus [37]. Moreover, piperine was combined with other nutraceuticals such as curcumin, epigallocatechin gallate, α-lipoic acid, N-acetylcysteine, B vitamins, vitamin C, and folate in a medical food cocktails that was administered for 6 months to the Tg2576 mouse model of AD. At the end of the treatment, the transgenic mice showed improved cortical- and hippocampal-dependent learning and their performance was indistinguishable from the non-transgenic control mice [38].

Basing on these already known properties of piperine, Suresh and Srinivasan orally administered 500 mg curcumin, 170 mg piperine or a combination of the two in a single formulation to Wistar male albino rats. Interestingly, they found that curcumin stayed significantly

longer in the body tissues when administered concomitant with piperine; moreover curcumin has been detected in the brain up to 96 h after the treatment [39].

Curcumin is only one of a multitude of compounds extracted from turmeric rhizome and the debate about the bioactivity of every single molecule is still open. It has been suggested that among the numerous non-curcuminoid components of turmeric, there are some, which could increase curcumin absorption and bioavailability. Taking advantage of the synergism between the sesquiterpenoids naturally present in turmeric and the curcuminoids, Jäger and colleagues compared a combination of curcuminoids and volatile oils of turmeric rhizome (CTR), a curcumin inclusion in a lipophilic matrix composed by curcumin, soy lecithin and microcrystalline cellulose 1:2:2 (CP), standard curcumin (CS) and a water soluble formulation of turmeric extract, hydrophilic carrier, cellulosic derivatives and natural antioxidants (CHC). All these formulations, with exception of CHC, were previously found to increase curcumin absorption with different potency [40-41]. After a single oral administered dose of 376 mg CP, CTR or CHC, or 1800 mg CS in human healthy volunteers, a 45.9-fold increase in CHC relative absorption compared to CS was observed, with a non statistically significant change of CTR (vs CS) and a weak increase of CP (vs CS) [42]. Thus, the volatile oils naturally occurring in turmeric rhizome are not increasing curcumin absorption, while the antioxidants tocopherol and ascorbyl palmitate combined with the polyvinyl pyrrolidone water-soluble carrier in the CHC formulation significantly improved it. This study suggests that the presence of a carrier is essential for ameliorating curcumin absorption and distribution. To further investigate the importance of an adequate profile for curcumin pharmacokinetics, a clinical study on human healthy volunteers was carried out with a patented formulation named BCM-95 CG (Biocurcumax^{TM}) in comparison with a combination of curcumin-lecithin-piperine, which was previously demonstrated to enhance curcumin bioavailability, and

normal curcumin. BCM-95 CG is a formulation generated by micronizing curcumin and adding turmeric rhizome essential oils. The absorption of BCM-95 CG was faster than curcumin and curcumin-lecithin-piperine; moreover it remained longer in the blood because of a lower elimination rate constant [40]. A more recent double-blind study compared the previous described Biocurcumax^{TM} with other two commercial formulations: Meriva, curcumin complex with phosphatidylcholine from soy lecithin [41], and Theracurmin, curcumin dispersed with colloidal submicron particles [43]. In this study, the change of curcumin concentration in plasma, the maximum concentration and the bioavailability have been evaluated, indicating that Theracurmin possesses higher absorption efficiency in comparison with Meriva and BCM-95 CG curcumin commercial formulations [44].

Alternative drug delivery

In recent years, researchers have focused their attention in nanotechnology-based delivery systems because of their promising potential and advantages over the conventional approaches (Fig. 2). The development of these systems could overcome the pharmaceutical issue related to curcumin delivery enhancing the dissolution rate, prolonging the residence in plasma, improving the pharmacokinetic profile and the cellular uptake.

The ability of curcumin to penetrate organs and different brain regions has been shown to be affected by nanoparticulation. Curcumin-loaded PLGA nanoparticles (C-NPs) increased curcumin circulation time when injected in the body of rats [45]. C-NPs were found mainly distributed in the spleen and the lung. Furthemore, C-NPs crossed the blood-brain barrier, thus prolonging retention time of curcumin in the cerebral cortex and hippocampus.
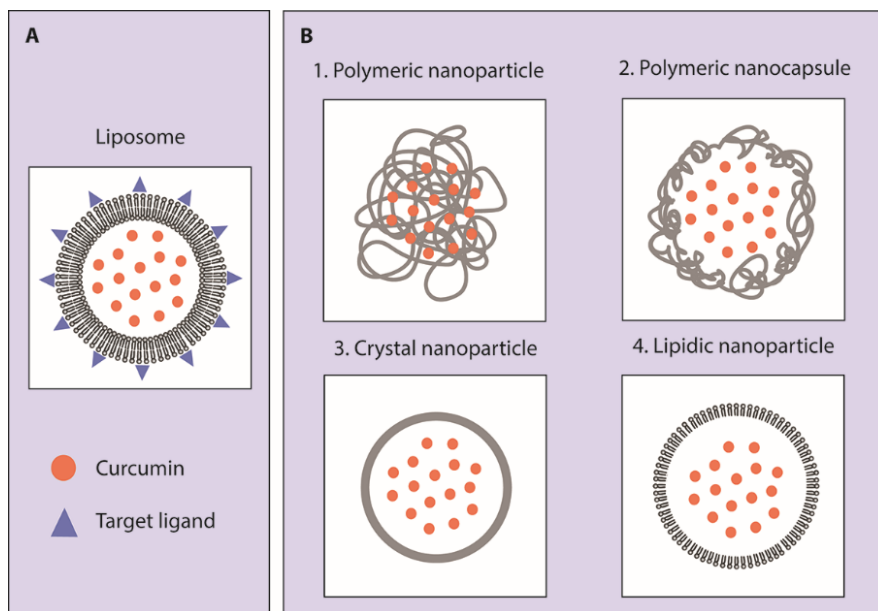
Figure 2: Curcumin drug delivery. Examples of nanotechnology-based delivery systems. A) Liposomes entrapped with curcumin and decorated with molecules able to specifically target the brain; B) Different types of nanoparticles: 1. Polymeric nanoparticle 2. Polymeric nanocapsule 3) Crystal nanoparticle 4) Lipidic nanoparticle. Figures have been done following the guidelines reported in [102].

A system of PLGA (poly lactide-co-glycolide) nanoparticles encapsulated with curcumin (Nps-Cur) was studied by Doggui and colleagues *in vitro* using SK-N-SH human neuroblastoma cell line. Nps-Cur formulation has been shown to be stable up to six months, non-toxic to neurons and internalized by SK-N-SH cells due to their size of around 100 nm. Moreover, Nps-Cur can prevent ROS increase in dichlorofluorescein assay and protect cells against oxidative damage induced by a treatment with 500 μM H_2O_2. Thus, PLGA-nanoparticles provide an efficient delivery system for encapsulated curcumin [46].

NanoCurc^{TM} is a polymeric nanoparticle encapsulated curcumin formulation that has been developed to increase curcumin systemic bioavailability. It is soluble in aqueous media and readily

administered parenterally by injection. This formulation showed to be protective *in vitro* in SK-N-SH differentiated cells against H_2O_2-induced oxidative stress. *In vivo* analysis demonstrated the presence of NanoCurc[TM] in the brain tissues of athymic mice and the ability of this formulation to downregulate the activity of caspase 3 and 7, critical mediators of the apoptotic pathway, in mice cortex. Moreover, after parenteral 25 mg/kg NanoCurc[TM] administration twice a day, in rodent brains a reduction in H_2O_2 content and an increase in the ratio of free versus oxidized glutathione [47] have been observed. These data suggest that this formulation could be promising also in AD, where oxidative stress and alterations in glutathione levels have been involved in the pathologic mechanism leading to the development of this type of dementia [48].

A novel lipopeptide composed by an aliphatic hydrophobic chain of palmitic acid, a microtubules stabilizing octapeptide and some hydrophilic residues, has been designed and synthesized by Ghosh's group [49]. This peptide spontaneously self-assembled in a β-sheet structure entrapping water molecules and forming a hydrogel with multiple functions. Furthermore, it slowly degrades releasing the neuroprotective octapeptide, and can be used to encapsulate curcumin, being a delivery vehicle for hydrophobic and poor soluble drugs. Investigating the activity of the lipopeptide *in vitro* with Neuro-2a cells, Adak and colleagues found that it promotes neurite outgrowth in absence of external growth factors. Moreover, in PC-12 cells differentiated with nerve growth factor (NGF) and then treated with anti-NGF, a known inducer of Aβ overproduction and cell death, the hydrogel was able to ameliorate neural cell morphology and health, being neuroprotective [50]. These data are interesting since they suggest how a specific formulation may ameliorate the intrinsic properties of curcumin itself. Several and recent data of literature highlighted as curcumin may also have positive and very encouraging effects on neurogenesis and neuronal differentiation pathways, a very promising ability for incurable neurodegenerative and

neuropsychiatric disorders that take a huge toll on society [51]. Curcumin has been related to hippocampal neurogenesis, since it can enhance neural plasticity and repair through the positive modulation of Wnt/beta-catenin pathway [52]. In addition, to overcome the problems related to pharmacokinetic limitations and improve the bioavailability of curcumin, the latter was encapsulated in polylactic-co-glycolic NPs (Cur_PLGA_NPs) to stimulate neural stem cells proliferation and neuronal differentiation *in vitr*o and in adult rats [52]. The nanomaterials used in this paper have been demonstrated to ameliorate the availability of curcumin, since Cur_PLGA_NPs was effective at much lower doses *in vivo* in comparison of free curcumin that did not induce neurogenesis below a minimum threshold level. Moreover, curcumin can promote brain-derived neurotrophic factor (BDNF) release [53], and showed, only after a chronic administration, to ameliorate AD-related cognitive deficits (working and spatial reference memory) through an upregulation of BDNF-ERK signaling in the hippocampus of rats subjected to a ventricular injection of Aβ1-42 [54]. In addition, in curcumin has been recognized the potential as a DNA methyltransferase (DNMT) inhibitor, thus modulating DNA methylation patterns interfering with signaling pathways and transcriptional factors related to cell differentiation [55]. In this context, the effects of curcumin on neuronal differentiation and neurite outgrowth were investigated in the PC-12 Adh cell line alone and after NGF treatment [56]. The combination of curcumin and NGF has a more prominent effect on cell differentiation and neurite elongation than curcumin alone, with the synergic effect related to the upregulation of GAP-43 and β-tubulin mRNA expression levels. These approaches suggest to be corrective not only on curcumin, but also on other factors crucial for maintaining the integrity of neurons throughout an individual lifetime, such as NGF. There is growing evidence that an imbalance of neurotrophic support is significant in the pathogenesis of neurodegenerative diseases, but the implementation of neurotrophic factors is restricted by their poor

penetration of the blood-brain barrier (BBB) and undesirable apoptotic effect.

As for NGF, the challenge of curcumin administration for brain disorders treatment is also represented by BBB penetration to reach the target organ. To achieve this goal, liposomes with cardiolipin (CL) and wheat germ agglutinin (WGA) carrying curcumin and NGF were developed and tested *in vitro* for their ability to permeate a monolayer of human brain-microvascular endothelial cells. Results were promising: WGA contributed to enhance the permeability of liposomes across the BBB and, at the same time, CL carried curcumin and NGF to Aβ fibrils inducing neuronal protection and apoptosis counteraction [57]. Mathew et al. adopted a different strategy to specifically target neurons and to reach the brain: they coupled curcumin-encapsulated PLGA-nanoparticles with Tet-1 peptide [58], which has affinity for neurons and retrograde transportation properties. Tet-1 is a 12 aminoacids peptide previously described by the groups of Boulis [58] and Pun [59]. This peptide possesses binding properties similar to the tetanus toxin, in fact it can specifically interact with motor neurons, being capable of retrograde delivery in neuronal cells. These peculiar characteristics of Tet-1 peptide were found interesting for an application in the drug delivery to the brain in the context of neurodegenerative diseases treatment. The study by Mathew et al. investigated the anti-amyloid and anti-oxidative properties mediated by the coupling of curcumin with PLGA-nanoparticles and Tet-1 peptide. This formulation slightly affected the free-radical scavenging activity of curcumin measured by DPPH assay becoming around 60% versus 80% of raw curcumin. On the contrary, anti-amyloid activity remained unchanged: Tet-1 conjugated PLGA-curcumin nanoparticles decreased the size of Aβ aggregates when co-incubated for 12, 24 or 48 h with a considerably reduction in plaques size [60].

Again with the goal to specifically target the brain, Mulik and co-workers tested the possibility to use ApoE3 as a ligand for brain

targeted delivery of curcumin [61]. Apolipoprotein E3 can form complexes with Aβ preventing its transport through the BBB, thus being neuroprotective. Furthermore, it can be taken up by the choroid plexus reaching the cerebrospinal fluid (CSF) by crossing the choroidal epithelium and enter brain parenchymal cells by low density lipoprotein receptor (LDL-R) mediated endocytosis, competing with Aβ [62]. Apolipoprotein E3-mediated poly(butyl) cyanoacrylate nanoparticles containing curcumin (ApoE3-C-PBCA NPs) have been formulated and have been shown to exhibit a protective role *in vitro* in SH-SY5Y cells against Aβ-induced cytotoxicity. This effect can be mainly ascribed to curcumin, whereas to ApoE3 to a lesser extent, because the control nanoparticles carrying ApoE, but without curcumin (ApoE-B-PBCA NPs), showed a slight protective effect. A similar result was obtained measuring the antioxidant and anti-apoptotic properties after Aβ treatment: ApoE3-C-PBCA NPs act counteracting oxidative stress and apoptosis with higher extent than ApoE-B-PBCA NPs [61].

Liposomes functionalized with a curcumin-alkyne derivative named TREG (described in 63) can sequester Aβ 1-42 in human biological fluids from sporadic AD patients and Down syndrome subjects [64]. This interesting finding supports the idea that a reduction in brain and plasma levels of Aβ 1-42 through the peripheral "sink effect" could be a useful therapeutic strategy. The same curcumin derivative was previously studied [65-66] for its ability to bind Aβ with high affinity, but only when the structure planarity was maintained. Moreover different liposome formulations were tested and the more effective in Aβ inhibition of aggregation was the one with TREG molecules protruding from the liposome surface, rather than the one with TREG internalized in the bilayer. More recently, TREG liposomes were further functionalized with BBB-targeting ligands [67] to evaluate the co-presence of more ligands on their functionality. Interestingly, these multi-functional liposomes maintained their ability to bind Aβ and to inhibit its aggregation. In addition, they showed an increase in

transport across monolayers suggesting the involvement of transporters for their translocation across the BBB [68]. The same liposomes were also injected intravenously in APP/PS1 mice for *in vivo* live animal imaging and *ex vivo* studies, and the results confirmed their high potential as theranostic (therapeutic and diagnostic) system for AD [69].

A functionalization strategy to specifically target Aβ, and inhibit its aggregation is the use of carriers conjugated with a combination of curcumin and specific antibodies. One example are the PEGylated biodegradable poly(alkyl cyanoacrylate) (PACA) nanoparticles (NPs) described by Le Droumaguet and co-workers. An anti-Aβ$_{1-42}$ antibody positioned at the PACA NPs surface showed a strong affinity towards Aβ$_{1-42}$ monomers and fibrils and curcumin functionalization offered a significant inhibition of Aβ aggregation [70].

In a context not specifically related to neurodegeneration and Alzheimer's disease, Storka et al. investigated safety and tolerability of Lipocurc^{TM} in healty humans. Lipocurc^{TM} is a liposomal formulation of curcumin specifically developed for intravenous administration to overcome the bioavailability and pharmacokinetic limitations of the oral administration. A concentration of 6.9 mg/mL of curcumin was embedded into DMPC and DMPG liposomal membranes in a molar ratio of 9:1. The results of this study showed that a single intravenous infusion was well tolerated without symptoms or local reactions at doses up to 120 mg/m^2 and can be considered safe [71].

A change in the way of administration was further investigated by McClure and co-workers. In a very recent study they tested, in an animal model of Alzheimer's disease, the efficacy of aerosol delivered curcumin. The advantages of aerosolized drug administration are multiple: the absence of first-pass effect, the direct absorption via the olfactory epithelium, the absence of systemic delivery with the consequent limitation of systemic side effects and, important for targeting the brain, the ability to enter the central nervous system also

for drugs incapable to permeate the BBB. 5XFAD mice treated with 5 mg/kg curcumin via aerosol showed improved cognitive functions, prevention of inflammation, reduction of plaque burden and dystrophic neurites [72].

Hybridation strategy for new efficient compounds

As for major chronic diseases, the pluralism of AD causes affords complex networks, suggesting that acting against a single pathogenic mechanism with high potency and selectivity might be insufficient to face the multifactorial nature of the disease [73]. The use of different drugs, as both drug cocktails or single pill drug combinations, represents the most simple and immediate way to modify AD phenotype by modulating simultaneously multiple nodes of the disease networks. Besides, a new polypharmacological approach has recently emerged, which proposes single chemical entities endowed with multiple biological activities as a promising strategy to obtaining potentially innovative medicines for multifactorial diseases. Interestingly, multitarget drugs offer the prospect of maintaining the positive outcomes of drug combinations, but with the benefits of a single-molecule therapy, as the issue of drug–drug interactions would be avoided, and the therapeutic regimen radically simplified [74].

Multitarget drugs can be rationally designed by linking, by means of suitable spacers, or fusing the key pharmacophoric functions, or through amalgamation of the pharmacophoric groups essential for activity into one hybrid molecule [75]. These strategies have led to the development of many multitarget neuroprotective agents, which are now tested as potential drug for Alzheimer's disease [76-77].

Because of its large spectrum of biological activities related to AD, curcumin represents a suitable starting point for multitarget drug design. Starting from this, many different curcumin analogues and hybrids have been synthetized and are now under testing phase.

Hybridation of Curcumin and Melatonin

Melatonin (N-acetyl-5-methoxytryptamine) is an indoleamine produced mainly in the pineal gland and plays a fundamental role in the regulation of circadian rhythms [78]. The decline in melatonin levels and the alteration of circadian rhythms during the aging contributes to the development of many neurodegenerative disorders [79-80]. Searching for a new efficient compound as a potential AD-modifying agent, Chojnacki et al. developed various hybrids fusing curcumin and melatonin according to the hybrid molecule design strategy [81]. As the phenolic substitution pattern and the β-diketone moiety of curcumin have been demonstrated to be important for its antioxidant, anti-inflammatory, and metal chelating properties [82] and, as the 5-methoxy group and the acetamide moiety of melatonin have been shown to be important for its antioxidant and free radical scavenging properties [83], the hybrid compounds were designed considering these structural features.

The neuroprotective activities of these compounds were evaluated in MC65 cells, a cellular AD model associated with Aβ- and oxidative stress-induced cellular toxicities, under tetracycline removal (−TC) conditions [84]. In this study, some compounds dose-dependently suppressed the production of Aβ-oligomers, but not the Aβ aggregation, counteracted the intracellular oxidative stress and significantly protected cells from induced toxicity. Neuroprotective activities of curcumin derivatives were strictly related to the hydroxy substituent on the phenyl ring, while the double bond and the conjugation system have been demonstrated to be not necessary. In addition, the ability of compounds to cross the BBB both *in vitro* and *in vivo* has also been evaluated, and one compound (Table 1, hybrid number 1) quickly and efficiently reached brain tissue after oral ingestion of a single daily dose. It has further been tested in a transgenic AD mice model showing an excellent bioavailability, thus encouraging further studies and optimizations for novel disease-modifying agents in AD [85].

Hybridation of Curcumin and acetylcholinesterase inhibitors

One of the most accredited theories on the pathogenesis of AD is the cholinergic hypothesis that has been successfully applied in clinic with the development of acetylcholinesterase (AChE) inhibitors. Tacrine has been the first drug with this profile to be used. In this context, hybrids have been synthesized combining the pharmacophore of curcumin in monoanionic form with that of tacrine with the aim of obtaining a single more efficient molecule [86]. The choice to use monoanionic curcumin is due to the fact that in this form curcumin may chelate metal ions [87], and it is well known that the imbalance of metal ions, such as copper (Cu^{2+}) and iron (Fe^{2+}) in turn increases the production of ROS [88]. Curcumin-tacrine hybrids have been tested in PC12 cell lines, showing a potent inhibition of AChE typical of tacrine. Particularly, one compound (Table 1, hybrid number 2) has been shown to have a higher potency when compared with Tacrine. The higher potency has been related to the β-diketone moiety of curcumin that made this hybrid more neuroprotective against H_2O_2- or $A\beta_{1-42}$-induced toxicity than curcumin alone, and showed a remarkable ions-chelating ability, suggesting a potential of the hybrid compound to halt ion-induced Aβ aggregation.

Among the acetylcholinesterase inhibitors, donepezil is the most used to date in the clinical treatment of AD. Yan et al. fused the pharmacophores of curcumin and donepezil to obtain a series of derivatives expected to be inhibitors of AChE activity and Aβ aggregation, metal chelators and antioxidants [89].

In this library of hybrids, one of the compounds (Table 1, hybrid number 3) turned out to be a potent AChE and Aβ aggregation inhibitor fusing the qualities of the original single molecules. Furthermore, this molecule has also been able to cross the BBB, indicating a great permeability and encouraging further studies.

Hybridation of Curcumin and Steroids

The addition of heterocyclic rings to steroids has often led to a change of their physiological activity and the appearance of new interesting pharmacological and biological properties [90]. On this basis, Elmegeed and co-workers synthetized novel curcumin hybrids fusing a promising steroidic heterocyclic nucleus to the essential phenolic feature of curcumin, one of which is shown in Table 1 (hybrid number 4) [91]. When tested in an AD rat model, the hybrids showed to enhance acetylcholine synthesis and increase the levels of glutathione and paraoxenase, a protein with anti-inflammatory and anti-oxidative properties. Notably, conjugation of curcumin with cholesterol was previously exploited to direct the antioxidant and antiaggregating efficacy of the polyphenolic feature to cell membrane/lipid rafts, using cholesterol as the anchor motif [92-93]. As for other curcumin congeners [94-95], targeting of antioxidant features to the main sites of ROS production through derivatization strategies was herein envisioned as a promising therapeutic approach.

Hybridation of Curcumin and diallyl sulfide from garlic

The idea to synthesize new other hybrids raised by the knowledge that hydroxycinnamoyl recurring motif, present in curcumin, has been shown to modulate several pathways related to aging and dementia [96-97]. Simoni et al. [98-99] synthetized a set of new hybrids, by combining a hydroxycinnamoyl function from curcumin and diallyl sulfides from garlic. In addition, diallyl sulfides, garlic-derived organosulfur compounds carrying allyl mercaptan moieties, are able to counteract oxidative stress through antioxidant enzyme expression [100]. A catechol derivative with remarkable anti-aggregating ability and antioxidant properties (Table 1, hybrid number 5) has been initially identified. The characterization of the anti-aggregating and antioxidant profile of this new nature-inspired compound demonstrated that the activation of the Keap1-Nrf2 system is essential for counteracting oxidative stress and Aβ-induced toxicity [99].

This evidence suggests that this novel design strategy is an efficient and promising approach that, in the near future, could lead to the development of new efficient molecules to counteract multifactorial diseases like AD.
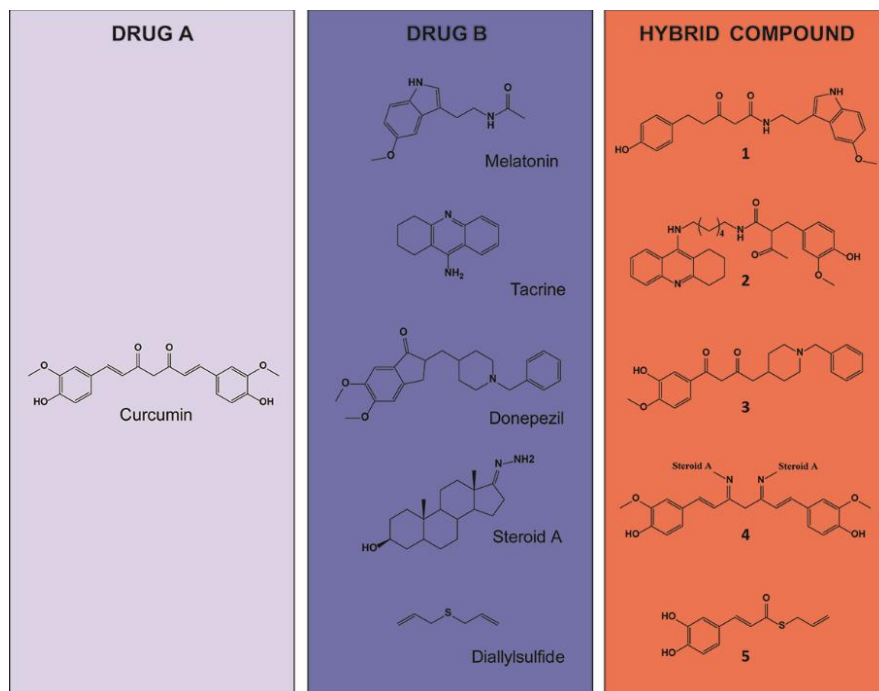

Table 1: Hybrids synthesis. Examples of different hybrid compounds from the combination of curcumin (drug A column) and other molecules (drug B column).

Conclusions

Curcumin is a minor constituent of the traditional medicine known as spice turmeric. Many scientific papers have been published on curcumin in different clinical fields ranging from cancer, neurodegenerative diseases, such as Alzheimer's disease, erectile dysfunction, hirsutism, to make some examples. These reported activities led to consider curcumin as a panacea. However, many limitations have been recognized for a therapeutic use of curcumin: its poor pharmacokinetic/pharmacodynamic properties, its chemical

instabililty, its low efficacy in different *in vitro* and *in vivo* disease models, its toxic profile under certain experimental settings [101], and very recently its PAINS character [34]. New formulations, changes in the way of administration, the direct delivery to the brain taking advantage from the development of nanotechnology-based delivery systems and the hybridization approach can overcome the critical pharmaceutical issues linked to curcumin pharmacokinetics improving therapeutic efficacy and giving new hopes for a clinical application of this natural compound. These approaches, besides possibly leading to new promising chemical entities, however, need further validation through expensive preclinical work to be approved for clinical trials.

Acknowledgements

References

1. Alzheimer's Association. 2016 Alzheimer's disease facts and figures. Alzheimers Dement. 2016 Apr;12(4):459-509.
2. Walsh DM, Selkoe DJ. Deciphering the molecular basis of memory failure in Alzheimer's disease. Neuron. 2004 Sep 30;44(1):181-93. doi: 10.1016/j.neuron.2004.09.010.
3. Cummings JL. Treatment of Alzheimer's disease: current and future therapeutic approaches. Rev Neurol Dis. 2004 Spring;1(2):60-9.
4. Schneider LS, Mangialasche F, Andreasen N, Feldman H, Giacobini E, Jones R, Mantua V, Mecocci P, Pani L, Winblad B, Kivipelto M. Clinical trials and late-stage drug development for Alzheimer's disease: an appraisal from 1984 to 2014. J Intern Med. 2014 Mar;275(3):251-83. doi: 10.1111/joim.12191.

5. Kim KS, Kim HS, Park JM, Kim HW, Park MK, Lee HS, Lim DS, Lee TH, Chopp M, Moon J. Long-term immunomodulatory effect of amniotic stem cells in an Alzheimer's disease model. Neurobiol Aging. 2013 Oct;34(10):2408-20. doi: 10.1016/j.neurobiolaging.2013.03.029.

6. Wisniewski T, Boutajangout A. Immunotherapeutic approaches for Alzheimer's disease in transgenic mouse models. Brain Struct Funct. 2010 Mar;214(2-3):201-18. doi: 10.1007/s00429-009-0236-2.

7. Wisniewski T, Goñi F. Immunotherapeutic approaches for Alzheimer's disease. Neuron. 2015 Mar 18;85(6):1162-76. doi: 10.1016/j.neuron.2014.12.064.

8. Jiang S, Han J, Li T, Xin Z, Ma Z, Di W, Hu W, Gong B, Di S, Wang D, Yang Y. Curcumin as a potential protective compound against cardiac diseases. Pharmacol Res. 2017 May;119:373-383. doi: 10.1016/j.phrs.2017.03.001.

9. Lelli D, Sahebkar A, Johnston TP, Pedone C. Curcumin use in pulmonary diseases: State of the art and future perspectives. Pharmacol Res. 2017 Jan;115:133-148. doi: 10.1016/j.phrs.2016.11.017.

10. Fadus MC, Lau C, Bikhchandani J, Lynch HT. Curcumin: An age-old anti-inflammatory and anti-neoplastic agent. J Tradit Complement Med. 2016 Sep 9;7(3):339-346. doi: 10.1016/j.jtcme.2016.08.002.

11. Ammon HP, Wahl MA. Pharmacology of Curcuma longa. Planta Med. 1991 Feb;57(1):1-7. doi: 10.1055/s-2006-960004.

12. Ahmed T, Gilani AH. Therapeutic potential of turmeric in Alzheimer's disease: curcumin or curcuminoids? Phytother Res. 2014 Apr;28(4):517-25. doi:10.1002/ptr.5030.

13. Ahmed T, Gilani AH. Inhibitory effect of curcuminoids on acetylcholinesterase activity and attenuation of scopolamine-

induced amnesia may explain medicinal use of turmeric in Alzheimer's disease. Pharmacol Biochem Behav. 2009 Feb;91(4):554-9. doi: 10.1016/j.pbb.2008.09.010.

14. Park SY, Kim DS. Discovery of natural products from Curcuma longa that protect cells from beta-amyloid insult: a drug discovery effort against Alzheimer's disease. J Nat Prod. 2002 Sep;65(9):1227-31. doi: 10.1021/np010039x.

15. Kim DS, Park SY, Kim JK. Curcuminoids from Curcuma longa L. (Zingiberaceae) that protect PC12 rat pheochromocytoma and normal human umbilical vein endothelial cells from betaA(1-42) insult. Neurosci Lett. 2001 Apr 27;303(1):57-61. doi: 10.1016/S0304-3940(01)01677-9.

16. Kim H, Park BS, Lee KG, Choi CY, Jang SS, Kim YH, Lee SE. Effects of naturally occurring compounds on fibril formation and oxidative stress of beta-amyloid. J Agric Food Chem. 2005 Nov 2;53(22):8537-41. doi: 10.1021/jf051985c.

17. Shi X, Zheng Z, Li J, Xiao Z, Qi W, Zhang A, Wu Q, Fang Y. Curcumin inhibits Aβ-induced microglial inflammatory responses in vitro: Involvement of ERK1/2 and p38 signaling pathways. Neurosci Lett. 2015 May 6;594:105-10. doi: 10.1016/j.neulet.2015.03.045.

18. Cianciulli A, Calvello R, Porro C, Trotta T, Salvatore R, Panaro MA. PI3k/Akt signalling pathway plays a crucial role in the anti-inflammatory effects of curcumin in LPS-activated microglia. Int Immunopharmacol. 2016 Jul;36:282-90. doi: 10.1016/j.intimp.2016.05.007.

19. Liu ZJ, Li ZH, Liu L, Tang WX, Wang Y, Dong MR, Xiao C. Curcumin Attenuates Beta-Amyloid-Induced Neuroinflammation via Activation of Peroxisome Proliferator-Activated Receptor-Gamma Function in a Rat Model of Alzheimer's Disease. Front Pharmacol. 2016 Aug 19;7:261. doi: 10.3389/fphar.2016.00261.

20. Sahebkar A, Cicero AF, Simental-Mendía LE, Aggarwal BB, Gupta SC. Curcumin downregulates human tumor necrosis factor-α levels: A systematic review and meta-analysis ofrandomized controlled trials. Pharmacol Res. 2016 May;107:234-42. doi: 10.1016/j.phrs.2016.03.026.

21. Derosa G, Maffioli P, Simental-Mendía LE, Bo S, Sahebkar A. Effect of curcumin on circulating interleukin-6 concentrations: A systematic review and meta-analysis of randomized controlled trials. Pharmacol Res. 2016 Sep;111:394-404. doi: 10.1016/j.phrs.2016.07.004.

22. Gibellini L, Bianchini E, De Biasi S, Nasi M, Cossarizza A, Pinti M. Natural Compounds Modulating Mitochondrial Functions. Evid Based Complement Alternat Med. 2015. doi: 10.1155/2015/527209.

23. Uğuz AC, Öz A, Nazıroğlu M. Curcumin inhibits apoptosis by regulating intracellular calcium release, reactive oxygen species and mitochondrial depolarization levels in SH-SY5Y neuronal cells. J Recept Signal Transduct Res. 2016 Aug;36(4):395-401. doi: 10.3109/10799893.2015.1108337.

24. Fan CD, Li Y, Fu XT, Wu QJ, Hou YJ, Yang MF, Sun JY, Fu XY, Zheng ZC, Sun BL. Reversal of Beta-Amyloid-Induced Neurotoxicity in PC12 Cells by Curcumin, the Important Role of ROS-Mediated Signaling and ERK Pathway. Cell Mol Neurobiol. 2017 Mar;37(2):211-222. doi: 10.1007/s10571-016-0362-3.

25. Ono K, Hasegawa K, Naiki H, Yamada M. Curcumin has potent anti-amyloidogenic effects for Alzheimer's beta-amyloid fibrils in vitro. J Neurosci Res. 2004 Mar 15;75(6):742-50. doi: 10.1002/jnr.20025.

26. Zhang L, Fiala M, Cashman J, Sayre J, Espinosa A, Mahanian M, Zaghi J, Badmaev V, Graves MC, Bernard G, Rosenthal M. Curcuminoids enhance amyloid-beta uptake by

macrophages of Alzheimer's disease patients. J Alzheimers Dis. 2006 Sep;10(1):1-7. doi: 10.3233/JAD-2006-10101.

27. Shimmyo Y, Kihara T, Akaike A, Niidome T, Sugimoto H. Epigallocatechin-3-gallate and curcumin suppress amyloid beta-induced beta-site APP cleaving enzyme-1 upregulation. Neuroreport. 2008 Aug 27;19(13):1329-33. doi: 10.1097/WNR.0b013e32830b8ae1.

28. Garcia-Alloza M, Borrelli LA, Rozkalne A, Hyman BT, Bacskai BJ. Curcumin labels amyloid pathology in vivo, disrupts existing plaques, and partially restores distorted neurites in an Alzheimer mouse model. J Neurochem. 2007 Aug;102(4):1095-104. doi: 10.1111/j.1471-4159.2007.04613.x.

29. Wang YJ, Thomas P, Zhong JH, Bi FF, Kosaraju S, Pollard A, Fenech M, Zhou XF. Consumption of grape seed extract prevents amyloid-beta deposition and attenuates inflammation in brain of an Alzheimer's disease mouse. Neurotox Res. 2009 Jan;15(1):3-14. doi: 10.1007/s12640-009-9000-x.

30. Goozee KG, Shah TM, Sohrabi HR, Rainey-Smith SR, Brown B, Verdile G, Martins RN. Examining the potential clinical value of curcumin in the prevention and diagnosis of Alzheimer's disease. Br J Nutr. 2016 Feb 14;115(3):449-65. doi: 10.1017/S0007114515004687.

31. Tang M, Taghibiglou C. The Mechanisms of Action of Curcumin in Alzheimer's Disease. J Alzheimers Dis. 2017 May 17. doi: 10.3233/JAD-170188.

32. Patil R, Gangalum PR, Wagner S, Portilla-Arias J, Ding H, Rekechenetskiy A, Konda B, Inoue S, Black KL, Ljubimova JY, Holler E. Curcumin Targeted, Polymalic Acid-Based MRI Contrast Agent for the Detection of Aβ Plaques in Alzheimer's Disease. Macromol Biosci. 2015 Sep;15(9):1212-7. doi: 10.1002/mabi.201500062.

33. Brondino N, Re S, Boldrini A, Cuccomarino A, Lanati N, Barale F, Politi P. Curcumin as a therapeutic agent in dementia: a mini systematic review of human studies. ScientificWorldJournal. 2014 Jan 22;2014:174282. doi: 10.1155/2014/174282.

34. Nelson KM, Dahlin JL, Bisson J, Graham J, Pauli GF, Walters MA. The Essential Medicinal Chemistry of Curcumin. J Med Chem. 2017 Mar 9;60(5):1620-1637. doi: 10.1021/acs.jmedchem.6b00975.

35. Anand P, Kunnumakkara AB, Newman RA, Aggarwal BB. Bioavailability of curcumin: problems and promises. Mol Pharm. 2007 Nov-Dec;4(6):807-18. doi: 10.1021/mp700113r.

36. Srinivasan K. Black pepper and its pungent principle-piperine: a review of diverse physiological effects. Crit Rev Food Sci Nutr. 2007;47(8):735-48. doi: 10.1080/10408390601062054.

37. Chonpathompikunlert P, Wattanathorn J, Muchimapura S. Piperine, the main alkaloid of Thai black pepper, protects against neurodegeneration and cognitive impairment in animal model of cognitive deficit like condition of Alzheimer's disease. Food Chem Toxicol. 2010 Mar;48(3):798-802. doi: 10.1016/j.fct.2009.12.009.

38. Parachikova A, Green KN, Hendrix C, LaFerla FM. Formulation of a medical food cocktail for Alzheimer's disease: beneficial effects on cognition and neuropathology in a mouse model of the disease. PLoS One. 2010 Nov 17;5(11):e14015. doi: 10.1371/journal.pone.0014015.

39. Suresh D, Srinivasan K. Tissue distribution & elimination of capsaicin, piperine & curcumin following oral intake in rats. Indian J Med Res. 2010 May;131:682-91.

40. Antony B, Merina B, Iyer VS, Judy N, Lennertz K, Joyal S. A Pilot Cross-Over Study to Evaluate Human Oral Bioavailability of BCM-95CG (Biocurcumax), A Novel

Bioenhanced Preparation of Curcumin. Indian J Pharm Sci. 2008 Jul-Aug;70(4):445-9. doi: 10.4103/0250-474X.44591.

41. Cuomo J, Appendino G, Dern AS, Schneider E, McKinnon TP, Brown MJ, Togni S, Dixon BM. Comparative absorption of a standardized curcuminoid mixture and its lecithin formulation. J Nat Prod. 2011 Apr 25;74(4):664-9. doi: 10.1021/np1007262.

42. Jäger R, Lowery RP, Calvanese AV, Joy JM, Purpura M, Wilson JM. Comparative absorption of curcumin formulations. Nutr J. 2014 Jan 24;13:11. doi: 10.1186/1475-2891-13-11.

43. Sasaki H, Sunagawa Y, Takahashi K, Imaizumi A, Fukuda H, Hashimoto T, Wada H, Katanasaka Y, Kakeya H, Fujita M, Hasegawa K, Morimoto T. Innovative preparation of curcumin for improved oral bioavailability. Biol Pharm Bull. 2011;34(5):660-5. doi: 10.1248/bpb.34.660.

44. Sunagawa Y, Hirano S, Katanasaka Y, Miyazaki Y, Funamoto M, Okamura N, Hojo Y, Suzuki H, Doi O, Yokoji T, Morimoto E, Takashi T, Ozawa H, Imaizumi A, Ueno M, Kakeya H, Shimatsu A, Wada H, Hasegawa K, Morimoto T. Colloidal submicron-particle curcumin exhibits high absorption efficiency-a double-blind, 3-way crossover study. J Nutr Sci Vitaminol (Tokyo). 2015;61(1):37-44. doi: 10.3177/jnsv.61.37.

45. Tsai YM, Chien CF, Lin LC, Tsai TH. Curcumin and its nano-formulation: the kinetics of tissue distribution and blood-brain barrier penetration. Int J Pharm. 2011 Sep 15;416(1):331-8. doi: 10.1016/j.ijpharm.2011.06.030.

46. Doggui S, Sahni JK, Arseneault M, Dao L, Ramassamy C. Neuronal uptake and neuroprotective effect of curcumin-loaded PLGA nanoparticles on the human SK-N-SH cell line. J Alzheimers Dis. 2012;30(2):377-92. doi: 10.3233/JAD-2012-112141.

47. Ray B, Bisht S, Maitra A, Maitra A, Lahiri DK. Neuroprotective and neurorescue effects of a novel polymeric nanoparticle formulation of curcumin (NanoCurc™) in the neuronal cell culture and animal model: implications for Alzheimer's disease. J Alzheimers Dis. 2011;23(1):61-77. doi: 10.3233/JAD-2010-101374.

48. Chiang GC, Mao X, Kang G, Chang E, Pandya S, Vallabhajosula S, Isaacson R, Ravdin LD; Alzheimer's Disease Neuroimaging Initiative, Shungu DC. Relationships among Cortical Glutathione Levels, Brain Amyloidosis, and Memory in Healthy Older Adults Investigated In Vivo with 1H-MRS and Pittsburgh Compound-B PET. AJNR Am J Neuroradiol. 2017 Jun;38(6):1130-1137. doi: 10.3174/ajnr.A5143.

49. Biswas A, Kurkute P, Jana B, Laskar A, Ghosh S. An amyloid inhibitor octapeptide forms amyloid type fibrous aggregates and affects microtubule motility. Chem Commun (Camb). 2014 Mar 11;50(20):2604-7. doi: 10.1039/c3cc49396b.

50. Adak A, Das G, Barman S, Mohapatra S, Bhunia D, Jana B, Ghosh S. Biodegradable Neuro-Compatible Peptide Hydrogel Promotes Neurite Outgrowth, Shows Significant Neuroprotection, and Delivers Anti-Alzheimer Drug. ACS Appl Mater Interfaces. 2017 Feb 15;9(6):5067-5076. doi: 10.1021/acsami.6b12114.

51. Uliassi E, Gandini A, Perone RC, Bolognesi ML. Neuroregeneration versus neurodegeneration: toward a paradigm shift in Alzheimer's disease drug discovery. Future Med Chem. 2017 Jun;9(10):995-1013. doi: 10.4155/fmc-2017-0038.

52. Tiwari, S. S. K., Agarwal, S., Seth, B., Yadav, A., Nair, S., Bhatnagar, P., et al. (2014). Curcumin-loaded nanoparticles potently induce adult neurogenesis and reverse cognitive deficits in Alzheimer's disease model via canonical Wnt/b-

catenin pathway. ACS Nano, 8(1), 76–103. doi:10.1021/nn405077y.

53. Liu, D., Wang, Z., Gao, Z., Xie, K., Zhang, Q., Jiang, H., & Pang, Q. (2014). Effects of curcumin on learning and memory deficits, BDNF, and ERK protein expression in rats exposed to chronic unpredictable stress. Behavioural Brain Research, 271C, 116–121. doi:10.1016/j.bbr.2014.05.068.

54. Zhang L, Fang Y, Xu Y, Lian Y, Xie N, Wu T, Zhang H, Sun L, Zhang R, Wang Z. Curcumin Improves Amyloid β-Peptide (1-42) Induced Spatial Memory Deficits through BDNF-ERK Signaling Pathway. PLoS One. 2015 Jun 26;10(6):e0131525. doi: 10.1371/journal.pone.0131525.

55. Bora-Tatar G, Erdem-Yurter H: Investigations of curcumin and resveratrol on neurite outgrowth: Perspectives on spinal muscular atrophy. BioMed Res Int 2014. doi: 10.1155/2014/709108.

56. Dikmen M. Comparison of the Effects of Curcumin and RG108 on NGF-Induced PC-12 Adh Cell Differentiation and Neurite Outgrowth. J Med Food. 2017 Apr;20(4):376-384. doi: 10.1089/jmf.2016.3889.

57. Kuo YC, Lin CC. Rescuing apoptotic neurons in Alzheimer's disease using wheat germ agglutinin-conjugated and cardiolipin-conjugated liposomes with encapsulated nerve growth factor and curcumin. Int J Nanomedicine. 2015 Apr 1;10:2653-72. doi: 10.2147/IJN.S79528.

58. Liu JK, Teng Q, Garrity-Moses M, Federici T, Tanase D, Imperiale MJ, Boulis NM. A novel peptide defined through phage display for therapeutic protein and vector neuronal targeting. Neurobiol Dis. 2005 Aug;19(3):407-18. doi: 10.1016/j.nbd.2005.01.022.

59. Park IK, Lasiene J, Chou SH, Horner PJ, Pun SH. Neuron-specific delivery of nucleic acids mediated by Tet1-modified

poly(ethylenimine). J Gene Med. 2007 Aug;9(8):691-702. doi: 10.1002/jgm.1062.

60. Mathew A, Fukuda T, Nagaoka Y, Hasumura T, Morimoto H, Yoshida Y, Maekawa T, Venugopal K, Kumar DS. Curcumin loaded-PLGA nanoparticles conjugated with Tet-1 peptide for potential use in Alzheimer's disease. PLoS One. 2012;7(3). doi: 10.1371/journal.pone.0032616.

61. Mulik RS, Mönkkönen J, Juvonen RO, Mahadik KR, Paradkar AR. ApoE3 mediated poly(butyl) cyanoacrylate nanoparticles containing curcumin: study of enhanced activity of curcumin against beta amyloid induced cytotoxicity using in vitro cell culture model. Mol Pharm. 2010 Jun 7;7(3):815-25. doi: 10.1021/mp900306x.

62. Martel CL, Mackic JB, Matsubara E, Governale S, Miguel C, Miao W, McComb JG, Frangione B, Ghiso J, Zlokovic BV. Isoform-specific effects of apolipoproteins E2, E3, and E4 on cerebral capillary sequestration and blood-brain barrier transport of circulating Alzheimer's amyloid beta. J Neurochem. 1997 Nov;69(5):1995-2004. doi: 10.1046/j.1471-4159.1997.69051995.x.

63. Airoldi C, Zona C, Sironi E, Colombo L, Messa M, Aurilia D, Gregori M, Masserini M, Salmona M, Nicotra F, La Ferla B. Curcumin derivatives as new ligands of Aβ peptides. J Biotechnol. 2011 Dec 20;156(4):317-24. doi: 10.1016/j.jbiotec.

64. Conti E, Gregori M, Radice I, Da Re F, Grana D, Re F, Salvati E, Masserini M, Ferrarese C, Zoia CP, Tremolizzo L. Multifunctional liposomes interact with Abeta in human biological fluids: Therapeutic implications for Alzheimer's disease. Neurochem Int. 2017 Feb 24. doi: 10.1016/j.neuint.2017.02.012.

65. Taylor M, Moore S, Mourtas S, Niarakis A, Re F, Zona C, La Ferla B, Nicotra F, Masserini M, Antimisiaris SG, Gregori M,

Allsop D. Effect of curcumin-associated and lipid ligand-functionalized nanoliposomes on aggregation of the Alzheimer's Aβ peptide. Nanomedicine. 2011 Oct;7(5):541-50. doi: 10.1016/j.nano.2011.06.015.

66. Mourtas S, Canovi M, Zona C, Aurilia D, Niarakis A, La Ferla B, Salmona M, Nicotra F, Gobbi M, Antimisiaris SG. Curcumin-decorated nanoliposomes with very high affinity for amyloid-β1-42 peptide. Biomaterials. 2011 Feb;32(6):1635-45. doi: 10.1016/j.biomaterials.2010.10.027.

67. Markoutsa E, Pampalakis G, Niarakis A, Romero IA, Weksler B, Couraud PO, Antimisiaris SG. Uptake and permeability studies of BBB-targeting immunoliposomes using the hCMEC/D3 cell line. Eur J Pharm Biopharm. 2011 Feb;77(2):265-74. doi: 10.1016/j.ejpb.2010.11.015.

68. Papadia K, Markoutsa E, Mourtas S, Giannou AD, La Ferla B, Nicotra F, Salmona M, Klepetsanis P, Stathopoulos GT, Antimisiaris SG. Multifunctional LUV liposomes decorated for BBB and amyloid targeting. A. In vitro proof-of-concept. Eur J Pharm Sci. 2017 Apr 1;101:140-148. doi: 10.1016/j.ejps.2017.02.019.

69. Papadia K, Giannou AD, Markoutsa E, Bigot C, Vanhoute G, Mourtas S, Van der Linded A, Stathopoulos GT, Antimisiaris SG. Multifunctional LUV liposomes decorated for BBB and amyloid targeting - B. In vivo brain targeting potential in wild-type and APP/PS1 mice. Eur J Pharm Sci. 2017 May 1;102:180-187. doi: 10.1016/j.ejps.2017.

70. Le Droumaguet B, Nicolas J, Brambilla D, Mura S, Maksimenko A, De Kimpe L, Salvati E, Zona C, Airoldi C, Canovi M, Gobbi M, Magali N, La Ferla B, Nicotra F, Scheper W, Flores O, Masserini M, Andrieux K, Couvreur P. Versatile and efficient targeting using a single nanoparticulate platform: application to cancer and Alzheimer's disease. ACS Nano. 2012 Jul 24;6(7):5866-79. doi: 10.1021/nn3004372.

71. Storka A, Vcelar B, Klickovic U, Gouya G, Weisshaar S, Aschauer S, Bolger G, Helson L, Wolzt M. Safety, tolerability and pharmacokinetics of liposomal curcumin in healthy humans. Int J Clin Pharmacol Ther. 2015 Jan;53(1):54-65. doi: 10.5414/CP202076.

72. McClure R, Ong H, Janve V, Barton S, Zhu M, Li B, Dawes M, Jerome WG, Anderson A, Massion P, Gore JC, Pham W. Aerosol Delivery of Curcumin Reduced Amyloid-β Deposition and Improved Cognitive Performance in a Transgenic Model of Alzheimer's Disease. J Alzheimers Dis. 2017;55(2):797-811. doi: 10.3233/JAD-160289.

73. Rosini M, Simoni E, Caporaso R, Minarini A. Multitarget strategies in Alzheimer's disease: benefits and challenges on the road to therapeutics. Future Med Chem. 2016 Apr;8(6):697-711. doi: 10.4155/fmc-2016-0003.

74. Rosini M. Polypharmacology: the rise of multitarget drugs over combination therapies. Future Med Chem. 2014 Apr;6(5):485-7. doi: 10.4155/fmc.14.25.

75. Bottegoni G, Favia AD, Recanatini M, Cavalli A. The role of fragment-based and computational methods in polypharmacology. Drug Discov Today. 2012 Jan;17(1-2):23-34. doi: 10.1016/j.drudis.2011.08.002. doi: 10.1016/j.drudis.2011.08.002.

76. Weinreb O, Amit T, Bar-Am O, Youdim MB. Neuroprotective effects of multifaceted hybrid agents targeting MAO, cholinesterase, iron and β-amyloid in ageing and Alzheimer's disease. Br J Pharmacol. 2016 Jul;173(13):2080-94. doi:10.1111/bph.13318.

77. Rosini M, Simoni E, Minarini A, Melchiorre C. Multi-target design strategies in the context of Alzheimer's disease: acetylcholinesterase inhibition and NMDA receptor antagonism as the driving forces. Neurochem Res. 2014 Oct;39(10):1914-23. doi: 10.1007/s11064-014-1250-1.

78. Pévet P. Melatonin and biological rhythms. Biol Signals Recept. 2000 May-Aug;9(3-4):203-12. doi: 14640.

79. Zhou JN, Liu RY, Kamphorst W, Hofman MA, Swaab DF. Early neuropathological Alzheimer's changes in aged individuals are accompanied by decreased cerebrospinal fluid melatonin levels. J Pineal Res. 2003 Sep;35(2):125-30. doi: 10.1034/j.1600-079X.2003.00065.x.

80. Hatfield CF, Herbert J, van Someren EJ, Hodges JR, Hastings MH. Disrupted daily activity/rest cycles in relation to daily cortisol rhythms of home-dwelling patients with early Alzheimer's dementia. Brain. 2004 May;127(Pt 5):1061-74. doi: 10.1093/brain/awh129.

81. Chojnacki JE, Liu K, Yan X, Toldo S, Selden T, Estrada M, Rodríguez-Franco MI, Halquist MS, Ye D, Zhang S. Discovery of 5-(4-hydroxyphenyl)-3-oxo-pentanoic acid [2-(5-methoxy-1H-indol-3-yl)-ethyl]-amide as a neuroprotectant for Alzheimer's disease by hybridization of curcumin and melatonin. ACS Chem Neurosci. 2014 Aug 20;5(8):690-9. doi: 10.1021/cn500081s.

82. Esatbeyoglu T, Huebbe P, Ernst IM, Chin D, Wagner AE, Rimbach G. Curcumin--from molecule to biological function. Angew Chem Int Ed Engl. 2012 May 29;51(22):5308-32. doi: 10.1002/anie.201107724.

83. Rosales-Corral SA, Acuña-Castroviejo D, Coto-Montes A, Boga JA, Manchester LC, Fuentes-Broto L, Korkmaz A, Ma S, Tan DX, Reiter RJ. Alzheimer's disease: pathological mechanisms and the beneficial role of melatonin. J Pineal Res. 2012 Mar;52(2):167-202. doi: 10.1111/j.1600-079X.2011.00937.x.

84. Sopher BL, Fukuchi K, Kavanagh TJ, Furlong CE, Martin GM. Neurodegenerative mechanisms in Alzheimer disease. A role for oxidative damage in amyloid beta protein precursor-

mediated cell death. Mol Chem Neuropathol. 1996 Oct-Dec;29(2-3):153-68.

85. Gerenu G, Liu K, Chojnacki JE, Saathoff JM, Martínez-Martín P, Perry G, Zhu X, Lee HG, Zhang S. Curcumin/melatonin hybrid 5-(4-hydroxy-phenyl)-3-oxo-pentanoic acid [2-(5-methoxy-1H-indol-3-yl)-ethyl]-amide ameliorates AD-like pathology in the APP/PS1 mouse model. ACS Chem Neurosci. 2015 Aug 19;6(8):1393-9. doi: 10.1021/acschemneuro.5b00082.

86. Liu Z, Fang L, Zhang H, Gou S, Chen L. Design, synthesis and biological evaluation of multifunctional tacrine-curcumin hybrids as new cholinesterase inhibitors with metal ions-chelating and neuroprotective property. Bioorg Med Chem. 2017 Apr 15;25(8):2387-2398. doi: 10.1016/j.bmc.2017.02.049.

87. Banerjee S, Chakravarty AR. Metal complexes of curcumin for cellular imaging, targeting, and photoinduced anticancer activity. Acc Chem Res. 2015 Jul 21;48(7):2075-83. doi: 10.1021/acs.accounts.5b00127.

88. Zatta P, Drago D, Bolognin S, Sensi SL. Alzheimer's disease, metal ions and metal homeostatic therapy. Trends Pharmacol Sci. 2009 Jul;30(7):346-55. doi: 10.1016/j.tips.2009.05.002.

89. Yan J, Hu J, Liu A, He L, Li X, Wei H. Design, synthesis, and evaluation of multitarget-directed ligands against Alzheimer's disease based on the fusion of donepezil and curcumin. Bioorg Med Chem. 2017 Jun 15;25(12):2946-2955. doi: 10.1016/j.bmc.2017.02.048.

90. Mohamed NR, Abdelhalim MM, Khadrawy YA, Elmegeed GA, Abdel-Salam OM. One-pot three-component synthesis of novel heterocyclic steroids as a central antioxidant and anti-inflammatory agents. Steroids. 2012 Nov;77(13):1469-76. doi: 10.1016/j.steroids.2012.09.001.

91. Elmegeed GA, Ahmed HH, Hashash MA, Abd-Elhalim MM, El-kady DS. Synthesis of novel steroidal curcumin derivatives as anti-Alzheimer's disease candidates: Evidences-based on in vivo study. Steroids. 2015 Sep;101:78-89. doi: 10.1016/j.steroids.2015.06.003.

92. Lenhart JA, Ling X, Gandhi R, Guo TL, Gerk PM, Brunzell DH, Zhang S. "Clicked" bivalent ligands containing curcumin and cholesterol as multifunctional abeta oligomerization inhibitors: design, synthesis, and biological characterization. J Med Chem. 2010 Aug 26;53(16):6198-209. doi: 10.1021/jm100601q.

93. Liu K, Gandhi R, Chen J, Zhang S. Bivalent ligands targeting multiple pathological factors involved in Alzheimer's disease. ACS Med Chem Lett. 2012 Nov 8;3(11):942-946. doi: 10.1021/ml300229y.

94. Simoni E, Bergamini C, Fato R, Tarozzi A, Bains S, Motterlini R, Cavalli A, Bolognesi ML, Minarini A, Hrelia P, Lenaz G, Rosini M, Melchiorre C. Polyamine conjugation of curcumin analogues toward the discovery of mitochondria-directed neuroprotective agents. J Med Chem. 2010 Oct 14;53(19):7264-8. doi:10.1021/jm100637k.

95. Simoni E, Caporaso R, Bergamini C, Fiori J, Fato R, Miszta P, Filipek S, Caraci F, Giuffrida ML, Andrisano V, Minarini A, Bartolini M, Rosini M. Polyamine Conjugation as a Promising Strategy To Target Amyloid Aggregation in the Framework of Alzheimer's Disease. ACS Med Chem Lett. 2016 Sep 26;7(12):1145-1150. doi: 10.1021/acsmedchemlett.6b00339.

96. Pocernich CB, Lange ML, Sultana R, Butterfield DA. Nutritional approaches to modulate oxidative stress in Alzheimer's disease. Curr Alzheimer Res. 2011 Aug;8(5):452-69. doi: https://doi.org/10.2174/156720511796391908.

97. Stefani M, Rigacci S. Protein folding and aggregation into amyloid: the interference by natural phenolic compounds. Int J Mol Sci. 2013 Jun 13;14(6):12411-57. doi: 10.3390/ijms140612411.

98. Simoni E, Serafini MM, Bartolini M, Caporaso R, Pinto A, Necchi D, Fiori J, Andrisano V, Minarini A, Lanni C, Rosini M. Nature-Inspired Multifunctional Ligands: Focusing on Amyloid-Based Molecular Mechanisms of Alzheimer's Disease. ChemMedChem. 2016 Jun 20;11(12):1309-17. doi: 10.1002/cmdc.201500422.

99. Simoni E, Serafini MM, Caporaso R, Marchetti C, Racchi M, Minarini A, Bartolini M, Lanni C, Rosini M. Targeting the Nrf2/Amyloid-Beta Liaison in Alzheimer's Disease: A Rational Approach. ACS Chem Neurosci. 2017 Apr 25. doi: 10.1021/acschemneuro.7b00100.

100. Kim S, Lee HG, Park SA, Kundu JK, Keum YS, Cha YN, Na HK, Surh YJ. Keap1 cysteine 288 as a potential target for diallyl trisulfide-induced Nrf2 activation. PLoS One. 2014 Jan 28;9(1):e85984. doi: 10.1371/journal.pone.0085984.

101. Burgos-Morón E, Calderón-Montaño JM, Salvador J, Robles A, López-Lázaro M. The dark side of curcumin. Int J Cancer. 2010 Apr 1;126(7):1771-5. doi:10.1002/ijc.24967. doi: 10.1002/ijc.24967.

102. Roskoski R Jr Guidelines for preparing color figures for everyone including the colorblind.Pharmacol Res. 2017 May;119:240-241. doi: 10.1016/j.phrs.2017.02.005.

Part 2.

The following manuscript has been accepted with minor revision for publication in Oxidative Medicine and Cellular Longevity (2018) as:

Characterization of the antioxidant effects of γ-Oryzanol: involvement of the Nrf2 pathway

Wiramon Rungratanawanich[1,§], Giulia Abate[1,§], **Melania Maria Serafini**[2,3], Michela Guarienti[1], Michele Catanzaro[3], Mariagrazia Marziano[1], Maurizio Memo[1], Cristina Lanni[3] and Daniela Uberti[*,1]

[1]Department of Molecular and Translational Medicine, University of Brescia, Viale Europa 11, 25123 Brescia, Italy

[2]Scuola Universitaria Superiore IUSS Pavia, P.zza Vittoria 15, 27100 Pavia, Italy

[3]Department of Drug Sciences (Pharmacology Section), University of Pavia, V.le Taramelli 14, 27100 Pavia, Italy

[§] The authors contributed equally to this work

Abstract

γ-oryzanol (ORY) is a ferulate compound very abundant in rice (*Oryza sativa L.*), from which its name derived. ORY is well-known for its antioxidant properties. However, the mechanism by which ORY exerts its antioxidant effects is still little known. In this paper, we demonstrated that ORY acts through the activation of nuclear factor (erythroid-derived 2)-like 2 (Nrf2) transcriptional pathway, the "master regulator" of cellular antioxidant defenses, actively involved in the aging process. In particular, in Human Embryonic Kidney cells (HEK-293), 24 h of ORY exposure modulated Nrf2 pathway both in basal condition and after an oxidative insult. The results of this study clearly suggest that ORY could be an early Nrf2 inducer, as demonstrated by its nuclear translocation. Furthermore ORY was able to promote the endogenous up-regulation of Nrf2-dependent defensive genes, such as NAD(P)H quinone reductase (NQO1), heme oxygenase-1 (HO-1), and glutathione synthetase (GSS), both at mRNA and protein levels. In conclusion this study, beside confirming the regulation of antioxidant enzymes by ORY, has been the first to demonstrate the long lasting antioxidant effect of ORY through the Nrf2 pathway activation, suggesting its newly potential role in preventing ageing process.

Keywords

Introduction

According with the Harmann theory of aging, oxidative stress is at the base of the mechanisms involved in aging processes [1] and contributes to the development of many age-related diseases, including cancer, atherosclerosis, hypertension, diabetes, and neurodegenerative disorders [2, 3]. Oxidative stress is defined as the imbalance among the production of free radicals, the efficiency of

antioxidant enzyme systems and the ability to activate antioxidant-promoting intracellular pathways. Reactive oxygen and nitrogen species (ROS/RNS) are usually produced by living organisms as a result of normal cellular metabolism, but they can also be induced by different endogenous and exogenous insults [4]. Thus, during the life span, the organism is continuously at risk to be exposed to ROS/RNS levels, beyond such a threshold for which the body tissues fail to counteract the damage. It is well known that at low to moderate concentrations ROS/RNS take part in physiological cell processes, but at high concentrations, they produce adverse modifications to the cellular macromolecules such as lipids, proteins and DNA, affecting cell functions and even its survival [3, 5]. Antioxidant enzyme cascade, involving superoxide dismutase (SOD), catalase and glutathione peroxidase (GPx), acts as first line of protection counteracting ROS/RNS generation. These three enzymes, working sequentially, neutralize free radicals: SOD catalyzes the dismutation of superoxide anion to hydrogen peroxide (H_2O_2), which is in turn neutralized to H_2O by catalase or GPx [6]. In addition, antioxidant-promoting intracellular pathways participate in maintaining redox steady state and in preventing ROS/RNS detrimental effects induced by stressors.

The transcription factor Nrf2 (NFE2-related factor 2) has emerged as a master regulator of cellular detoxification response and redox status, since it protects the organism from pathologies that are caused or exacerbated by oxidative stress. Very recently, a key role of the Nrf2 pathway has also emerged in the aging processes and in preventing age-related diseases [10-12]. The Nrf2 pathway is an intrinsic mechanism of defense able to reduce oxidative stress by inducing the transcription of up to 10% of human genes, which take part in different cellular functions such as ROS/RNS elimination, detoxification, xenobiotic metabolism, drug excretion, glutathione and NADPH synthesis. Among the antioxidant enzymes, the Nrf2 pathway promotes the transcription of NAD(P)H quinone reductase

(NQO1), heme oxygenase-1 (HO-1), and glutathione synthetase (GSS), to name a few, because of the presence of an antioxidant responsive element (ARE) sequence in their promoter region [7, 8]. The activation of Nrf2 is mediated by disrupting its interaction and binding to Kelch-like ECH associated protein 1 (Keap1), a cytosolic Nrf2 repressor that, in basal conditions, recruits the Cul3 ubiquitin ligase to induce Nrf2 degradation via proteasome, thus acting as a sensor of oxidative stress [9].

In recent years, natural compounds have gained more attention, since their therapeutic effects have been found important in the improvement of a life-style as well as in the protection against age-related diseases such as hyperlipidemia, inflammatory disorders, cardiovascular diseases and cancer [13-15]. These observations might change the concept of food consumption and nutrition, not only for diminishing starvation and malnutrition, but also for preventing morbidity and mortality of chronic diseases, particularly related to free radical damage. Thus, dietary antioxidants containing anti-oxidative phytochemicals become fundamental to counteract oxidative stress, consequently maintaining body homeostasis and redox balance [16].

Rice (*Oryza sativa L.*), a natural source of antioxidant, is rich in plenty of anti-oxidative components such as essential vitamin E complex, anthocyanins and phenolic compounds [17]. As compared to other cereal grains, rice contains the highest special phenolic compound that is ferulic acid, which is presented in the form of a steryl ferulate called "γ-oryzanol" (ORY). γ-oryzanol derived its name from rice because it was first discovered in rice bran oil and it is composed of a hydroxyl group [18-20]. Rice-derived extracts have been characterized by many metabolites of the ORY, a mixture of ferulic acid esters and phytosterols, among which triterpene alcohols and plant sterols [21]. The quantity of ORY and its metabolites vary in the different types of rice. Some varieties of rice may exhibit an amount

of ORY 8–10 times higher than vitamin E, to date one of the most potent natural antioxidants [22, 23].

The antioxidant properties of ORY have been first investigated in *in vivo* and *in vitro* experiments, demonstrating its ability in preventing and reducing the ROS/RNS formation [15, 21]. Jin Son et al. demonstrated that mice subjected to an high-fat diet supplemented with ORY showed significantly lower amount of oxidative stress and lipid peroxidation when compared to mice fed with high-fat diet alone [24]. Similarly, in Drosophila melanogaster, ORY was found to ameliorate antioxidant activities, thereby preventing the oxidative damage [25].

However, the mechanism by which ORY exerts it antioxidant effects is still little known. In this paper, we have deepened ORY antioxidant effects by studying the involvement of the activation of nuclear factor (erythroid-derived 2)-like 2 (Nrf2) transcriptional pathway. In particular, ORY was investigated as a putative Nrf2 inducer, and its ability of promoting the endogenous up-regulation of the Nrf2-dependent defensive genes was also assessed.

Material and Methods

Cell culture and treatments. Human Embryonic Kidney cells (HEK-293) were cultured in Dulbecco's modified Eagle's medium containing 10% foetal bovine serum, 2 mmol/L glutamine, 100 U/mL penicillin and 100 µg/mL streptomycin at 37°C in a 5% CO_2-containing atmosphere. Oxidative insult was induced adding 100 µM of H_2O_2 to cells at 80% confluent monolayers for different times according with the experimental paradigms.

Cell viability. Cell viability was evaluated 24 h after the oxidative insult by MTT assay. Cells were incubated with 500 mg/mL of MTT (3-(4,5-dimethylthiazol-2-yl)-2,5-diphenyltetrazolium bromide) for 3 h at 37°C. Then it was removed and cells were lysed with dimethyl sulfoxide. The absorbance at 595 nm was measured using a Bio-Rad

3350 microplate reader (Bio Rad Laboratories, Richmond, CA, USA). Cells, treated with 0.2% Triton-X100 solution (Sigma Aldrich, Merck KGaA, Darmastadt, Germany), were used to calculate the maximum toxicity, T_{max}. Data were expressed as percentage of cell viability over the corresponding controls.

Measurement of ROS/RNS generation. Intracellular ROS levels were measured using the fluorescent dye 2',7'-dichlorodihydrofluorescein diacetate (H₂DCF-DA) (Thermo Fisher Scientific, Waltham, Massachusetts USA), a nonpolar compound that is converted into a nonfluorescent polar derivative (H₂DCF) by cellular esterase after incorporation into cells. H₂DCF is membrane permeable and is rapidly oxidized to the highly fluorescent 2',7'-DCF (DCF) in the presence of intracellular ROS. For the experiments, HEK-293 was pretreated with ORY_{24h} and then exposed to H_2O_2 oxidative insult at different time points. At the end of the treatment, cells were washed in Hanks' Balanced Salt Solution (HBSS) and then incubated in nitrogen-saturated HBSS with 20 mM H₂DCF-DA dissolved in DMSO for 30 minutes at 37°C 5% CO_2. After washing twice in HBSS, intracellular DCF fluorescence, proportional to the amount of ROS/RNS, was evaluated by EnSight fluorescence 96-plate reader (EnSight™ Multimode Plate Reader, PerkinElmer), with excitation and emission wavelengths of 492 and 527 nm, respectively.

Subcellular Fractionation for Nrf2 Nuclear Translocation. Nuclear protein extracts were prepared by washing HEK-293 cells twice with ice-cold PBS. Cells were subsequently homogenized 15 times using a glass-glass dounce homogenizer in 0.32 M sucrose buffered with 20 mM Tris-HCl (pH 7.4) containing 2 mM EDTA, 0.5 mM EGTA, 50 mM β-mercaptoethanol and 20 μg/mL leupeptin, aprotinin, and pepstatin. The homogenate was centrifuged at 300 g for 5 minutes to obtain the nuclear fraction. An aliquot of the nuclear fraction was used for protein assay by the Bradford method, whereas

the remaining was boiled for 5 min after dilution with sample buffer and subjected to polyacrylamide gel electrophoresis and immunoblotting as described below.

Western blot analysis. Total protein extracts were prepared by harvesting cells in 80 µl of lysis buffer containing 50 mM Tris-HCl (pH 7.6), 150 mM NaCl, 5 mM EDTA, 1 mM phenyl methyl sulphonyl fluoride, 0.5 mg/mL leupeptin, 5 mg/mL aprotinin and 1 mg/mL pepstatin. Samples were sonicated and centrifuged at 15,000 g for 30 minutes at 4°C. The resulting supernatants were isolated and protein content determined by a conventional method (BCA protein assay Kit, Pierce, Rockford, IL) before processing for Western blot analysis. Protein samples (30 µg) of both total and nuclear extracts, were electrophoresed in 10% or 12% acrylamide gel and electro-blotted onto nitrocellulose membranes (Sigma-Aldrich, Merck KGaA, Darmastadt, Germany). Membranes were blocked for 1 h in 5% w/v Bovine Serum Albumin in TBS-T (0.1 M Tris-HCl pH 7.4, 0.15 M NaCl, 0.1% Tween 20) and incubated overnight at 4°C with primary antibodies. Primary antibodies were anti-Mn-superoxide dismutase (MnSOD) (anti-SOD2, 1:200 Sigma- Aldrich, Merck KGaA, Darmastadt, Germany), anti-Cu–Zn superoxide dismutase (anti-SOD1, 1:300, Santa Cruz Biotechnology Inc., Heidelberg, Germany), anti-Nrf2 (1:2000, Novus, Biotechne, Minneapolis USA), anti-NQO1 (1:100, Novus, Biotechne, Minneapolis USA), anti HO-1 (1:2000, Novus, Biotechne, Minneapolis USA), anti-β-actin (1:1000, BD Biosciences, Franklin lakes, NJ USA), anti-lamin A/C (1:1000, BD Biosciences, Franklin lakes, NJ USA) and anti-α tubulin (1:1000, Sigma-Aldrich, Merck KGaA, Darmastadt, Germany). IR Dye near-infrared dyes-conjugated secondary antibodies (LI-COR, Lincoln, Nebraska USA) were used. The immunodetection was performed using a dual-mode western imaging system Odyssey FC (LI-COR Lincoln, Nebraska USA). Quantification was performed using Image Studio Software (LI-COR, Lincoln, Nebraska USA) and

the results were normalized over the α-tubulin, β-actin or lamin A/C signal.

Antioxidant enzyme activities. SOD activity was measured following the inhibition of epinephrine oxidation, according to McCord method [26]. Total protein extracts and epinephrine 0,1 M (Sigma Aldrich, Merck KGaA, Darmastadt, Germany) were added to G buffer (0.05 M glycine and 0.1 M NaCl at pH 10.34), and the reaction was monitored measuring the decrease of absorbance at 480 nm. The activity of purified SOD enzyme (3000 U/mg Sigma Aldrich, Merck KGaA, Darmastadt, Germany) was also measured in each experiment as a positive control. Data were normalized for protein amount and results expressed as U/mg using the molar extinction coefficient of 4.02 at 480 nm.

Catalase activity was measured monitoring the decomposition of H_2O_2 according to Shangari and O'Brien [27]. In particular, total protein extracts were incubated in a substrate (65 µM hydrogen peroxide in 6.0 mM PBS buffer pH 7.4) at 37°C for 60 s. The enzymatic reaction was stopped by the addition of 32.4 mM ammonium molybdate (Sigma Aldrich, Merck KGaA, Darmastadt, Germany) and measured at 405 nm. The results were extrapolated by a standard curve (ranging from 12 U/mL to 0,25 U/mL) performed with purified CAT enzyme (20100 U Sigma Aldrich, Merck KGaA, Darmastadt, Germany).

Glutathione peroxidase activity was performed in accordance with Awasthi et al. [28], measuring NADPH oxidation at 340 nm in the reaction that involved oxidation of reduced glutathione (GSH) to glutathione (GSSG) followed by its reduction by glutathione reductase (GR). Total protein extracts were mixed with a reaction mix, containing 50 mM PBS with 0.4 mM EDTA, pH 7.0; 1.0 mM sodium azide solution; 1.0 mg β–NADPH; 100 U/mL GR, 200 mM GSH and 10 µl of 0.042% H_2O_2. The activity of purified GPx enzyme (116 U/mg) was also measured in each experiment as positive control.

All the reagents were purchased by Sigma Aldrich, Merck KGaA, Darmastadt, Germany. GPx activity was measured as nmol NADPH oxidized to NADP+/mg protein by using the molar extinction coefficient of 0.00622 at 340 nm, and the data were expressed as U/mg.

Quantitative real-time PCR. Total RNA was extracted from 5×10^6 cells following TRIzol® reagent protocol (Invitrogen Corporation, Carlsbad, CA USA). 2 μg of total RNA were retrotranscribed with MMLV reverse transcriptase (Promega, Madison, Wisconsin USA), using randomhexamers in a final volume of 40 μl. Parallel reactions containing no reverse transcriptase were used as negative controls to confirm the removal of all genomic DNA. Nrf2, NQO1, HO-1 and GAPDH primers were provided by Qiagen (Qiagen, Hilden, Germany). GAPDH was used as endogenous reference. Quantitative RT-PCR was performed with the ViiA7 Real Time PCR System (Applied Biosystems, Foster City, CA USA), using the iQ™SYBR Green Supermix method (Bio-Rad Laboratories, Richmond, CA, USA) according to manufacturer's instructions.

Statistical Analysis. Results are reported as mean ± standard error mean (SEM) or standard deviation (SD) of at least three independent experiments. Statistical differences were determined by analysis of variance (one-way ANOVA) followed, when significant, by an appropriate *post hoc* test as indicated in figure legends. p value of <0.05 was considered statistically significant.

Results
Oryzanol prevents H_2O_2-induced ROS/RNS generation and cell death. The antioxidant properties of ORY (Sigma Aldrich, Merck KGaA, Darmastadt, Germany) were evaluated in HEK-293 cells in baseline redox steady-state conditions and after an acute oxidative insult. Cells were pretreated for 24 h with ORY (ORY$_{24h}$) at different

concentrations, ranging from 1 to 20 µg/mL, followed by an acute oxidative insult elicited by 100 µM H_2O_2. 24 h later, cell viability was evaluated with MTT assay. As shown in Fig. 1A, ORY_{24h} did not affect cell viability at any examined concentration. H_2O_2 alone reduced cell viability of about 35% (p<0.001) but this mortality was rescued by ORY_{24h} already at 5 µg/mL (p<0.05) (Fig. 1A). The minimum efficient concentration was used for the following experiments.
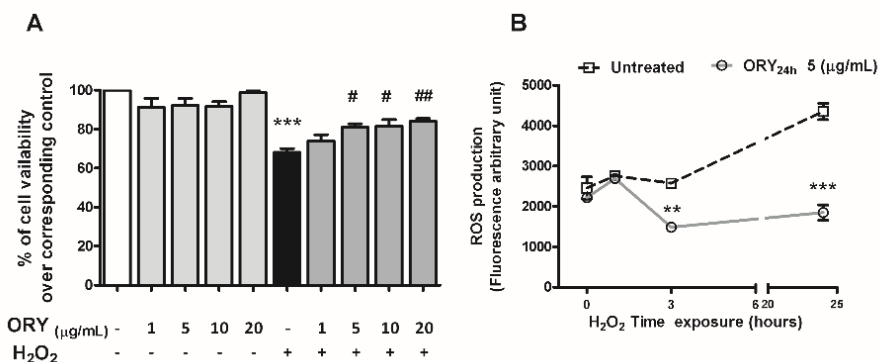
Figure 1. Oryzanol protects from cell death and decrease H_2O_2-induced ROS/RNS generation. (A) HEK-293 cells were pretreated for 24 h with ORY (ORY_{24h}) at different concentrations, and then stressed by the addition of 100 µM H_2O_2 for 24 h. Cell viability was evaluated with MTT assay. Data are shown as percentage of cell viability compared with untreated cells; *** p<0.001 vs untreated cells and ## p<0.01, # p<0.05, vs H_2O_2 group. (B) Effects of 5 µg/mL ORY_{24h} on H_2O_2-induced ROS/RNS production were determined by H_2DCF-DA oxidation using a fluorescence microplate reader. Fluorescence intensity of ORY_{24h} (open square symbol) after oxidative insult significantly decreased over time with ** p<0.01 at 3 h and *** p<0.001 at 24 h vs the corresponding untreated control group (open circle symbol). Bonferroni's multiple comparison test.

The effect of 5 µg/mL ORY_{24h} on H_2O_2-induced oxygen and nitrogen reactive species (ROS/RNS) production was studied by monitoring the oxidation of the 2'-7' dichlorofluorescein (DCF) probe that in a reduced state is not fluorescent and becomes florescent in the

presence of free radicals. 100 μM H_2O_2 exposure initially induced a moderate production of ROS/RNS, that anyway significantly increased over time, as assessed by accumulation of oxidized DCF (Fig. 1B open square symbol). ORY_{24h} reverted H_2O_2-induced ROS/RNS generation already at 3 h and this effect was sustained at least until 24 h (Fig. 1B open circle symbol).

Oryzanol modulates the antioxidant enzyme activities. Different studies suggested that ORY could exert its antioxidant effects by modulating the endogenous antioxidant enzyme activities. In particular, superoxide dismutase has been found to be positively regulated by ORY [25, 29, 30]. Here we evaluated the protein expression and activity of SOD enzymes in the presence of ORY_{24h} alone or followed by H_2O_2 insult. H_2O_2 insult did not affect the protein expression of MnSOD, but significantly increased the Cu-Zn SOD protein levels (Fig. 2B), that also reflected an increase of SOD activity induced by the oxidative insult (Fig. 2C). ORY_{24h} alone significantly enhanced the protein expression of both the mitochondrial MnSOD (mean ± SEM: untreated cells 0.078 ± 0.014 vs ORY_{24h} 0.143 ± 0.006; $p<0.001$) and cytosolic Cu-Zn SOD (mean ± SEM: untreated cells 0.059 ± 0.005 vs ORY_{24h} 0.150 ± 0.011; $p<0.01$) (Fig. 2A, B), as well as the total SOD activity (mean ± SEM: untreated cells 0.098 ± 0.066 vs ORY_{24h} 0.566 ± 0.072; $p< 0.001$ Fig. 2C).

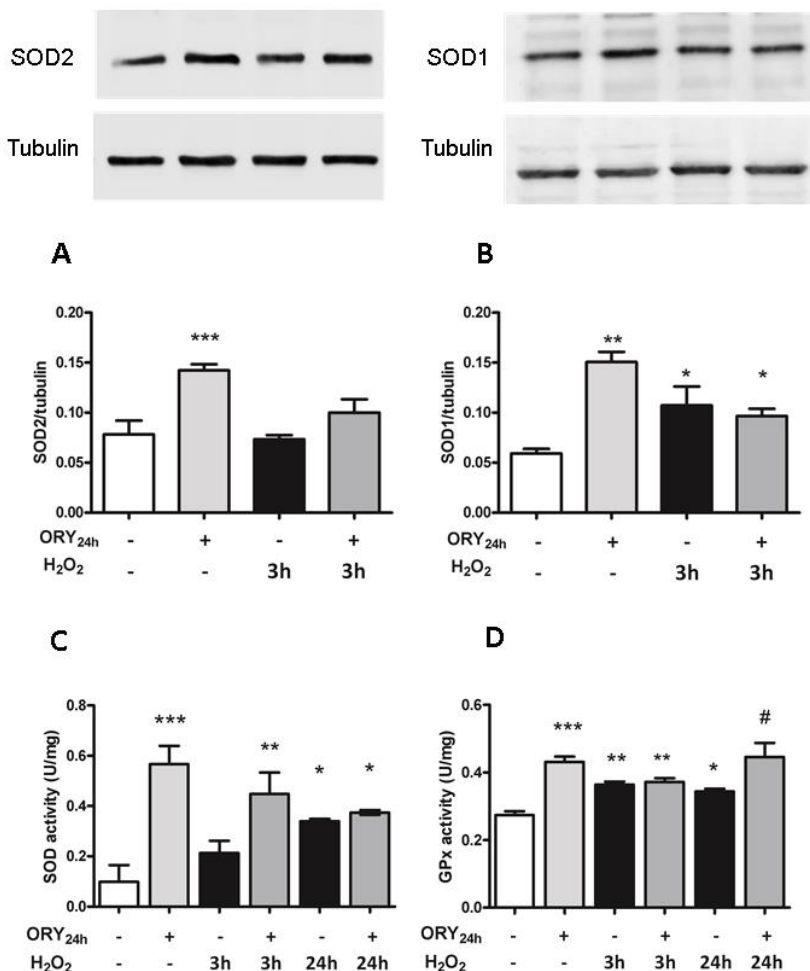**Figure 2. Oryzanol effect on antioxidant enzyme activities and MnSOD and Cu-ZnSOD expression.** HEK-293 cells were pretreated with 5 μg/mL ORY for 24 h followed by 100 μM H_2O_2 for 3 h or 24 h. A, B) Effect of ORY_{24h} on the expression of MnSOD and Cu-ZnSOD in H_2O_2-induced oxidative stress. The protein expression was assessed by western blotting. Tubulin expression was used as loading control. Data are presented as mean ± SEM; *** $p<0.001$, ** $p<0.01$ vs untreated cells. The activity of total SOD (C) and GPx (D) enzymes was assessed, as reported in the method section, before and after 3 h and 24 h of H_2O_2 oxidative insult. The results are represented as mean ± SEM; *** $p<0.001$, ** $p<0.01$, * $p<0.05$ vs untreated cells and # $p<0.05$ vs the corresponding H_2O_2 control group. Bonferroni's multiple comparison test.

The combination of ORY_{24h} followed by H_2O_2 still maintained significantly higher the Cu-Zn SOD protein expression compared with untreated cells (mean ± SEM: 0,097 ± 0,007; p<0.05), but no differences were highlighted compared with H_2O_2 alone (mean ± SEM: 0.107 ± 0.019). Interestingly, in presence of an acute oxidative insult (3 h of H_2O_2 treatment), ORY_{24h} still maintained higher the total SOD activity compared with H_2O_2 alone (mean ± SEM: ORY_{24h} + H_2O_2 0.4448 ± 0.085 vs H_2O_2 0.214 ± 0.048 Fig. 2C). We also evaluated the activity of Catalase and GPx, two enzymes that work downstream SOD. No differences in term of catalase activity were found comparing the different treatments (data not shown). Differently, GPx activity was found to be modulated by Oryzanol. ORY_{24h} alone increased GPx activity (mean ± SEM: 0.43 ± 0.016) compared to untreated one (mean ± SEM: 0.27 ± 0.011; p<0.001 Fig. 2D). H_2O_2 acute insults (3 h) also induced an increase in GPx activity that was confirmed by the Oryzanol pretreatment without further affecting the activity levels. A long lasting oxidative insult (H_2O_2 24 h) showed ORY_{24h} still maintained higher GPx activity after oxidative insult suggesting a still active alarm system that is ready to detoxify from radicals. All together these data confirmed the antioxidant effects of ORY throughout the modulation of endogenous antioxidant enzyme activities.

Oryzanol activates the Nrf2 pathway. Activation of the Keap1/Nrf2 pathway and the consequent induction of its antioxidant genes trigger an elaborate network of protective mechanisms against oxidative damage [31]. When exposed to an oxidative insult, Keap1, following conformational changes, disrupts its binding to Nrf2, in turn promoting Nrf2 translocation into the nucleus and the activation of transcription-mediated protective responses [32]. Thus, ORY was investigated to verify whether it might affect the Nrf2 pathway. We focused on the activation of Nrf2 signaling by analyzing its translocation into nucleus and its ability to induce NQO1 and HO-1,

two prototypical cytoprotective Nrf2-target genes related to cellular stress response.

In basal conditions, 3 h exposure of ORY significantly increased Nrf2 nuclear expression, that is further enhanced at 6 h and then decreased at 24 h, even if in an higher extent in comparison with untreated cells (mean ± SEM: ORY_{3h} 1.28 ± 0.11; ORY_{6h} 1.76 ± 0.25, ORY_{24h} 1.03 ± 0.02 vs untreated 0.64 ± 0.07; p<0.01, p<0.001, p<0.05 respectively Fig. 3A). As a positive control, also 3 h treatment with 100 μM H_2O_2 increased Nrf2 nuclear levels, that resulted higher than those found in untreated cells (mean 1.01 ± 0.07; p<0.05), and comparable with ORY_{24h} treatment (Fig. 3A). The pretreatment of cells with ORY_{24h} followed by 3 h H_2O_2 did not significantly differ in the extent of activation from the ORY_{24h} or H_2O_2 alone. To further sustain these results, we also investigated the Nrf2 expression in the cytosolic fraction. At 3, 6 and 24 h, ORY did not modify the Nrf2 cytoplasmatic expression, expressed as ratio Nrf2/tubulin (Fig. 3B). In the same way, a similar trend was observed in presence of H_2O_2 alone or combined with ORY (Fig. 3B).
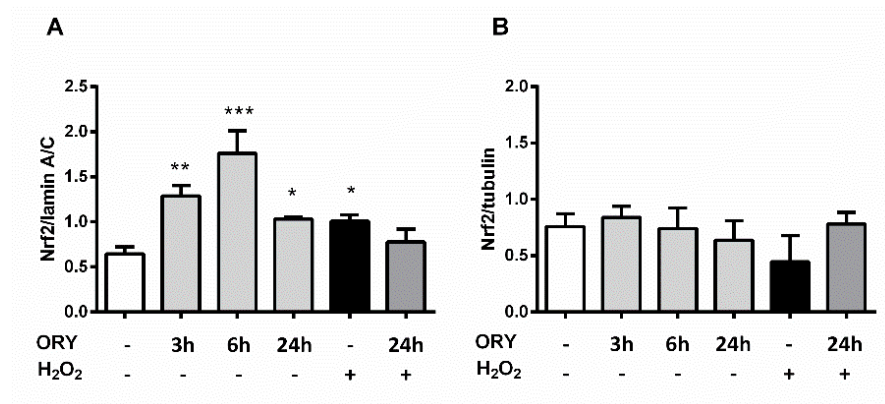

Figure 3. Nrf2 nuclear translocation induced by Oryzanol. HEK-293 cells were pretreated with ORY for 3, 6 and 24 h and then stressed with 100 μM H_2O_2 for 3h. Nuclear and cytoplasmic fractions were isolated as described in the methods section. (A) Nuclear expression of Nrf2 was assessed by western blotting and Lamin

A/C expression was used as loading control. Data are represented as mean ± SD; *** p<0.001, ** p<0.01, * p<0.05 vs untreated cells, Dunnett's multiple comparison test. (B) Cytoplasmic expression of Nrf2 was assessed by western blotting and Tubulin expression was used as loading control. Data are represented as mean ± SD.

The mRNA expression of Nrf2 was also evaluated in cells pretreated with ORY_{24h} alone or followed by a H_2O_2 time course (Fig. 4A). H_2O_2 alone transiently increased mRNA levels of Nrf2. ORY_{24h} alone did not affect Nrf2 expression, but when oxidative insult was present, ORY_{24h} significantly increased its mRNA levels at 1 and 3 h, without changing the transient pattern. The increase of mRNA reflected also an increase of Nrf2 protein levels at 24 h after H_2O_2 insult in presence or absence of ORY_{24h} (Fig. 5A).
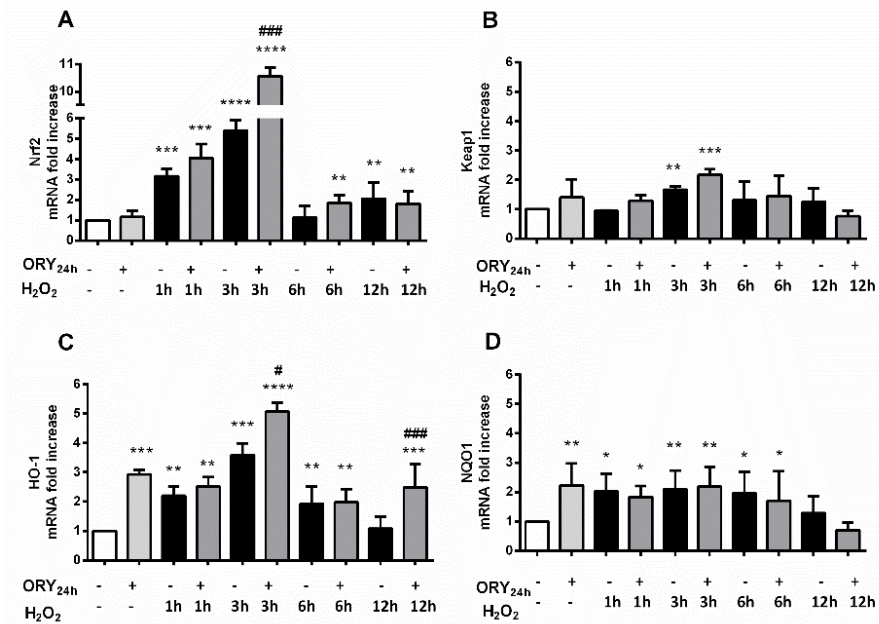

Figure 4. Oryzanol activates the transcription of Nrf2-target genes. HEK-293 cells were pretreated with 5 μg/mL ORY for 24 h followed by a time course of 100 μM H_2O_2 (1, 3, 6 and 12 h). After these periods of time cells were processed for measuring Nrf2 (A), Keap1 (B), HO-1 (C) and NQO1 (D) mRNA levels by real time PCR. GAPDH was used to normalized the results. Data are shown as mean ±

SEM. Statistically significant differences were represented as follow: **** $p < 0.0001$, *** $p < 0.001$, ** $p < 0.01$, * $p < 0.05$ vs untreated cells and ### $p < 0.001$, # $p < 0.05$ vs the corresponding H_2O_2 control group, Bonferroni's multiple comparison test.

Since Keap1 is the other key factor involved in the regulation of Nrf2 pathway activation, its mRNA expression was also investigated (Fig. 4B). ORY_{24h} did not change Keap1 mRNA levels respect to untreated cells. H_2O_2 alone induced a slight increase of Keap1 mRNA level that resulted significant only at 3 h. While the combined treatment ORY_{24h} and H_2O_2, although appeared to further enhance Keap1 mRNA, only at 3 h of oxidative insult resulted significant.

To verify the complete activation of the Nrf2 pathway, we then analyzed the induction of the cytoprotective Nrf2-target genes. Figure 4 and 5 reported the mRNA expression and protein levels of HO-1 and NQO1 in cells exposed to ORY_{24h} alone or followed by H_2O_2.

ORY_{24h} treatment increased the mRNA levels of HO-1 and NQO1 by nearly two fold and one fold respectively (Fig. 4C, D). HO-1 mRNA expression was also transiently induced by oxidative insult, with a highest expression at 3 h, that returned at basal levels at 12 h. Interestingly after treatment with ORY_{24h} followed by oxidative insult, HO-1 mRNA remained still high at 12 h (Fig. 4C). HO-1 protein expression reflected the mRNA results, significantly increasing after ORY_{24h} or H_2O_2 alone as well as remaining high after the combined treatment ORY_{24h} plus oxidative insult (Fig. 5B). Similarly, NQO1 mRNA was transiently increased by H_2O_2 alone or in combination with ORY_{24h}, although the magnitude of fold increase was lower than that observed for HO-1 at any time point (Fig. 4D). NQO1 protein expression reflected the mRNA results, showing a significant increase after ORY_{24h} or H_2O_2 alone and then decreasing after the combined treatment ORY_{24h} plus H_2O_2 (Fig. 5D).
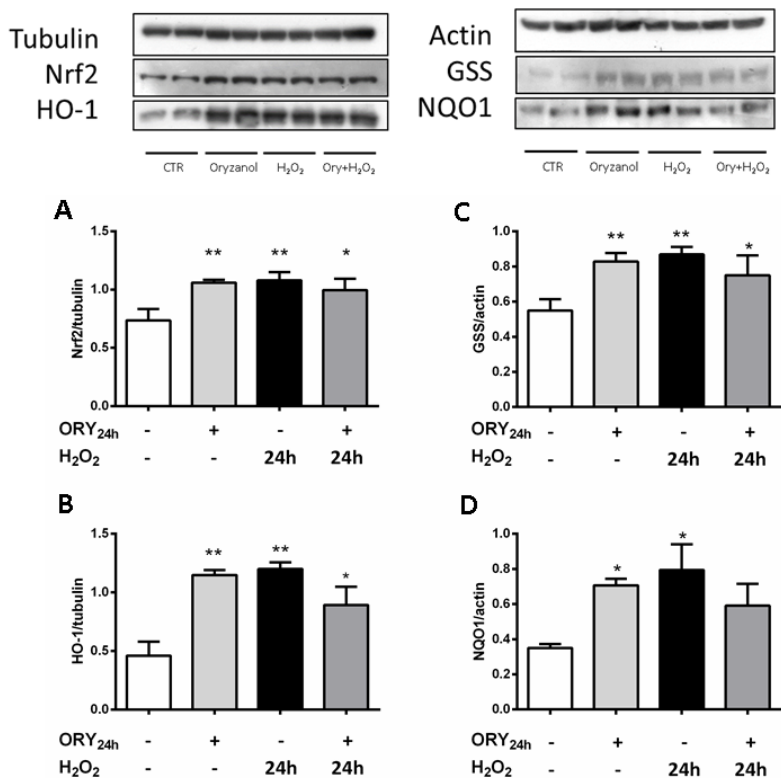
Figure 5. Oryzanol induces an increase in Nrf2-target genes protein levels.
HEK-293 cells were pretreated with 5 µg/mL ORY for 24 h followed by 24 h of
100 µM H_2O_2. After that, cells were processed for measuring Nrf2 (A), HO-1 (B),
GSS (C) and NQO1 (D) protein levels by western blotting. Tubulin or actin were
used as loading control according with the molecular weight of above investigated
proteins. Data are shown as mean ± SD; ** $p<0.01$, * $p<0.05$ vs untreated cells,
Dunnett's multiple comparison test.

Since the increase in GPx activity due to ORY pretreatment, we also
decided to investigate protein levels of glutathione synthetase (GSS),
another Nrf2-target gene. GSS protein expression was in accordance
with the results obtained for HO-1, since it significantly increased
after ORY_{24h} or H_2O_2 alone and then decreased after the combined
pretreatment with ORY and oxidative insult.

These data confirmed an early activation of Nrf2 pathway due to ORY pretreatment highlighting its ability to modulate efficiently the relative expression of Nrf2 target gene both at mRNA and protein levels.

Discussion

Before the westernization of East countries, with the introduction and diffusion of Western foods, the East populations were known for their longevity and for the low incidence of certain illness, like cardiovascular disease [33]. Rice has been, and is even now, at the base of diet of such populations and it has been related to the prevention of aging and age-related disease, but its importance and consumptions are not really well claimed. Rice exerts beneficial effects on health, being a source of fiber, minerals, vitamins and phenols with antioxidant activities [18, 19, 34, 35]. Rice-derived ORY has been well studied for its ability to prevent oxidative stress by inducing antioxidant enzyme expression and activity [15, 21].

Our results support these data and further validate the antioxidant effects exerted by ORY by inhibiting H_2O_2-induced ROS/RNS generation. In particular, we showed that, in basal conditions, ORY regulated the protein expression of SOD enzymes, also inducing an increased enzyme activity. Furthermore, GPx enzyme activity was also enhanced by ORY in H_2O_2-induced ROS/RNS and baseline conditions. In addition, following an oxidative insult, when ROS/RNS are excessively produced, ORY sustained the antioxidant cellular response, maintaining a higher enzymatic activity, thus efficiently turning off ROS burst. Through this mechanism, rice-derived ORY may represent a valid first defense line against oxidative hits. Moreover, beyond its antioxidant properties, ORY was found to possess further potential functionalities, including anti-hyperlipidemic, anti-diabetic and anti-inflammatory effects, thus suggesting a potential role also against the development of the related diseases [15, 21, 35-37].

All these disorders are related to redox imbalance, thus suggesting that other mechanisms associated with the regulation of redox homeostasis and the protection against long-lasting oxidative insults could be involved. Here we showed that ORY exhibited a remarkable free radical scavenging property and we further deepened the antioxidant profile of ORY by demonstrating for the first time its ability to trigger the Nrf2 pathway in terms of up-regulation of Nrf2 expression, translocation into the nucleus and induction of the Nrf2-dependent defensive genes.

These results are also very interesting, because they may suggest ORY or ORY-inspired compounds as an integrative intervention to impact the aging process and longevity, taking into account that, with aging, Nrf2 activity decreases alongside increased oxidant stress [38, 39].

Induction by reactive oxygen species is the best understood mechanism of Nrf2 activation. In our experimental models, H_2O_2 was able to induce Nrf2 translocation and activation of its target genes involved in cellular responses against xenobiotics. NAD(P)H quinone dehydrogenase 1 (NQO1), heme oxygenase-1 (HO-1) mRNA and protein levels were found enhanced in HEK-293 cells treated with H_2O_2. SOD1, is another target gene of Nrf2. H_2O_2 induced an increase in the expression of cytosolic SOD, suggesting that it could be under the regulation of Nrf2. The mechanism by which free radicals activate Nrf2 pathway is via the modification of cysteine residues on Keap1, thus resulting in Nrf2 accumulation in the cytoplasm and translocation into the nucleus. Oxidative insult also induced the increased of mRNA and protein expression of Nrf2 (Fig. 4A). Two ARE-like motifs in the 5 flanking region of the Nrf2 promoter are responsible for the induction of Nrf2 upon activation [40], ensuring a feed-forward process with Nrf2 activation promoting its own expression and thus facilitating a profound cellular response to stress. Therefore, all these data highlighted the answer that the cells put in place in the tentative to detoxify themselves by the oxidative insult that finally

failed because ROS/RNS production took the lead. In addition, Nrf2 can also be activated by different phytochemicals [41-43] as well as various pharmaceuticals (reviewed in [44]) via overlapping and distinct mechanisms.

Here we demonstrated that ORY alone was able to transiently induce Nrf2 translocation that was still present when oxidative insult was added. The mechanism of action by which ORY is able to modulate Nrf2 pathway could be due by its intrinsic chemical structure (Fig.6). The hydroxyl group of the phenolic ring of ORY and an electron delocalization of ferulate residue induced by the presence of ROS/RNS [15, 21] might be involved in the modification of cysteine thiols of Keap1, leading to the inhibition of Keap1-Nrf2 binding. The consequence of Nrf2 nuclear translocation is the transactivation of its target genes. Here we found that ORY_{24h} induced the transiently transcription of at least three Nrf2 target genes, HO1, NQO1 and GSS. HO-1 and NQO1 gene transactivation was confirmed by the increase of their protein expression. It is noteworthy that HO-1 mRNA was still higher after 12 h of pretreatment with ORY followed by oxidative insult, suggesting the existence of putative alternative mechanisms able to sustain in parallel its expression. Finally, ORY_{24h}-induced Cu-Zn-SOD (SOD1) increased protein expression could be also under the control of Nrf2.

In conclusion, this study demonstrates that the antioxidant properties of ORY are sustained by the Nrf2 pathway. The beneficial effects of ORY have been here reinforced by understanding its mechanism of action. Since Nfr2 has been also proposed as a "master regulator of the aging process" playing a role in regulating longevity as well as age-related diseases, in future we will further investigate ORY properties as a possible longevity-promoting inducer.

Acknowledgement

References

1. Harman, D., "Aging: a theory based on free radical and radiation chemistry," J Gerontol, vol. 3, pp. 298-300, 1956.
2. Olinski, R., et al., "Oxidative damage to DNA and antioxidant status in aging and age-related diseases," Acta Biochim Pol, vol. 1, pp. 11-26, 2007.
3. Uttara, B., et al., "Oxidative stress and neurodegenerative diseases: a review of upstream and downstream antioxidant therapeutic options," Curr Neuropharmacol, vol. 1, pp. 65-74, 2009.
4. McCord, J.M., "The evolution of free radicals and oxidative stress," Am J Med, vol. 8, pp. 652-9, 2000.
5. Fang, Y.Z., S. Yang, and G. Wu, "Free radicals, antioxidants, and nutrition," Nutrition, vol. 10, pp. 872-9, 2002.
6. Ghosh, N., R. Ghosh, and S.C. Mandal, "Antioxidant protection: A promising therapeutic intervention in neurodegenerative disease," Free Radic Res, vol. 8, pp. 888-905, 2011.
7. Wilson, A.J., et al., "Keap calm, and carry on covalently," J Med Chem, vol. 19, pp. 7463-76, 2013.
8. Itoh, K., et al., "An Nrf2/small Maf heterodimer mediates the induction of phase II detoxifying enzyme genes through antioxidant response elements," Biochem Biophys Res Commun, vol. 2, pp. 313-22, 1997.
9. Lu, M.C., et al., "The Keap1-Nrf2-ARE Pathway As a Potential Preventive and Therapeutic Target: An Update," Med Res Rev, vol. 5, pp. 924-63, 2016.

10. Castillo-Quan, J.I., K.J. Kinghorn, and I. Bjedov, "Genetics and pharmacology of longevity: the road to therapeutics for healthy aging," Adv Genet, vol., pp. 1-101, 2015.

11. Bruns, D.R., et al., "Nrf2 Signaling and the Slowed Aging Phenotype: Evidence from Long-Lived Models," Oxid Med Cell Longev, vol., pp. 732596, 2015.

12. Sykiotis, G.P., et al., "The role of the antioxidant and longevity-promoting Nrf2 pathway in metabolic regulation," Curr Opin Clin Nutr Metab Care, vol. 1, pp. 41-8, 2011.

13. Ismail, N., et al., "Mechanistic basis for protection of differentiated SH-SY5Y cells by oryzanol-rich fraction against hydrogen peroxide-induced neurotoxicity," BMC Complement Altern Med, vol., pp. 467, 2014.

14. Ismail, N., et al., "Neuroprotective effects of germinated brown rice against hydrogen peroxide induced cell death in human SH-SY5Y cells," Int J Mol Sci, vol. 8, pp. 9692-708, 2012.

15. Islam, M.S., et al., "Biological abilities of rice bran-derived antioxidant phytochemicals for medical therapy," Curr Top Med Chem, vol. 14, pp. 1847-53, 2011.

16. Masisi, K., T. Beta, and M.H. Moghadasian, "Antioxidant properties of diverse cereal grains: A review on in vitro and in vivo studies," Food Chem, vol., pp. 90-7, 2016.

17. Soobrattee, M.A., et al., "Phenolics as potential antioxidant therapeutic agents: mechanism and actions," Mutat Res, vol. 1-2, pp. 200-13, 2005.

18. Butsat, S. and S. Siriamornpun, "Antioxidant capacities and phenolic compounds of the husk, bran and endosperm of Thai rice," Food Chemistry, vol. 2, pp. 606-613, 2010.

19. Lerma-García, M.J., et al., "Composition, industrial processing and applications of rice bran γ-oryzanol," Food Chemistry, vol. 2, pp. 389-404, 2009.

20. Tsuchiya, T.a.K., R., "New compound in rice bran and germ oils (Abstract in English)," Kogyo Kagaku Zasshi, vol., pp. 526-529, 1954.

21. Minatel, I.O., et al., "Antioxidant Activity of gamma-Oryzanol: A Complex Network of Interactions," Int J Mol Sci, vol. 8, 2016.

22. Minatel, I.O., et al., "Fat-soluble bioactive components in colored rice varieties," J Med Food, vol. 10, pp. 1134-41, 2014.

23. Xu, Z., N. Hua, and J.S. Godber, "Antioxidant activity of tocopherols, tocotrienols, and gamma-oryzanol components from rice bran against cholesterol oxidation accelerated by 2,2'-azobis(2-methylpropionamidine) dihydrochloride," J Agric Food Chem, vol. 4, pp. 2077-81, 2001.

24. Jin Son, M., et al., "Influence of Oryzanol and Ferulic Acid on the Lipid Metabolism and Antioxidative Status in High Fat-Fed Mice," J Clin Biochem Nutr, vol. 2, pp. 150-6, 2010.

25. Araujo, S.M., et al., "Effectiveness of gamma-oryzanol in reducing neuromotor deficits, dopamine depletion and oxidative stress in a Drosophila melanogaster model of Parkinson's disease induced by rotenone," Neurotoxicology, vol., pp. 96-105, 2015.

26. McCord, J.M. and I. Fridovich, "Superoxide dismutase. An enzymic function for erythrocuprein (hemocuprein)," J Biol Chem, vol. 22, pp. 6049-55, 1969.

27. Shangari, N. and P.J. O'Brien, "Catalase activity assays," Curr Protoc Toxicol, vol., pp. Unit 7.7.1-15, 2006.

28. Awasthi, Y.C., et al., "Purification and properties of glutathione peroxidase from human placenta," Biochem J, vol. 2, pp. 471-6, 1979.

29. Panchal, S.S., et al., "Anti-Inflammatory and Antioxidative Stress Effects of Oryzanol in Glaucomatous Rabbits," J Ophthalmol, vol., pp. 1468716, 2017.

30. Ghatak, S.B. and S.S. Panchal, "Anti-diabetic activity of oryzanol and its relationship with the anti-oxidant property," International Journal of Diabetes in Developing Countries, vol. 4, pp. 185-192, 2012.

31. Baird, L. and A.T. Dinkova-Kostova, "The cytoprotective role of the Keap1-Nrf2 pathway," Arch Toxicol, vol. 4, pp. 241-72, 2011.

32. Suzuki, T. and M. Yamamoto, "Molecular basis of the Keap1-Nrf2 system," Free Radic Biol Med, vol. Pt B, pp. 93-100, 2015.

33. Odegaard, A.O., et al., "Western-style fast food intake and cardiometabolic risk in an Eastern country," Circulation, vol. 2, pp. 182-8, 2012.

34. Laokuldilok, T., et al., "Antioxidants and antioxidant activity of several pigmented rice brans," J Agric Food Chem, vol. 1, pp. 193-9, 2011.

35. Chalermpong, S., "Antioxidant and anti-inflammatory activities of gamma-oryzanol rich extracts from Thai purple rice bran," Journal of Medicinal Plants Research, vol. 6, 2012.

36. Parrado, J., et al., "Prevention of brain protein and lipid oxidation elicited by a water-soluble oryzanol enzymatic extract derived from rice bran," Eur J Nutr, vol. 6, pp. 307-14, 2003.

37. Sakai, S., et al., "gamma-Oryzanol reduces adhesion molecule expression in vascular endothelial cells via suppression of nuclear factor-kappaB activation," J Agric Food Chem, vol. 13, pp. 3367-72, 2012.

38. Safdar, A., J. deBeer, and M.A. Tarnopolsky, "Dysfunctional Nrf2-Keap1 redox signaling in skeletal muscle of the sedentary old," Free Radic Biol Med, vol. 10, pp. 1487-93, 2010.

39. Suh, J.H., et al., "Decline in transcriptional activity of Nrf2 causes age-related loss of glutathione synthesis, which is

reversible with lipoic acid," Proc Natl Acad Sci U S A, vol. 10, pp. 3381-6, 2004.

40. Kwak, M.K., et al., "Enhanced expression of the transcription factor Nrf2 by cancer chemopreventive agents: role of antioxidant response element-like sequences in the nrf2 promoter," Mol Cell Biol, vol. 9, pp. 2883-92, 2002.

41. Surh, Y.J., J.K. Kundu, and H.K. Na, "Nrf2 as a master redox switch in turning on the cellular signaling involved in the induction of cytoprotective genes by some chemopreventive phytochemicals," Planta Med, vol. 13, pp. 1526-39, 2008.

42. Donovan, E.L., et al., "Phytochemical activation of Nrf2 protects human coronary artery endothelial cells against an oxidative challenge," Oxid Med Cell Longev, vol., pp. 132931, 2012.

43. Reuland, D.J., et al., "Upregulation of phase II enzymes through phytochemical activation of Nrf2 protects cardiomyocytes against oxidant stress," Free Radic Biol Med, vol., pp. 102-11, 2013.

44. Hybertson, B.M., et al., "Oxidative stress in health and disease: the therapeutic potential of Nrf2 activation," Mol Aspects Med, vol. 4-6, pp. 234-46, 2011.

Chapter III

The following preliminary data are part of a two-year project started on October 1ˢᵗ 2017 and funded by the Fondo di Ricerca di Ateneo, Blue Sky Research.

The title of the project is:

Eye-light on Age-related Macular Degeneration: targeting the Nrf2 pathway as a novel therapeutic strategy

Principal Investigator: Marialaura Amadio [1]
Co-investigator: **Melania Maria Serafini** [1,2]

[1]*Department of Drug Sciences (Pharmacology Section), University of Pavia, V.le Taramelli 14, 27100 Pavia, Italy*

[2]*Scuola Universitaria Superiore IUSS Pavia, P.zza Vittoria 15, 27100 Pavia, Italy*

Introduction

Age-related macular degeneration (AMD) is a severe neurodegenerative disease and the main cause of irreversible blindness in the elderly worldwide because of the progressive loss of central vision,due to degenerative and vascular changes in the macula, a retinal region responsible for fine and color vision [1].

AMD pathology shows various phenotypes and severity: it is classified in dry (~90%) and wet (~10%) forms, in early and late stages. It is possible, in some cases, that the dry AMD form converts into the wet form. Dry AMD is hardly detectable at the earlier stage, and its advanced form, named geographic atrophy, is responsible for the majority of blindness cases [2]. To date, no cure is available for dry AMD. On the contrary, in the wet form, monthly intravitreal injections of anti-VEGF drugs arer used to contrast neoangiogenesis, but this therapy can only delay the symptoms and slow down the disease progression [3].

The lack of effective AMD treatments is due to the poor understanding of AMD at molecular and cellular levels. The available AMD animal models do not recapitulate all the features of human disease [4], making more difficult the identification of new possible therapy targets. Furthermore, the etiology of AMD is complex: well-known risk factors have been identified in aging and genetic, and in environmental and behavioral factors, including unhealthy lifestyle. Among the earliest factors triggering this pathology there is the degeneration of retinal pigment epithelium (RPE) primarily responsible for photoreceptor homeostasis [5]. RPE cells are involved in several functions of the retina, and their degeneration cause adverse effects on photoreceptors and choriocapillaries, finally leading to visual loss [6].

The AMD pathogenic mechanisms are unknown; however, oxidative stress, inflammation, and protein aggregation, have been indicated as main determinants [7-9].

In AMD, RPE shows increased susceptibility to oxidative stress with higher levels of reactive oxygen species (ROS) and inflammation, reduced mitochondrial activity and autophagy impairment with increased protein aggregation [10, 11].

AMD microscopic pathological hallmarks are intracellular and extracellular depositions of toxic materials, which usually are removed by the autophagic pathway. In AMD RPE, these deposits, observed both in early and late stages, result in cell apoptosis [12] and in ROS generation. The increase of oxidative stress, in turn, induces protein aggregation contributing to inflammation and triggering a vicious cycle [13].

The main system used by RPE to neutralize oxidative stress and maintain cellular homeostasis is the Keap1/Nrf2/ARE pathway [14]. In basal conditions, Nrf2 is sequestered in the cytosol by Kelch-like ECH-associated protein 1 (Keap1), which recruits an ubiquitin ligase and mediates Nrf2 ubiquitination and proteasomal degradation. Upon oxidative stress conditions, Keap1 undergoes a conformational change and dissociates from Nrf2 that is free to translocate into the nucleus, where it binds to the antioxidant response element (ARE) in the promoter of target genes, such as SOD1, catalase and HO-1, thus promoting their transcription [15-17].

Interestingly, Nrf2 expression level decreases in aged retina [18], its signaling pathway is impaired in aged RPE exposed to an oxidative insult [19], and in human AMD Nrf2 labeling is decreased in RPE associated with drusen [20]. Moreover, KO animals for Nrf2 or its downstream genes develop age-related RPE degeneration and other AMD-like features [21-24] strongly suggesting that Nrf2 pathway impairment contributes to RPE degeneration in AMD [25].

It is widely known that Nrf2 activation suppresses inflammation indirectly through redox control [26]. More recently, evidence also demonstrated that Nrf2 acts directly as negative regulator of pro-inflammatory cytokine genes by binding to their promoters and inhibiting RNA Polimerase II recruitment [27].

Furthermore, triggering Nrf2 pathway blocks IL-1 and IL-6 expression, and displays antioxidant and anti-inflammatory effects *in vitro* and *in vivo* in ocular injury animal model [28]. These findings suggest that many anti-inflammatory effects observed in previous studies and attributed to the Nrf2-mediated transcription of ROS-scavengers, might depend upon Nrf2 direct effects on the transcription of cytokines and other genes related to inflammation. Moreover, Nrf2 has been found to be crucial in the activation of the inflammasome, with Nrf2-inducing compounds, including the anti-inflammatory drug dimethyl fumarate (DMF), being able to block the activation of the NLRP3 inflammasome, independently on Nrf2-induced gene expression [29]. The inflammasome is a group of protein complexes inducing an inflammatory response following stress factors [30].

In AMD, the inflammasome activation is related to RPE damage in both dry and wet forms [31, 32], and it has been hypothesized that it might trigger retinal cells death by pyroptosis, a mechanism depending on caspase-1 [33].

As previously said, in addition to increased oxidative stress and inflammation, AMD shows aberrant protein deposition. Thus clearance alteration has been frequently linked to AMD and autophagy process, the main clearing system in RPE cells, has been involved [9].

Autophagy is a catabolic process that directs degradation of unnecessary cellular molecules such as unfolded or damaged proteins, aggregates and organelles by delivering them to lysosomes, where they are degraded and recycled [34]. It is an internal quality control mechanism fundamental for assuring cellular homeostasis, and its alterations can contribute to several pathologies [35-37]. Aging is characterized by a general decrease of autophagic activity in all tissues, including the eye, and a further impairment of autophagy has been suggested in AMD [9, 38].

Among the genes involved in protein aggregates clearance via autophagy and proteasome pathway, p62 is a stress response factor with a role in AMD [39, 40]. In fact, p62 exerts a cytoprotective role in RPE against oxidative stress [41] and it is considered the link between autophagy and Nrf2 signaling [42] because it can directly bind Keap1 allowing Nrf2 activation [43-45]. Notably, Nrf2 can induce the expression of autophagy genes, like Hsp70 and p62 itself [46-48] suggesting a crosstalk between the two signaling cascades.

Given its central role in the modulation of different pathways involved in AMD, the Nrf2 transcription factor represents an attracting target for drug discovery. Many Nrf2-activating drugs have been evaluated *in vivo* and *in vitro* in degenerative diseases and in retinal tissues [49-55]. The results of these studies shown that Nrf2 activity increase protects against oxidative stress, inflammation and protein deposition [56-58]. However, to our knowledge, none of Nrf2 activators is under clinical testing for eye diseases. Thus, new nature-inspired compounds able to activate Nrf2-pathway (described in Chapter I, Part 3 and 4 of this thesis) are of great interest.

Background data
In the context of a potential therapeutic intervention for AMD, nature may represent a structural muse. Natural products have already proven to be a rich source of therapeutics and, by offering a great chemical diversity, they may be of inspiration to create new bioactive compounds. Thanks to an active collaboration with the research group coordinated by professor Michela Rosini of the Department of Pharmacy and Biotechnology at the Alma Mater Studiorum University of Bologna with a strong expertise in molecular design and synthesis, the combination of the hydroxycinnamoyl function of polyphenols and the allyl mercaptan moiety of garlic-derived organosulfur compounds, led to the synthesis of new nature-inspired chemical entities, which have been shown to possess a polypharmacological profile.

Their first characterization concerned the investigation of the molecular mechanisms potentially involved in aging and dementia, and led us to identify the catechol derivative, compound 1, with remarkable anti-aggregating ability and antioxidant properties [59, 60]. Deepening insight the antioxidant profile of compound 1, we observed its ability to induce the activation of Nrf2 pathway in human neuroblastoma cells (Chapter I, Part 4).

The prospect for tuning the Nrf2-mediated inducible antioxidant response is offered by Keap1 cysteine residues, which covalently conjugate electrophilic species. As a consequence, electrophiles and proelectrophiles from synthetic and natural sources have increasingly attracted interest in the drug discovery community. Among others, the catechol motif (red color, Figure 1) emerged as privileged structure as it becomes active electrophilic ortho-quinone on oxidation, prospecting benefits of proelectrophiles, which should provide major neuroprotection in oxidative conditions.
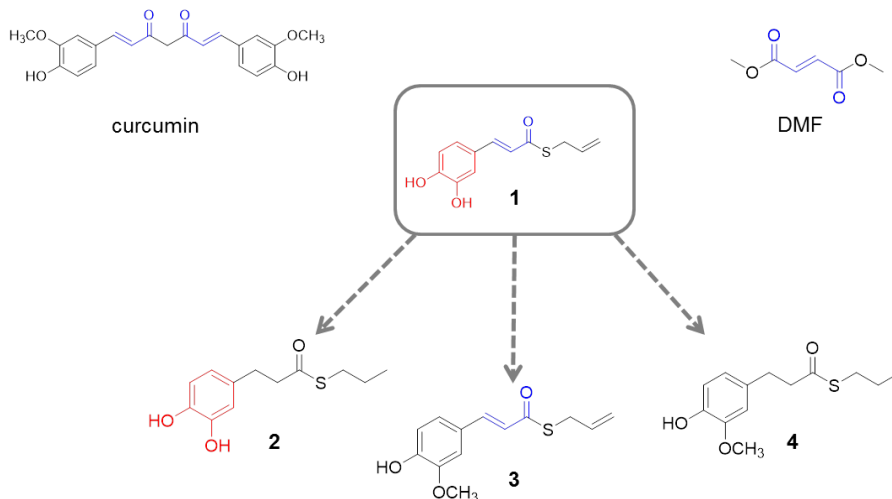

Figure 1. Design strategy for molecules 2,3 and 4 from leading compound 1. The catechol moiety (red color) and the electrophilic α,β-unsaturated carbonyl group (blue color) in Michael-type acceptor compounds such as curcumin and DMF, should be protective in oxidative stress conditions.

The electrophilic α,β-unsaturated carbonyl group (blue color, Figure 1) in Michael acceptor-type compounds, such as curcumin (CURC) and dimethylfumarate, represents an additional source for Nrf2 activation. These modifications should provide selectivity toward the binding site of Keap1, and prospect an optimized profile for these new molecules as Nrf2 inducers.

We already characterized these new natural hybrids as Nrf2 inducers in human neuroblastoma SH-SY5Y cells finding a better potency on Nrf2 activation profile than molecules already known in literature, such as DMF, a known Nrf2 activator approved by FDA that is currently used in clinic for multiple sclerosis (Chapter I, Part 4).

In addition to the antioxidant profile previously described and keeping in mind the centrality of the autophagy process impairment in AMD etiology, we investigated the ability of the leading compound 1 to modulate the expression of p62 and Hsp70 which are known to be autophagy genes (Figure 2).
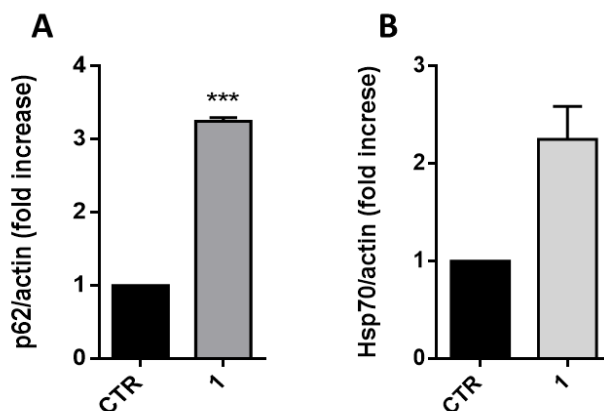

Figure 2. Modulation of p62 and Hsp70 protein expression in SH-SY5Y cells. SH-SY5Y human neuroblastoma cells were treated for 24 hours with compound 1 [5 μM]. After treatment, cells were harvested, washed and lysed. Whole cells extracts were examined by Western blot using an antibody against p62 or Hsp70. β-actin expression was detected to normalize the samples. Each value represents the mean ± SEM of three independent experiments. Statistical analysis was performed with unpaired T-test with ***$p < 0.001$ versus CTR (vehicle-treated cells).

Hybrid 1 showed to induce an increase in p62 protein expression and to be able to positively modulate, although not in a statistically significant manner (p value = 0,0667), Hsp70 levels in SH-SY5Y human neuroblastoma cells. Thus, confirming the crosstalk between the Nrf2 pathway and the autophagy process.

Finally, we preliminarily evaluated the potential anti-inflammatory activity of nature-inspired compounds in another cellular model, the THP-1 human monocytic cell line derived from an acute monocytic leukemia patient, which is responsive to an inflammatory stimulus such as lipopolysaccharide (LPS). The new natural hybrids diminished the LPS-induced increase in the production of tumor necrosis factor alpha (TNF-α) and interleukin (IL)-8 (Figure 3). Surprisingly, also compound 4, which lacks both functionalities essential for Nrf2 activation, showed a similar effect on pro-inflammatory cytokines, thus suggesting that the anti-inflammatory activity may be independent from Nrf2 activation.
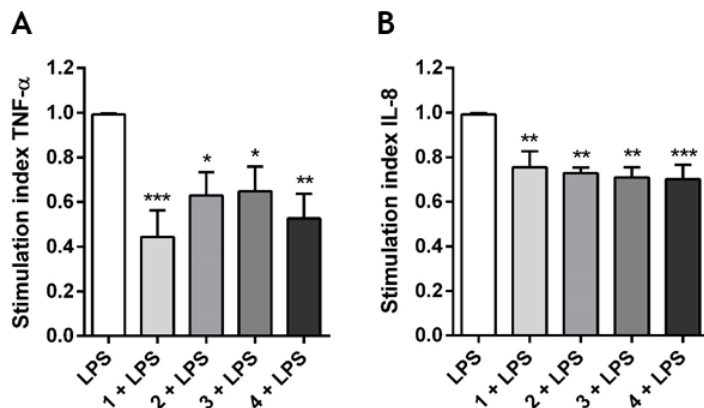

Figure 3. TNF-α and IL-8 modulation in THP-1 cells. THP-1 cells were seeded and pre-treated 24 h with compounds 1-4 [5 μM]. After treatment, cells were exposed to LPS (10 ng·mL^{-1}) for additional 3 h. TNF-α (**A**) and IL-8 (**B**) release were evaluated in cell-free supernatants by ELISA, following the manufacturer's instructions. Each value in the graph represents the mean ± SEM of three

independent experiments. Statistical analysis was performed with Dunnett's multiple comparison test with **$p < 0.01$, ***$p < 0.001$ versus LPS.

Preliminary results

On the basis of the above reported data, we performed some pilot experiments to start to investigate the activity of nature-inspired hybrids in the cell model suitable for the study of AMD: the ARPE-19 retinal pigmented epithelium (RPE) cell line.

In order to define the range of concentration to be used in cellular experimental settings, the cytotoxicity of compounds 1, 4, curcumin and dimethyl fumarate was assessed in ARPE-19 cells.

Cells were exposed to the compounds at increasing concentrations ranging from 1 to 100 µM (1, 2.5, 5, 7.5, 10, 25, 50, 75 and 100 µM) for 24 h and cell viability was evaluated by MTT assay. As shown in Figure 1, all the compounds were well tolerated, in fact they do not induce any statistically significant decrease in ARPE-19 cell viability.
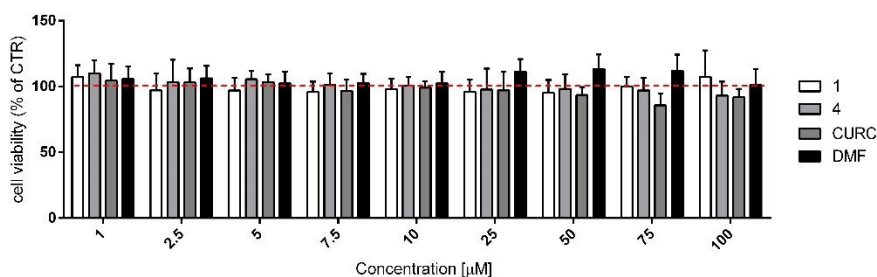

Figure 1. Cell viability of ARPE-19 cells treated with nature-inspired hybrids. ARPE-19 cells were treated for 24 hours with increasing concentrations of hybrid 1, and their viability was assessed by MTT assay. The cell toxicity of curcumin (CURC), dimethyl fumarate (DMF), and the non(pro)electrophilic derivative hybrid 4, were also tested. Each value represents the mean ± SEM of three independent experiments. Dunnett's multiple comparisons test versus CTR (100%, dotted red line).

Once assessed the safety of the hybrids on the ARPE-19 cell line, we verify the ability of compound 1 to induce the Nrf2 transcription factor translocation from the cytosol to the nucleus. Cells were treated with two different concentrations of compound 1 (500 nM and 5 µM) for 3 h and then fractionated to separate the nuclear extracts. As shown in Figure 2, hybrid 1, at the highest concentration tested (5 µM), triggered Nrf2 translocation to the nucleus.
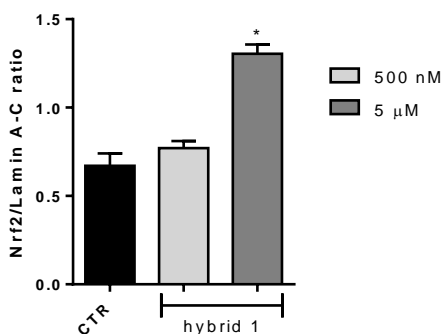

Figure 2. Nrf2 nuclear translocation in ARPE-19 cells. ARPE-19 cells were treated for 3 h with hybrid 1 at two different concentrations, and then were subjected to cell fractionation. Nuclear extracts were examined by Western blot using an antibody against Nrf2. Lamin A/C expression was detected to normalize the samples. Each value represents the mean ± SEM of three independent experiments. *p < 0.05 Dunnett's multiple comparisons test versus CTR.

Finally, to assess the complete Nrf2 pathway activation, we investigate the modulation of the expression of HO-1, one of the well-known Nrf2-target genes. ARPE-19 cells were treated with compound 1 (500 nM and 5 µM) for increasing times (3, 6, 9, 16, 24 h) and then fractionated to obtain the cytosolic fraction. As shown in Figure 3, the treatment with 5 µM hybrid 1 induced a long-lasting increase in HO-1 protein levels that is statistically significant from 6 to 24 h. Moreover, at 24 h, also the lower concentration of 500 nM seemed to be effective.
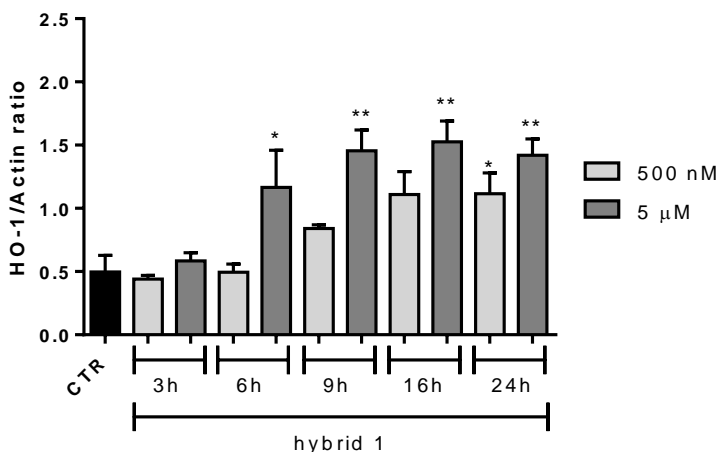
Figure 3. Nrf2-target HO-1 expression levels in ARPE-19 cells. Cytoplasm extracts were examined by Western blot using an antibody against HO-1. Actin expression was detected to normalize the samples. Each value represents the mean ± SEM of three independent experiments. *$p < 0.05$, **$p < 0.01$. Dunnett's multiple comparisons test versus CTR.

In conclusion, these preliminary results confirmed the ability of nature-inspired hybrid 1 to trigger the Nrf2 pathway also in the cell line ARPE-19 which represents the retinal pigmented epithelium and are the suitable cell model for the study of AMD pathogenesis.

Further experiments will be performed in the next months and for the next two years thanks to the funding received by the Fondo di Ricerca di Ateneo, Blue Sky Research. This research field will open future perspective for my work after the PhD.

Material and methods

Cell Culture and Treatments. Human ARPE-19 cells were obtained from the American Type Culture Collection (ATCC) and grown to confluence in a humidified 5% CO_2 atmosphere at 37°C. ARPE-19 cells were cultured in Dulbecco's MEM/Nut MIX F-12 (1:1) medium containing 10% inactivated FBS, 100 units/ml penicillin, 100 µg/ml

streptomycin and 2 mM L-glutamine. The cells were treated with vehicle (DMSO), hybrid 1, 2, 3, 4, curcumin or DMF, at the concentrations indicated in the figure legends.

Cell fractioning and Western blotting. Cells were seeded in 100 mm^2 dishes and treated as reported in figure legends. Cells were then washed and homogenized using a glass-glass dounce homogenizer in 0.32 M sucrose buffered with 20 mM TrisHCl (pH 7.4) containing 2 mM EDTA, 0.5 mM EGTA, 50 mM β-mercaptoethanol, and 20 μg/mL leupeptin, aprotinin, and pepstatin. The homogenate was centrifuged at 300g for 5 min to separate the nuclear and cytoplasmic fractions. Proteins of both the cellular fractions were separated on SDS-polyacrylamide gel electrophoresis and processed following standard procedures. The nitrocellulose membranes signals were detected by chemiluminescence. Statistical analysis of Western blot data were performed on the densitometric values obtained with the NIH image software 1.61 (http://rsb.info.nih.gov/nih-image).

Cell viability. Mitochondrial enzymatic activity was used to estimate the cell viability of ARPE-19 cells by MTT [3-(4,5-dimethylthiazol-2-yl)-2,5-diphenyltetrazolium bromide] assay following standard procedure. Absorbance values were measured at 595 nm in a microplate reader and the results expressed as % with respect to control.

Statistical analysis. The statistical analysis were performed by using GraphPad InStat software. All results were analyzed by Dunnett's multiple comparisons test ; differences were considered statistically significant when $p < 0.05$.

References

1. Jager RD, Mieler WF, Miller JW. Age-related macular degeneration. N Engl J Med. 2008 Jun 12;358(24):2606-17. doi: 10.1056/NEJMra0801537.

2. Lim LS, Mitchell P, Seddon JM, Holz FG, Wong TY. Age-related macular degeneration. Lancet. 2012 May 5;379(9827):1728-38. doi:10.1016/S0140-6736(12)60282-7.

3. Amadio M, Govoni S, Pascale A. Targeting VEGF in eye neovascularization: What's new?: A comprehensive review on current therapies and oligonucleotide-based interventions under development. Pharmacol Res. 2016 Jan;103:253-69. doi: 10.1016/j.phrs.2015.11.027.

4. Lyzogubov VV, Bora PS, Wu X, Horn LE, de Roque R, Rudolf XV, Atkinson JP, Bora NS. The Complement Regulatory Protein CD46 Deficient Mouse Spontaneously Develops Dry-Type Age-Related Macular Degeneration-Like Phenotype. Am J Pathol. 2016 Aug;186(8):2088-2104. doi: 10.1016/j.ajpath.2016.03.021.

5. Strauss O. The retinal pigment epithelium in visual function. Physiol Rev. 2005 Jul;85(3):845-81. doi: 10.1152/physrev.00021.2004.

6. Ambati J, Fowler BJ. Mechanisms of age-related macular degeneration. Neuron. 2012 Jul 12;75(1):26-39. doi: 10.1016/j.neuron.2012.06.018.

7. Reibaldi M, Longo A, Pulvirenti A, Avitabile T, Russo A, Cillino S, Mariotti C, Casuccio A. Geo-Epidemiology of Age-Related Macular Degeneration: New Clues Into the Pathogenesis. Am J Ophthalmol. 2016 Jan;161:78-93.e1-2. doi:10.1016/j.ajo.2015.09.031.

8. Boya P, Esteban-Martínez L, Serrano-Puebla A, Gómez-Sintes R, Villarejo-Zori B. Autophagy in the eye: Development, degeneration, and aging. Prog Retin Eye Res.

2016 Nov;55:206-245. doi: 10.1016/j.preteyeres.2016.08.001.

9. Kaarniranta K, Tokarz P, Koskela A, Paterno J, Blasiak J. Autophagy regulates death of retinal pigment epithelium cells in age-related macular degeneration. Cell Biol Toxicol. 2017 Apr;33(2):113-128. doi: 10.1007/s10565-016-9371-8.

10. Ferrington DA, Sinha D, Kaarniranta K. Defects in retinal pigment epithelial cell proteolysis and the pathology associated with age-related macular degeneration. Prog Retin Eye Res. 2016 Mar;51:69-89. doi:10.1016/j.preteyeres.2015.09.002.

11. Kauppinen A, Paterno JJ, Blasiak J, Salminen A, Kaarniranta K. Inflammation and its role in age-related macular degeneration. Cell Mol Life Sci. 2016 May;73(9):1765-86. doi: 10.1007/s00018-016-2147-8.

12. Crabb JW, Miyagi M, Gu X, Shadrach K, West KA, Sakaguchi H, Kamei M, Hasan A, Yan L, Rayborn ME, Salomon RG, Hollyfield JG. Drusen proteome analysis: an approach to the etiology of age-related macular degeneration. Proc Natl Acad Sci U S A. 2002 Nov 12;99(23):14682-7. doi: 10.1073/pnas.222551899.

13. Liu J, Copland DA, Theodoropoulou S, Chiu HA, Barba MD, Mak KW, Mack M, Nicholson LB, Dick AD. Impairing autophagy in retinal pigment epithelium leads to inflammasome activation and enhanced macrophage-mediated angiogenesis. Sci Rep. 2016 Feb 5;6:20639. doi: 10.1038/srep20639.

14. Cano M, Thimmalappula R, Fujihara M, Nagai N, Sporn M, Wang AL, Neufeld AH, Biswal S, Handa JT. Cigarette smoking, oxidative stress, the anti-oxidant response through Nrf2 signaling, and Age-related Macular Degeneration. Vision Res. 2010 Mar 31;50(7):652-64. doi: 10.1016/j.visres.2009.08.018.

15. hang DD. Mechanistic studies of the Nrf2-Keap1 signaling pathway. Drug Metab Rev. 2006;38(4):769-89. doi: 10.1080/03602530600971974.

16. Loboda A, Damulewicz M, Pyza E, Jozkowicz A, Dulak J. Role of Nrf2/HO-1 system in development, oxidative stress response and diseases: an evolutionarily conserved mechanism. Cell Mol Life Sci. 2016 Sep;73(17):3221-47. doi:10.1007/s00018-016-2223-0.

17. Fuse Y, Kobayashi M. Conservation of the Keap1-Nrf2 System: An Evolutionary Journey through Stressful Space and Time. Molecules. 2017 Mar 9;22(3). pii: E436. doi: 10.3390/molecules22030436.

18. Lenox AR, Bhootada Y, Gorbatyuk O, Fullard R, Gorbatyuk M. Unfolded protein response is activated in aged retinas. Neurosci Lett. 2015 Nov 16;609:30-5. doi: 10.1016/j.neulet.2015.10.019.

19. Sachdeva MM, Cano M, Handa JT. Nrf2 signaling is impaired in the aging RPE given an oxidative insult. Exp Eye Res. 2014 Feb;119:111-4. doi:10.1016/j.exer.2013.10.024.

20. Wang L, Kondo N, Cano M, Ebrahimi K, Yoshida T, Barnett BP, Biswal S, Handa JT. Nrf2 signaling modulates cigarette smoke-induced complement activation in retinal pigmented epithelial cells. Free Radic Biol Med. 2014 May;70:155-66. doi:10.1016/j.freeradbiomed.2014.01.015.

21. Zhao Z, Chen Y, Wang J, Sternberg P, Freeman ML, Grossniklaus HE, Cai J. Age-related retinopathy in NRF2-deficient mice. PLoS One. 2011 Apr 29;6(4):e19456. doi: 10.1371/journal.pone.0019456.

22. Mitter SK, Song C, Qi X, Mao H, Rao H, Akin D, Lewin A, Grant M, Dunn W Jr, Ding J, Bowes Rickman C, Boulton M. Dysregulated autophagy in the RPE is associated with increased susceptibility to oxidative stress and AMD.

Autophagy. 2014;10(11):1989-2005. doi:10.4161/auto.36184.

23. Yao J, Jia L, Khan N, Lin C, Mitter SK, Boulton ME, Dunaief JL, Klionsky DJ, Guan JL, Thompson DA, Zacks DN. Deletion of autophagy inducer RB1CC1 results in degeneration of the retinal pigment epithelium. Autophagy. 2015;11(6):939-53. doi: 10.1080/15548627.2015.1041699.

24. Pujol-Lereis LM, Schäfer N, Kuhn LB, Rohrer B, Pauly D. Interrelation Between Oxidative Stress and Complement Activation in Models of Age-Related Macular Degeneration. Adv Exp Med Biol. 2016;854:87-93. doi:10.1007/978-3-319-17121-0_13.

25. Datta S, Cano M, Ebrahimi K, Wang L, Handa JT. The impact of oxidative stress and inflammation on RPE degeneration in non-neovascular AMD. Prog Retin Eye Res. 2017 Sep;60:201-218. doi: 10.1016/j.preteyeres.2017.03.002.

26. Ahmed SM, Luo L, Namani A, Wang XJ, Tang X. Nrf2 signaling pathway: Pivotal roles in inflammation. Biochim Biophys Acta. 2017 Feb;1863(2):585-597. doi:10.1016/j.bbadis.2016.11.005.

27. Kobayashi EH, Suzuki T, Funayama R, Nagashima T, Hayashi M, Sekine H, Tanaka N, Moriguchi T, Motohashi H, Nakayama K, Yamamoto M. Nrf2 suppresses macrophage inflammatory response by blocking proinflammatory cytokine transcription. Nat Commun. 2016 May 23;7:11624. doi: 10.1038/ncomms11624.

28. Ildefonso CJ, Jaime H, Brown EE, Iwata RL, Ahmed CM, Massengill MT, Biswal MR, Boye SE, Hauswirth WW, Ash JD, Li Q, Lewin AS. Targeting the Nrf2 Signaling Pathway in the Retina With a Gene-Delivered Secretable and Cell-Penetrating Peptide. Invest Ophthalmol Vis Sci. 2016 Feb;57(2):372-86. doi:10.1167/iovs.15-17703.

29. Garstkiewicz M, Strittmatter GE, Grossi S, Sand J, Fenini G, Werner S, French LE, Beer HD. Opposing effects of Nrf2 and Nrf2-activating compounds on the NLRP3 inflammasome independent of Nrf2-mediated gene expression. Eur J Immunol. 2017 May;47(5):806-817. doi:10.1002/eji.201646665.

30. Strowig T, Henao-Mejia J, Elinav E, Flavell R. Inflammasomes in health and disease. Nature. 2012 Jan 18;481(7381):278-86. doi: 10.1038/nature10759.

31. Tarallo V, Hirano Y, Gelfand BD, Dridi S, Kerur N, Kim Y, Cho WG, Kaneko H, Fowler BJ, Bogdanovich S, Albuquerque RJ, Hauswirth WW, Chiodo VA, Kugel JF, Goodrich JA, Ponicsan SL, Chaudhuri G, Murphy MP, Dunaief JL, Ambati BK, Ogura Y, Yoo JW, Lee DK, Provost P, Hinton DR, Núñez G, Baffi JZ, Kleinman ME, Ambati J. DICER1 loss and Alu RNA induce age-related macular degeneration via the NLRP3 inflammasome and MyD88. Cell. 2012 May 11;149(4):847-59. doi:10.1016/j.cell.2012.03.036.

32. Tseng WA, Thein T, Kinnunen K, Lashkari K, Gregory MS, D'Amore PA, Ksander BR. NLRP3 inflammasome activation in retinal pigment epithelial cells by lysosomal destabilization: implications for age-related macular degeneration. Invest Ophthalmol Vis Sci. 2013 Jan 7;54(1):110-20. doi: 10.1167/iovs.12-10655.

33. Wang Y, Hanus JW, Abu-Asab MS, Shen D, Ogilvy A, Ou J, Chu XK, Shi G, Li W, Wang S, Chan CC. NLRP3 Upregulation in Retinal Pigment Epithelium in Age-Related Macular Degeneration. Int J Mol Sci. 2016 Jan 8;17(1). pii: E73. doi:10.3390/ijms17010073.

34. Hyttinen JM, Amadio M, Viiri J, Pascale A, Salminen A, Kaarniranta K. Clearance of misfolded and aggregated proteins by aggrephagy and implications for aggregation

diseases. Ageing Res Rev. 2014 Nov;18:16-28. doi:10.1016/j.arr.2014.07.002.

35. Li YJ, Jiang Q, Cao GF, Yao J, Yan B. Repertoires of autophagy in the pathogenesis of ocular diseases. Cell Physiol Biochem. 2015;35(5):1663-76. doi:10.1159/000373980.

36. Lippai M, Szatmári Z. Autophagy-from molecular mechanisms to clinical relevance. Cell Biol Toxicol. 2017 Apr;33(2):145-168. doi:10.1007/s10565-016-9374-5.

37. Morel E, Mehrpour M, Botti J, Dupont N, Hamaï A, Nascimbeni AC, Codogno P. Autophagy: A Druggable Process. Annu Rev Pharmacol Toxicol. 2017 Jan 6;57:375-398. doi: 10.1146/annurev-pharmtox-010716-104936.

38. Iannaccone A, Giorgianni F, New DD, Hollingsworth TJ, Umfress A, Alhatem AH, Neeli I, Lenchik NI, Jennings BJ, Calzada JI, Satterfield S, Mathews D, Diaz RI, Harris T, Johnson KC, Charles S, Kritchevsky SB, Gerling IC, Beranova-Giorgianni S, Radic MZ; Health ABC study. Circulating Autoantibodies in Age-Related Macular Degeneration Recognize Human Macular Tissue Antigens Implicated in Autophagy, Immunomodulation, and Protection from Oxidative Stress and Apoptosis. PLoS One. 2015 Dec 30;10(12):e0145323. doi: 10.1371/journal.pone.0145323.

39. Viiri J, Amadio M, Marchesi N, Hyttinen JM, Kivinen N, Sironen R, Rilla K, Akhtar S, Provenzani A, D'Agostino VG, Govoni S, Pascale A, Agostini H, Petrovski G, Salminen A, Kaarniranta K. Autophagy activation clears ELAVL1/HuR-mediated accumulation of SQSTM1/p62 during proteasomal inhibition in human retinal pigment epithelial cells. PLoS One. 2013 Jul 29;8(7):e69563. doi:10.1371/journal.pone.0069563.

40. Wang L, Ebrahimi KB, Chyn M, Cano M, Handa JT. Biology of p62/sequestosome-1 in Age-Related Macular Degeneration

(AMD). Adv Exp Med Biol. 2016;854:17-22. doi:10.1007/978-3-319-17121-0_3.

41. Wang L, Cano M, Handa JT. p62 provides dual cytoprotection against oxidative stress in the retinal pigment epithelium. Biochim Biophys Acta. 2014 Jul;1843(7):1248-58. doi: 10.1016/j.bbamcr.2014.03.016.

42. Jiang T, Harder B, Rojo de la Vega M, Wong PK, Chapman E, Zhang DD. p62 links autophagy and Nrf2 signaling. Free Radic Biol Med. 2015 Nov;88(Pt B):199-204. doi: 10.1016/j.freeradbiomed.2015.06.014.

43. Lau A, Wang XJ, Zhao F, Villeneuve NF, Wu T, Jiang T, Sun Z, White E, Zhang DD. A noncanonical mechanism of Nrf2 activation by autophagy deficiency: direct interaction between Keap1 and p62. Mol Cell Biol. 2010 Jul;30(13):3275-85. doi:10.1128/MCB.00248-10.

44. Copple IM, Lister A, Obeng AD, Kitteringham NR, Jenkins RE, Layfield R, Foster BJ, Goldring CE, Park BK. Physical and functional interaction of sequestosome 1 with Keap1 regulates the Keap1-Nrf2 cell defense pathway. J Biol Chem. 2010 May 28;285(22):16782-8. doi:10.1074/jbc.M109.096545.

45. Komatsu M, Kurokawa H, Waguri S, Taguchi K, Kobayashi A, Ichimura Y, Sou YS, Ueno I, Sakamoto A, Tong KI, Kim M, Nishito Y, Iemura S, Natsume T, Ueno T, Kominami E, Motohashi H, Tanaka K, Yamamoto M. The selective autophagy substrate p62 activates the stress responsive transcription factor Nrf2 through inactivation of Keap1. Nat Cell Biol. 2010 Mar;12(3):213-23. doi:10.1038/ncb2021.

46. Jain A, Lamark T, Sjøttem E, Larsen KB, Awuh JA, Øvervatn A, McMahon M, Hayes JD, Johansen T. p62/SQSTM1 is a target gene for transcription factor NRF2 and creates a positive feedback loop by inducing antioxidant response

element-driven gene transcription. J Biol Chem. 2010 Jul 16;285(29):22576-91. doi:10.1074/jbc.M110.118976.

47. Pietrocola F, Izzo V, Niso-Santano M, Vacchelli E, Galluzzi L, Maiuri MC, Kroemer G. Regulation of autophagy by stress-responsive transcription factors. Semin Cancer Biol. 2013 Oct;23(5):310-22. doi: 10.1016/j.semcancer.2013.05.008.

48. Pajares M, Jiménez-Moreno N, García-Yagüe ÁJ, Escoll M, de Ceballos ML, Van Leuven F, Rábano A, Yamamoto M, Rojo AI, Cuadrado A. Transcription factor NFE2L2/NRF2 is a regulator of macroautophagy genes. Autophagy. 2016 Oct 2;12(10):1902-1916. doi:10.1080/15548627.2016.1208889

49. Hanneken A, Lin FF, Johnson J, Maher P. Flavonoids protect human retinal pigment epithelial cells from oxidative-stress-induced death. Invest Ophthalmol Vis Sci. 2006 Jul;47(7):3164-77. doi:10.1167/iovs.04-1369.

50. Koskela A, Reinisalo M, Hyttinen JM, Kaarniranta K, Karjalainen RO. Pinosylvin-mediated protection against oxidative stress in human retinal pigment epithelial cells. Mol Vis. 2014 Jun 2;20:760-9.

51. Chang CF, Cho S, Wang J. (-)-Epicatechin protects hemorrhagic brain via synergistic Nrf2 pathways. Ann Clin Transl Neurol. 2014 Apr 1;1(4):258-271. doi:10.1002/acn3.54.

52. Zhang H, Liu YY, Jiang Q, Li KR, Zhao YX, Cao C, Yao J. Salvianolic acid A protects RPE cells against oxidative stress through activation of Nrf2/HO-1 signaling. Free Radic Biol Med. 2014 Apr;69:219-28. doi:10.1016/j.freeradbiomed.2014.01.025.

53. Liu X, Ward K, Xavier C, Jann J, Clark AF, Pang IH, Wu H. The novel triterpenoid RTA 408 protects human retinal pigment epithelial cells against H2O2-induced cell injury via NF-E2-related factor 2 (Nrf2) activation. Redox Biol. 2016 Aug;8:98-109. doi: 10.1016/j.redox.2015.12.005.

54. Fang Y, Su T, Qiu X, Mao P, Xu Y, Hu Z, Zhang Y, Zheng X, Xie P, Liu Q. Protective effect of alpha-mangostin against oxidative stress induced-retinal cell death. Sci Rep. 2016 Feb 18;6:21018. doi: 10.1038/srep21018.

55. Inoue Y, Shimazawa M, Noda Y, Nagano R, Otsuka T, Kuse Y, Nakano Y, Tsuruma K, Nakagami Y, Hara H. RS9, a novel Nrf2 activator, attenuates light-induced death of cells of photoreceptor cells and Müller glia cells. J Neurochem. 2017 Jun;141(5):750-765. doi: 10.1111/jnc.14029.

56. Lu MC, Ji JA, Jiang ZY, You QD. The Keap1-Nrf2-ARE Pathway As a Potential Preventive and Therapeutic Target: An Update. Med Res Rev. 2016 Sep;36(5):924-63. doi: 10.1002/med.21396.

57. Gazaryan IG, Thomas B. The status of Nrf2-based therapeutics: current perspectives and future prospects. Neural Regen Res. 2016 Nov;11(11):1708-1711. doi: 10.4103/1673-5374.194706.

58. Pajares M, Cuadrado A, Rojo AI. Modulation of proteostasis by transcription factor NRF2 and impact in neurodegenerative diseases. Redox Biol. 2017 Apr;11:543-553. doi: 10.1016/j.redox.2017.01.006.

59. Simoni E, Serafini MM, Bartolini M, Caporaso R, Pinto A, Necchi D, Fiori J, Andrisano V, Minarini A, Lanni C, Rosini M. Nature-Inspired Multifunctional Ligands: Focusing on Amyloid-Based Molecular Mechanisms of Alzheimer's Disease. ChemMedChem. 2016 Jun 20;11(12):1309-17. doi: 10.1002/cmdc.201500422.

60. Simoni E, Serafini MM, Caporaso R, Marchetti C, Racchi M, Minarini A, Bartolini M, Lanni C, Rosini M. Targeting the Nrf2/Amyloid-Beta Liaison in Alzheimer's Disease: A Rational Approach. ACS Chem Neurosci. 2017 Jul 19;8(7):1618-1627. doi: 10.1021/acschemneuro.7b00100.

List of publications (from 2014 to 2017)

1. **Serafini MM**, Catanzaro M, Rosini M, Racchi M, Lanni C. *Curcumin in Alzheimer's disease: Can we think to new strategies and perspectives for this molecule?* Pharmacol Res. 2017 Oct;124:146-155. doi: 10.1016/j.phrs.2017.08.004.

2. Simoni E, **Serafini MM**, Caporaso R, Marchetti C, Racchi M, Minarini A, Bartolini M, Lanni C, Rosini M. *Targeting the Nrf2/Amyloid-Beta Liaison in Alzheimer's Disease: A Rational Approach.* ACS Chem Neurosci. 2017 Jul 19;8(7):1618-1627. doi: 10.1021/acschemneuro.7b00100.

3. Racchi M, Buoso E, Ronfani M, **Serafini MM**, Galasso M, Lanni C, Corsini E. *Role of Hormones in the Regulation of RACK1 Expression as a Signaling Checkpoint in Immunosenescence.* Int J Mol Sci. 2017 Jul 6;18(7). pii: E1453. doi: 10.3390/ijms18071453.

4. Buoso E, Galasso M, **Serafini MM**, Ronfani M, Lanni C, Corsini E, Racchi M. *Transcriptional regulation of RACK1 and modulation of its expression: Role of steroid hormones and significance in health and aging.* Cell Signal. 2017 Jul;35:264-271. doi: 10.1016/j.cellsig.2017.02.010.

5. Buoso E, Galasso M, Ronfani M, **Serafini MM**, Lanni C, Corsini E, Racchi M. *Role of spliceosome proteins in the regulation of glucocorticoid receptor isoforms by cortisol and dehydroepiandrosterone.* Pharmacol Res. 2017 Jun;120:180-187. doi: 10.1016/j.phrs.2017.03.019.

6. Simoni E, **Serafini MM**, Bartolini M, Caporaso R, Pinto A, Necchi D, Fiori J, Andrisano V, Minarini A, Lanni C, Rosini M. *Nature-Inspired Multifunctional Ligands: Focusing on Amyloid-Based Molecular Mechanisms of Alzheimer's*

Disease. ChemMedChem. 2016 Jun 20;11(12):1309-17. doi: 10.1002/cmdc.201500422.

7. Corsini E, Galbiati V, Papale A, Kummer E, Pinto A, **Serafini MM**, Guaita A, Spezzano R, Caruso D, Marinovich M, Racchi M. *Role of androgens in dhea-induced rack1 expression and cytokine modulation in monocytes.* Immun Ageing. 2016 May 29;13:20. doi: 10.1186/s12979-016-0075-y.

8. Necchi D, Pinto A, Tillhon M, Dutto I, **Serafini MM**, Lanni C, Govoni S, Racchi M, Prosperi E. *Defective DNA repair and increased chromatin binding of DNA repair factors in Down syndrome fibroblasts.* Mutat Res. 2015 Oct;780:15-23. doi: 10.1016/j.mrfmmm.2015.07.009.

9. Pinto A, Malacrida B, Oieni J, **Serafini MM**, Davin A, Galbiati V, Corsini E, Racchi M. *DHEA modulates the effect of cortisol on RACK1 expression via interference with the splicing of the glucocorticoid receptor.* Br J Pharmacol. 2015 Jun;172(11):2918-27. doi: 10.1111/bph.13097.

List of congress abstracts and posters (from 2014 to 2017)

1. **Serafini MM**, Catanzaro M, Marchesi N, Simoni E, Pascale A, Racchi M, Amadio M, Rosini M, Lanni C. *Modulation of oxidative and inflammatory pathways by nature-inspired new hybrids: relevance for Nrf2 transcription factor involvement.* Italian Society of Pharmacology (SIF) - 2017 Oct 24-28, Rimini, Italy.

2. Amadio M, **Serafini MM**, Marchesi N, Catanzaro M, Fagiani F, Simoni E, Pascale A, Rosini M, Lanni C. *Nature-inspired Nrf2 activators in retinal pigment epithelial cells: a source for therapeutics in Age-related Macular Degeneration.* European Association for Vision and Eye Research (EVER) - 2017 Sept 27-30, Nice, France.

3. **Serafini MM**, Poloni L, Racchi M, Bartolini M, Rosini M, Lanni C. *Nature-inspired new hybrids to counteract oxidative stress and inflammation in the central nervous system.* More than neurons: toward a less neuronocentric view of brain disorders – 2016 Dec 1-3, Torino, Italy.

4. **Serafini MM**, Poloni L, Ronfani M, Galasso M, Racchi M, Bartolini M, Rosini M, Lanni C. *Nature-inspired new hybrids to counteract oxidative stress in neurodegeneration.* Society for Neuroscience (SfN) annual meeting - 2016 Nov 12-16, San Diego, CA, USA.

5. **Serafini MM**, Pinto A, Racchi M, Necchi D, Lanni C. *p53 in neurodegeneration: impact of beta-amyloid/p53 interference on Alzheimer pathogenesis.* The 12th international conference on Alzheimer's and Parkinson's diseases (AD/PD) – 2015, Mar 18-22, Nice, France.